Optimal Detection in the Presence of Non-Gaussian Jamming

by

Khalid Ateyia Almahrog

A thesis submitted to the Faulty of Graduate and Postdoctoral Affairs
in partial fulfillment of the requirements for the degree of

Doctor of Philosophy in Electrical and Computer Engineering

Ottawa-Carleton Institute for Electrical and Computer Engineering
Department of Systems and Computer Engineering
Carleton University
Ottawa, Ontario
May 2022

© Khalid Ateyia Almahrog, 2022

Declaration of Authorship

I hereby certify that this thesis is entirely my own original work except where otherwise indicated. I am aware of the University's regulations concerning plagiarism, including those concerning consequent disciplinary actions. Any use of the works of any other author, in any form, is properly acknowledged at their point of use.

Abstract

The open nature of the wireless channel makes it vulnerable to many security attacks like jamming and eavesdropping. Jamming threatens the existence of wireless services and can lead to denial of service. Barrage jamming where the jammer emits white Gaussian noise that occupies the entire transmission bandwidth is known to be the most harmful when the jammer has no knowledge about the target system or when it targets many different systems. The majority of literature models the barrage jamming signal at the receiver as additive Gaussian noise. The accuracy of this model in mobile communication scenarios is questionable. The complex Gaussian signal transmitted over the unknown complex Gaussian channel induces a non-Gaussian signal at the receiver. Knowing the distribution of the received jamming signal is fundamental to develop detectors and to compute the probability of detection error. This thesis considers scenarios where a single-antenna transmitter sends complex symbols drawn from one-dimensional or multi-dimensional constellation to a receiver equipped with a single, double, or multiple antennas in the presence of a single-antenna barrage jammer. The exact likelihood expressions of the received signal and the likelihood expressions based on the Gaussian approximation of the signal induced by the jammer's transmissions are derived for scenarios in which the receiver has full channel state information (CSI), full channel distribution information (CDI), or partial CDI about the transmitter channel. The jammer CDI is assumed to be either partially or fully available at the receiver. Using the derived likelihood expressions, two maximum likelihood (ML) detectors are developed for each scenario. One detector is based on the exact likelihood expressions and the other is based on the Gaussian approximation expressions. The performance of each detector is investigated and cases in which the two detector are equivalent are identified analytically and experimentally. Furthermore, the effects of the number of receive antennas, and symbol length on the detection performance are investigated.

Acknowledgments

All praise and thanks are due to Allah, the almighty; without his welling, nothing can exist, nor it can be done.

I am deeply thankful to my supervisor Professor Ramy Gohary for his academic, financial, and personal support throughout my research. Professor Gohary was always there to solve problems related to mathematical derivations, software implementations, and writing with LaTeX. Working with Professor Gohary boosted my interest in scientific research and made me a tea connoisseur through the countless cups of hot, tasty tea he offered during every meeting. Finding words that may asymptotically approach my feeling of gratitude towards professor Gohary would be a good topic for another Ph.D. thesis.

I am also indebted to the university of Tripoli and the Libyan ministry of higher education and scientific research for the Ph.D. scholarship they offered me.

I would like to thank the members of my doctoral committee: Prof. Roshdy Hafez, Prof. Natalia Stepanova, Prof. Martin Bouchard, and Prof. Ha Nguyen for their inspiring discussion and insightful suggestions. My thanks also go to Prof. Halim Yanikomeroglu for suggesting the anti-jamming research topic, Dr. Amr El-Keyi for the support and encouragement during the early stages of this research, and Prof. Peter Galko for serving as a member of my proposal committee.

I would like to express my deep gratitude to my parents, my siblings, and my relatives for their emotional support and sincere prayers.

Last but not least, I am deeply indebted to my wife and children for all the love, joy, and patience they showed during all times.

Dedication

*To my father **Ateiya**, and my mother **Bariqa** for the sacrifices they made,*

*To the memory of brother **Taiseer**, grandmother **Zuhra**, uncle **Mahmoud**, and teacher*

***Musbah Saad**, for the principles and morals they embodied,*

To my brothers and sisters, for the unconditional support.

*And to my wife **Wafa** and my children for the endless love.*

Table of Contents

List of Figures **x**

List of Symbols **xii**

1 Introduction **1**

1.1 Fatality of jamming attacks 1

1.2 Optimality of Maximum Likelihood Detection 4

1.3 Contributions 6

1.4 Publications 7

1.5 Outline 8

2 Literature Review **9**

2.1 Jammer's Classes 9

2.2 Anti-jamming 12

2.3 Optimal Detection in the Presence of Jamming 16

3 SIMO with single transmission **19**

3.1 System Model and Problem Statement 19

3.1.1 System Model 19

3.1.2 Problem Statement 21

3.2 Likelihood function expressions for the different CSI cases 23

3.2.1 Statistical distribution of both $\boldsymbol{H}$ and $\boldsymbol{G}$ known: 24

3.2.2 Statistical distribution of $\boldsymbol{H}$ known and statistical distribution of $\boldsymbol{G}$ partially known: 25

3.2.3 Statistical distribution of $\boldsymbol{H}$ partially known and statistical distribution of $\boldsymbol{G}$ known: 26

3.2.4 Statistical distribution of both $\boldsymbol{H}$ and $\boldsymbol{G}$ partially known: 28

3.3 Conclusion 30

4 SISO with multiple transmissions **31**

4.1 System Model and Problem Statement 31

4.1.1 System Model 31

4.1.2 Problem Statement 33

4.2 Likelihood function expressions for the different CSI cases 35

4.2.1 Realization of $\boldsymbol{h}$ known and statistical distribution of $\boldsymbol{g}$ partially known 38

4.2.2 Realization of $\boldsymbol{h}$ and statistical distribution of $\boldsymbol{g}$ known 39

4.2.3 Statistical distribution of both $\boldsymbol{h}$ and $\boldsymbol{g}$ partially known 41

4.2.4 Statistical distribution of $\boldsymbol{h}$ partially known and statistical distribution of $\boldsymbol{g}$ known 43

4.2.5 Statistical distribution of $\boldsymbol{h}$ known and statistical distribution of $\boldsymbol{g}$ partially known 44

4.2.6 Statistical distribution of both $\boldsymbol{h}$ and $\boldsymbol{g}$ known 46

4.3 Simulation Results 47

4.4 Conclusion 54

5 SIDO with multiple transmissions **57**

5.1 Introduction 57

5.2 System Model and Problem Statement 58

5.3 Likelihood function expressions for the different CSI cases 62

5.3.1 Statistical distribution of both $\boldsymbol{H}$ and $\boldsymbol{G}$ partially known: 62

5.3.2 Statistical distribution of $\boldsymbol{H}$ partially known and statistical distribution of $\boldsymbol{G}$ known: 65

5.3.3 Statistical distribution of $\boldsymbol{H}$ known and statistical distribution of $\boldsymbol{G}$ partially known: 67

5.3.4 Statistical distribution of both $\boldsymbol{H}$ and $\boldsymbol{G}$ known: 69

5.4 Simulation Results 71

5.5 Conclusion 76

6 Conclusions and Future Work **78**

APPENDICES **80**

A **81**

A.1 Proof of Theorem 3.1 81

A.2 Proof of Theorem 3.2 84

A.3 Proof of Theorem 3.3 86

A.4 Proof of Theorem 3.4 88

A.5 Proof of Lemma 3.1 92

A.6 Proof of Theorem 3.5 93

B **98**

B.1 Proof of Theorem 4.1 98

B.2 Proof of Theorem 4.2 100

B.3 Proof of Theorem 4.3 102

B.4 Proof of Theorem 5.1 105

B.5 Proof of Lemma 4.1 108

B.6 Proof of corollary 4.5 109

C **113**

C.1 Proof of Theorem 5.1 113

C.2 Proof of Lemma 5.1 124

References **128**

List of Figures

2.1 Frequency Domain Overlap 11

3.1 System Model. 20

4.1 System Model. 32

4.2 $T=4$, $k_g=0$ and various values of k_h. 50

4.3 $T=2$, $k_h=5$ and various values of k_g. 51

4.4 $T=4$, $k_h=5$ and various values of k_g. 52

4.5 $T=6$, $k_h=5$ and various values of k_g. 53

4.6 $T=4$, $k_h=5$ and various values of k_g. 54

4.7 $T=4$, SJNR = 10 dB and various values of k_g and k_h. 55

4.8 $T=4$, SJNR = 20 dB and various values of k_g and k_h. 56

5.1 System Model. 59

5.2 $T=4$, $k_g=0$ and various values of k_h. 73

5.3 $T=4$, $k_h=0$ and various values of k_g. 74

5.4 Detection performance of double receive antenna vs. single receive antenna for $T = 4$ and various values of k_h and k_g. 75

5.5 Detection performance for different data rates and various values of T, $k_h = 0$ and $k_g = 0$. 76

List of Symbols

$*$	The linear convolution operator
$\mathbf{0}_N$	A column vector of N zeros
$\mathbf{1}_N$	A column vector of N ones
$\boldsymbol{G}$	The random jammer-receiver vector channel for a multiple-antenna receiver
$\boldsymbol{g}$	The random jammer-receiver scalar channel for a single-antenna receiver
$\boldsymbol{H}$	The random transmitter-receiver vector channel for a multiple-antenna receiver
$\boldsymbol{h}$	The random transmitter-receiver scalar channel for a single-antenna receiver
$\boldsymbol{V}$	Random vector representing the jamming signal samples
$\boldsymbol{X}$	Random vector representing the transmitted symbols
$\boldsymbol{Y}$	Random vector representing the received signal
$\boldsymbol{Z}$	Random vector representing the additive white Gaussian noise
$\Gamma(\cdot)$	The gamma function

$\mathrm{Im}\{z\}$	The imaginary part of a complex variable z
$\measuredangle z$	The phase of a complex variable z
$\otimes$	The Kronecker product
$\mathrm{Re}\{z\}$	The real part of a complex variable z
$\lvert M \rvert$	The determinant of matrix M
$\lVert U \rVert$	The Euclidean norm of vector U
$E\{\cdot\}$	The expectation operator
G	A given realization of $\boldsymbol{G}$
H	A given realization of $\boldsymbol{H}$
h	A given realization of $\boldsymbol{h}$
$I_\nu(\cdot)$	The modified Bessel functions of the first kind of order ν
I_N	The Identity matrix matrix of order N
$K_\nu(\cdot)$	The modified Bessel functions of the second kind of order ν
$M^\dagger$	The Hermitian transpose of matrix M
M^{-1}	The inverse of matrix M
R	Number of receive antennas
T	Transmitted symbol length
V	A given realization of $\boldsymbol{V}$

$vec(M)$ The vectorized version of matrix M

X A given realization of $\boldsymbol{X}$

Y A given realization of $\boldsymbol{Y}$

z^* The conjugate of a complex variable z

${}_1\tilde{F}_2(\cdot;\cdot,\cdot;\cdot)$ The regularized generalized hypergeomtric function

${}_1F_1\left(\cdot;\cdot;\cdot\right)$ The confluent hypergeometric function of the first kind

Chapter 1

Introduction

This chapter exposes the fatality of jamming attacks against wireless communication networks; hence, justifies the effort of combating jamming, and highlights the optimality condition of ML detection.

1.1 Fatality of jamming attacks

Services based on wireless communications became an essential part of everyday life. The disruption of these services can cause discomfort, erupt chaos, claim lives, and lead to catastrophic losses. The open nature of the wireless channel makes it vulnerable to many security attacks like jamming and eavesdropping. While eavesdropping threatens the confidentiality of wireless services, jamming threatens the existence of these services and can lead to denial of service (DoS) [1–3]. The wireless communication networks that can be targeted by jamming attacks including:

- Cellular wireless networks including legacy cellular networks like the Global System

for Mobile Communications (GSM) and the Universal Mobile Telecommunications System (UMTS) networks [4] [5], the widely used Long Term Evolution (LTE) networks [6], and the evolving fifth Generation (5G) networks [7] [8] which are anticipated to provide the communication infrastructure for public safety, disaster relief, and rescue operations.

- Wireless Local Area Networks (WLAN) [9] that are widely used for providing connectivity to internet gateways, printers and other shared resources in homes, office buildings, schools, universities, hospitals, malls, airports, and so on.

- Low Power Wide Area Networks (LPWANs) [10] which is a group of technologies that have many attractive features such as operating at low cost, having high power efficiency, connecting large number of low rate battery-powered devices over up to 5 kilometers in urban zones and 40 kilometers in rural zones. These features make LPWANs applicable in **smart agriculture** through monitoring of cattle, soil moisture, levels of chemicals in soil; **smart city** through smart street lights, parking, waste management, metering, flood sensors; **smart healthcare** through tracking of patients with Alzheimer's and dementia, monitoring of refrigerators storing vaccines, medications, blood, and so on.

- Low-Rate Wireless Personal Area Networks (LR-WPANs) and ZigBee Networks [11–13] which are employed in industrial control, environmental monitoring, health date collection, home automation, intruder and smoke warning, indoor localization, and disaster response.

- Bluetooth Networks [14] that are commonly used to connect computers to peripherals like mice, keyboards, and printers; for data transfer between smart devices at

homes and in offices; for data collection in hospitals; for remote control of smart appliances; and for home infotainment and in-car infotainment systems; for monitoring and keeping records of vital signs of patients and sending alarm signals when it is necessary in order to save lives.

- Wireless Sensor Networks (WSN) [15] which are used for forest fire detection and monitoring, long-duration and large-scale environmental monitoring, structural health monitoring, mechanical stress monitoring after earthquakes, smart agriculture, machine surveillance and preventive maintenance, etc.

- Cognitive Radio Networks (CRN) [16] which is a spectrum sharing technology that enables unlicensed users to coexist with what called incumbent users in licensed spectrum without generating interference. CRN anticipated applications include device-to-device (D2D) communications in disaster relief [17], smart grid networks, public safety broadband networks, and patient monitoring in wireless medical networks [18].

- Vehicular Ad hoc Networks [19] that are anticipated to be a key part of the Intelligent Transportation System (ITS) [20]. In addition to offering internet access to passengers and assisting drivers through providing traffic updates and road conditions notifications, VANETs could save lives by reducing the number of car accidents through the Cooperative Collision Warning (CCW) systems that use inter-vehicle wireless transmissions for applications such as Forward Collision Warning (FCW), Lane Change Assistance (LCA), and Electronic Emergency Brake Light (EEBL) that informs the driver when other vehicles ahead of him suddenly brake even though they might be obscured by other vehicles [21].

- Global Positioning Systems (GPS) [22] that are widely used in various fields of everyday life including navigation in land, marine, and aeronautics; public safety and

disaster relief; survey and mapping; precise agriculture; herd monitoring and tracking; tracking for law enforcement; preservation of endangered species; outdoor recreation; communication systems; and so on.

- Radio Frequency Identification (RIFD) systems [23] which are used for product tracking; inventory monitoring; toll road payment; storing information in passports and credit cards; e-voting systems [24]; and so on.

- Internet-of-Things (IoT) systems [25] that are for heart rate and glucose monitors in health care applications; controlling appliances and security related applications in smart homes; traffic monitoring, waste control, and water management in mart cities; monitoring and controlling the climate inside greenhouse in agriculture; quality control and inventory management in industrial applications, etc.

The ever-increasing reliance of individuals and societies' daily lives on services provided by wireless communication systems, and the low cost and simplicity of launching jamming attacks aggravate the threat of jamming and emphasizes the need for improving the resilience of these systems to such attacks. Improving the jamming immunity of wireless communication systems can save lives, prevent losses, enhance security, and increase productivity.

1.2 Optimality of Maximum Likelihood Detection

Let $\boldsymbol{y}$ be a sample of the signal resulting for transmitting symbol $\boldsymbol{x}$ through channel $\boldsymbol{h}$ mingled with an additive white noise sample $\boldsymbol{n}$, i.e.,

$$\boldsymbol{y} = \boldsymbol{h}\boldsymbol{x} + \boldsymbol{n}. \tag{1.1}$$

Detection is the process of determining the transmitted symbol, $\boldsymbol{x}$, based on a set of sufficient statistics extracted for the received sample, $\boldsymbol{y}$. There are many detection schemes that differ in terms of the extracted statistics, decision rule, complexity, and performance. Examples of the widely used detectors include the Maximum A Posteriori probability detector (MAP), the maximum likelihood detector (ML), the Zero Forcing detector (ZF), and the Minimum Mean Squared Error detector (MMSE). Among all detection schemes, MAP detector is shown to be the one that minimizes the probability of detection error, i.e., it is the optimal detection rule [26]. However, when the transmitted symbols are equally likely, it is proven that the MAP detector and the ML detector are equivalent. For the sake of completeness, we share the proof.

To minimizes the probability of erroneous detection decisions, the optimal detector must maximize the probability of correct detection decision for each received sample $\boldsymbol{y} = y$. Maximizing the probability of correct detection decision for each $\boldsymbol{y} = y$ is achieved by deciding in favor of the constellation symbol x^* that has the largest *a posteriori* probability, i.e.,

$$\begin{aligned} \hat{x} &= \arg\max_{x \in \mathcal{C}} P_r(x|y) \\ &= \arg\max_{x \in \mathcal{C}} \frac{P_r(x)P_r(y|x)}{P_r(y)}, \end{aligned} \tag{1.2}$$

where $\mathcal{C}$ is the symbol constellation, $P_r(u)$ is the probability of $\boldsymbol{u} = u$, $P_r(u|v)$ is the probability of $\boldsymbol{u} = u$ conditioned on that $\boldsymbol{v} = v$. Since $P_r(y)$ is constant, equation (1.2) can be written as:

$$\hat{x} = \arg\max_{x \in \mathcal{C}} P_r(x)P_r(y|x) \tag{1.3}$$

If all symbols are equally likely, i.e., $P_r(x_i) = \dfrac{1}{M}$, where M is the constellation size,

and $i \in \{1, \ldots, M\}$, equation (1.3) yields:

$$\hat{x} = \arg\max_{x \in \mathcal{C}} P_r(y|x) \tag{1.4}$$

i.e., when the constellation symbols are equally likely, the optimal decision rule is to decide in favor of the constellation symbol, x, that maximizes the likelihood of the received sample, y.

1.3 Contributions

The contributions of the work presented in this thesis are the following:

1. Deriving the likelihood expressions and developing the ML detector for a scenario wherein a single-antenna transmitter sends complex one-dimensional symbols to a multi-antenna receiver. The transmission is jammed by a single-antenna proactive jammer continuously emitting a zero-mean complex Gaussian signal over an unknown complex Gaussian channel. The ML detector is developed for cases corresponding to whether the receiver has either full CDI, or partial CDI about the transmitter channel. The jammer CDI is either partially or fully available at the receiver. The advantage of using the exact ML detector over the Gaussian approximation ML detector is investigated experimentally.

2. Deriving the likelihood expressions and developing the ML detector for a scenario wherein a single-antenna transmitter sends complex multi-dimensional symbols to a single-antenna receiver. The transmission occurs in the presence of a single-antenna jammer emitting, proactively and continuously, a zero-mean complex Gaussian signal

over an unknown complex Gaussian channel. The ML detector is developed for cases corresponding to whether the receiver has full CSI, full CDI, or partial CDI about the transmitter channel. The jammer CDI is either partially or fully available at the receiver. Moreover, the contributions for this this scenario include:

- Identifying cases where the non-Gaussian signals resulting from the jammer's transmission can be approximated by Gaussian signals without affecting the efficacy of the ML detector; and showing, analytically and numerically, the equivalence of the exact and Gaussian approximation ML detectors.
- Showing experimentally the advantage of the exact ML detector over the Gaussian approximation one for cases in which the two ML detectors are not equivalent.

3. Deriving the likelihood expressions and developing the ML detector for a scenario wherein a single-antenna transmitter sends complex multi-dimensional symbols to a double-antenna receiver. The transmission occurs in the presence of a single-antenna jammer emitting, proactively and continuously, a zero-mean complex Gaussian signal over an unknown complex Gaussian channel. The ML detector is developed for cases corresponding to whether the receiver has full CDI or partial CDI about the transmitter channel. The jammer CDI is either partially or fully available at the receiver. The advantage of using the exact ML detector over the Gaussian approximation ML detector is shown experimentally.

1.4 Publications

Some of the work presented in this thesis is published in the following papers:

1. K. A. Almahorg and R. H. Gohary, "Maximum Likelihood Detection in the Presence of Non-Gaussian Jamming," in IEEE Transactions on Signal Processing, vol. 68, pp. 5722-5735, 2020.

2. K. A. Almahorg and R. H. Gohary, "Optimal Detection in the Presence of Non-Gaussian Jamming," ICASSP 2021, pp. 4835-4839.

3. K. Almahorg and R. Gohary, "Maximum Likelihood Detection in Single-Input Double-Output Non-Gaussian Barrage-Jammed Systems," Submitted to the IEEE Trans. Signal processing, March 2022.

4. K. Almahorg and R. Gohary, "Optimal Detection in Barrage-Jammed Single-Input Double-Output Systems," Submitted to IEEE Globecom 2022 Conference.

1.5 Outline

This thesis is organized as follows. Chapter 2 reviews main techniques in anti-jamming, and highlights the challenges of optimal detection in the presence of jamming. Chapter 3 is dedicated to ML detection in barrage-jammed Single-Input Multiple-Output (SIMO) system using one-dimensional complex constellation, Chapter 4 deals with ML detection in a barrage-jammed Single-Input Single-Output (SISO) system using multi-dimensional complex constellation. Chapter 5 focuses on ML detection in barrage-jammed Single-Input Double-Output (SIDO) system using multi-dimensional complex constellation. Finally, Chapter 6 concludes this thesis and suggests potential future work directions.

Chapter 2

Literature Review

This chapter defines the different classes of jamming attacks, surveys anti-jamming techniques, introduces the challenges of optimal detection in the presence of jamming, and reviews previous works.

2.1 Jammer's Classes

Degrading the signal to noise ratio (SNR) at the receiver can disrupt wireless services; hence, the jammer could use a simple transmitter emitting random signals, e.g. noise generator, to launch his attack. Such a jammer is protocol-neutral, i.e., it can impact the performance of any wireless system, and can hit many different systems at the same time. Besides using simple noise generators, with the availability of inexpensive software-defined radio (SDR) devices such as the Universal Software Radio Peripheral (USRP) [27], jammers could build programmable systems to launch adaptive attacks [15] [28]. With the advancements in smartphone technology, jamming attacks can also be launched using off-

the-shelf smartphones [29]. Jamming attacks that use programmable devices are usually protocol-aware, i.e., they have prior knowledge about the communication protocols of the target system. Protocol-aware jamming attacks exploit vulnerabilities of communication protocols and procedures to disrupt wireless services. The protocols targeted by jammers include, but not limited to, the medium access control protocol (MAC) [30], [31], timing synchronization procedures [32], [33], frequency synchronization procedures [34–36], channel estimation procedures, [37–40], and the beamforming procedures [41].

Jammers can be classified according to the time at which they launch their attacks into [3]:

- **Proactive Jammers**: a proactive jammer attacks whether there is communication activity or not. A proactive jammer can be:
  - **Constant jammer** that attacks continuously.
  - **Random jammer** that attacks at randomly selected points in time.
- **Reactive Jammers**: a reactive jammer does not attack unless a communication activity is taking place; hence, it is more power efficient than the proactive jammer. A reactive jammer can be:
  - **Adaptive jammer** that adjusts its power according to the power of the legitimate signal.
  - **Intelligent jammer** that tailors its attack according to the type of the systems involved in the legitimate communication activity.
  - **Selective jammer** that targets a specific legitimate transmitter.
  - **Deceptive jammer** that uses traditional modulation techniques or sends regular packets to disguise as a legitimate user.

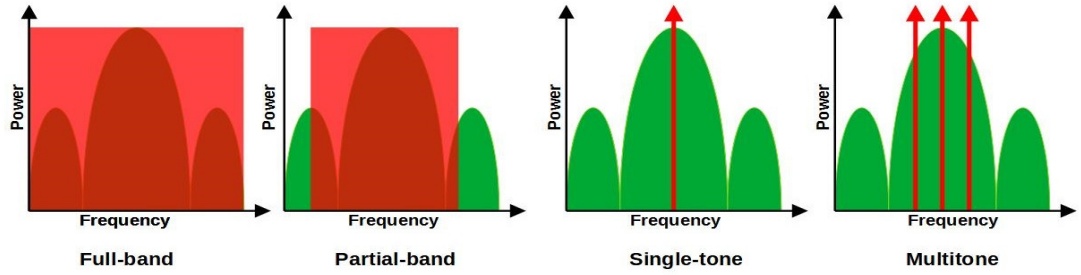

Figure 2.1: Frequency Domain Overlap

As depicted in Figure 2.1, Jammers can also be classified according to the jammed portion of the target system bandwidth, or the number of jammed subcarriers, into [42]:

- **Full-band** or **barrage jammer** that emits a white Gaussian noise occupying the entire bandwidth of the target system. However, barrage jamming is known for its high power consumption especially if the target system uses wide frequency band.
- **Partial-band jammer** that emits a signal occupying a frequency band that overlaps partially with the frequency band occupied by the legitimate transmission.
- **Single-tone jammer** that hits a single subcarrier of the set of subcarriers used by the target system. The jammer can shift its power rapidly from one subcarrier to another to have a more destructive effect. The latter jammer is called **Sweep jammer**.
- **Multitone jammer** that hits multiple subcarriers of the set of subcarriers used by the target system.

In this thesis, we assume that the jammer is a proactive constant barrage jammer since barrage jamming is the optimal jamming attack if the jammer has no prior knowledge of the target system [43].

2.2 Anti-jamming

Anti-jamming refers to the defense mechanisms aiming to eliminate or, at least, alleviate the effects of jamming attacks. Jamming avoidance is a mainstream anti-jamming mechanism in which the legitimate parties try to keep the jammer unaware of the ongoing communication activity or, at least, try to evade the jamming signal in time, frequency, or space. A reactive jammer can be avoided by transmitting a hard-to-detect signal, e.g., a low power Direct-Sequence spread spectrum (DSSS) signal or a short duration Ultra Wide Band (UWB) signal. In contrast, a partial-band proactive or random jammer can be avoided by using Frequency Hopping Spread Spectrum (FHSS) to evade the jammed frequency bands [44]. The FHSS hopping pattern and the DSSS chipping sequence can be generated using a secret key shared by the transmitter and the receiver; however, the key management in the wireless environment is challenging, especially under jamming. Uncoordinated Frequency Hopping (UFH) and DSSS (UDSSS) were proposed [45], [46] to solve the key management problem. The transmitter and the receiver randomly hop over many channels before they can communicate. Once they land on the same channel, they exchange the hopping pattern or chipping sequence. To speed up the algorithm's convergence, either the transmitter or the receiver has to hop faster than the other (e.g., 20 times faster). However, UFH is only applicable for point-to-point communication. For broadcast communication, the authors of [47] introduced the Randomized Differential DSSS (RD-DSSS) in which chipping sequences are randomly chosen from a publicly known pool of sequences. FHSS and DSSS can cope with partial band jamming; however, they can not cope with powerful broadband jamming attacks; moreover, FHSS and DSSS result in inefficient spectrum utilization.

Spatial retreat is a jamming avoidance technique in which the area plagued by the

jamming signal is evaded; however, this technique can be used only by mobile transmitters and receivers [48], [49]. The jammer can be avoided in space using beamforming techniques of multiple input multiple output (MIMO) systems. A receiver equipped with multiple antenna can nullify the jamming signal by steering a null of its antenna pattern towards the direction of arrival (DOA) of the jamming signal [50–53]. Similarly, a transmitter equipped with a sufficient number of antennas can steer a null of its antenna pattern towards a reactive jammer to keep him oblivious to the communication activity taking place. However, due to side-lobes or blunt main-lobe, there might be some leakage that the reactive jammer can sense. To solve this problem, the transmitter can beamform a decoy signal of a different frequency band towards the jammer. The decoy signal misleads the jammer to focus its power away from the band occupied by the legitimate signal [54], [55].

Jamming can also be avoided in signal space. The authors of [56] proposed a precoding technique that allows the transmitter's signal to avoid the subspace spanned by the jamming signal, i.e., to be orthogonal to it at the receiver. However, in addition to being inapplicable to single antenna systems, this technique requires high-quality channel state information at the transmitter (TCSI) and knowing some jammer channel properties. In mobile scenarios, e.g., drone transceivers and jammers, acquiring and updating this information is challenging. It was shown in [57] that knowing the jammer channel is unnecessary; it is sufficient to know the jammer's signal direction. The receiver can achieve this by taking the ratio of the jammer's signal at two receiver's antennas. Based on the work in [57], the authors of [58] presented a mechanism to estimate and track the transmitter's channel and the jammer's signal direction iteratively and alternatively. In addition to the preamble pilots, more pilots are embedded randomly in the data frame in this mechanism. Assuming a reactive jammer, the first few preamble pilots will not be jammed; hence, the receiver can use them to estimate the transmitter's channel. Then, the receiver

uses this estimate to remove the effect of the embedded pilots from the received signal and estimate the jammer's signal direction. Finally, the receiver sends back the estimate of the jammer's signal direction to the transmitter to use it for precoding purposes. The anti-jamming resilience of this work relies mainly on two assumptions. The first assumption is that randomizing the embedded pilot locations makes it difficult for the reactive jammer to hinder the channel estimation procedure. And the second assumption is that the jammer's channel remains constant between two consecutive embedded pilots; therefore, this work is not applicable in highly mobile systems, e.g., UAV and VANETs. The effect of pilot randomization on the jamming resilience of Orthogonal Frequency Division Multiplexing (OFDM) systems was investigated in [59]. It was found that Pilot randomization improves resilience when signal to jammer power ratio (SJR) is low; however, at a high SJR (SJR $\geqslant$ 5 dB), it degrades resilience. Differential encoding and jammer's signal direction are employed in [60] to combat a single-antenna constant jammer or a reactive jammer targeting single-antenna transmitter and double-antenna receiver. The authors of [61] proposed a blind, Space-Time Adaptive Processing (STAP) algorithm for combating jamming in GPS systems. They used a space-time adaptive filter whose weights form a matrix projecting onto a subspace orthogonal to the jamming signal. Similarly, the authors of [62] proposed a two-stage blind adaptive algorithm to suppress jamming in GPS systems. In the first stage, the received signal is projected onto the jamming signal's orthogonal complement space; then, in the second stage, the so-called CLEAN [63] algorithm is used to iteratively estimate the DOAs of the GPS signals to build the beamforming vector.

Frequency domain filtering using Adaptive Notch Filters (ANFs) is a classical technique for the excision of continuous-wave narrowband interference and jamming signals [64, 65]. The authors of [66] proposed an anti-jamming system composed of a cascade of ANFs. Each ANF is a second-order Infinite Impulse Response (IIR) digital filter [67] designed in

the time domain to detect, estimate, and block a single-tone continuous jamming signal. To improve the ANF ability to detect and cancel jamming, the authors of [68] proposed an enhanced Sort-Time Fourier Transform (STFT) [69] called multiple STFT (MSTFT) is to increase the accuracy of time-frequency resolution of the GPS signal.

A friendly eavesdropper who hears the jamming signal and describes it to the receiver on an orthogonal channel can reduce the jammer's impact [70]. Another option for the transmitter is to adjust its transmission power and transmission rate to improve the SNR at the receiver [71]; however, increasing the transmission power may increase the risk of eavesdropping attacks [72]. Game theory is a suitable tool used to model the interactions among the transmitter and the jammer and facilitate making optimal decisions related to power allocation, rate adjustment, and frequency hopping [73–75].

Optimal detection in the presence of jamming can alleviate the harmful effect of jamming; hence, it can be considered an anti-jamming technique. Maximum likelihood detection (ML) is well known to minimize the probability of detection error given that all symbols of the transmitter's alphabet are equally likely [26]; however, ML detection performance depends heavily on the accuracy of the likelihood expressions. As mentioned in the previous section, in this thesis, we consider a proactive constant barrage jammer. The overwhelming majority of existing literature models the barrage jamming signal at the receiver as additive Gaussian noise, e.g., [43, 70, 73, 76–78]. While this modeling is justifiable when both the jammer and the receiver are stationary, its accuracy in mobile communication scenarios is questionable. In the next section, we expose the invalidity of this modeling.

2.3 Optimal Detection in the Presence of Jamming

The assumption that the jammer's transmissions induce Gaussian-distributed signal at the receiver is valid when the jammer transmits Gaussian-distributed signals and the CSI of the channel between the jammer and the receiver is known. However, knowing this CSI is generally challenging since the jammer does not send pilots to train the receiver, nor does it send prescribed waveforms. The problem is compounded when either the jammer, the receiver, or both are mobile or air-borne, e.g., VANET or UAVs. In such a case, acquiring and updating the CSI of the channel between the jammer and the receiver is impractical [79], calling the Gaussian model of the jamming signal observed by the receiver into question. To see this, we note that when the jammer is mobile, the channel between the jammer and the receiver constitutes a random process, whereby the signal emitted by the jammer at any time instant is scaled by a complex random variable that alters both the amplitude and the phase of this signal. In this case, the distribution of the jammer's signal observed at the receiver is not Gaussian, but rather the distribution corresponding to the product of a Gaussian random variable and a random variable that depends on the fading model of the channel between the jammer and the receiver. For instance, if the channel between the jammer and the receiver is Rayleigh or Rician fading, the jamming signal at the receiver has the distribution of the product of two Gaussian random variables, which is not Gaussian [80,81]. Knowing the received jamming signal distribution is essential for deriving the exact likelihood expressions of the entire received signal. The likelihood expressions are fundamental to detectors' design and the computation of the probability of detection error. For example, consider a single input single output system in which a transmitter communicates with a receiver over a block fading channel in the presence of a proactive constant barrage jammer. The transmitter to receiver channel is denoted by $\boldsymbol{h}$, and the

jammer to receiver channel is denoted $\boldsymbol{g}$. Both channels are assumed to remain constant during the transmission of a block of T data symbols and take independent realizations in subsequent blocks. The transmitted signal is denoted by $\boldsymbol{X} \in \mathbb{C}^T$ and is drawn from a T-dimensional constellation $\mathcal{C}$. The jammer's signal is denoted by $\boldsymbol{V} \in \mathbb{C}^T$, and the additive noise at the receiver is denoted by $\boldsymbol{Z} \in \mathbb{C}^T$. The corresponding received signal is denoted by $\boldsymbol{Y} \in \mathbb{C}^T$. Using this notation we have,

$$\boldsymbol{Y} = \boldsymbol{h}\boldsymbol{X} + \boldsymbol{Z} + \boldsymbol{g}\boldsymbol{V} \tag{2.1}$$

We see from equation (2.1) that the received signal vector, $\boldsymbol{Y}$, is the sum of three vectors: the transmitted symbols vector, $\boldsymbol{X}$, shaped by the transmitter's channel, $\boldsymbol{h}$, the receiver's additive complex Gaussian noise vector, $\boldsymbol{Z}$, and the jamming signal samples vector, $\boldsymbol{V}$, shaped by the jammer's channel, $\boldsymbol{g}$. Given the transmitted symbols vector, the first two vectors on the right hand side of (2.1) are complex Gaussian, and so is their sum by virtue of Gaussianity [82]. However, the third vector is non-Gaussian since the product of two independent real or complex Gaussian random variables is non-Gaussian [80], [81]. Therefore, the exact likelihood expression is the probability density function (pdf) of the sum of a complex Gaussian vector and a non-Gaussian one. Since the pdf of the sum of two random vectors of any dimension results from the convolution of their respective pdfs [83], the derivation of the non-Gaussian pdf of the vector $\boldsymbol{g}\boldsymbol{V}$ is crucial to the derivation of the exact likelihood expression of the received signal vector, $\boldsymbol{Y}$.

The pdfs of the distribution of the product of two real or complex Gaussian random variables have been obtained in prior works, e.g., [84–86], In particular, the pdf of the inner product of two real Gaussian random vectors is given in [84]. In a complementary fashion, the characteristic function of the inner product of two complex Gaussian random vectors

was derived in [85]. However, this characteristic function does not yield a closed form expression for the corresponding pdf; the latter can be obtained by numerical evaluation of the inverse Fourier transform of the characteristic function. The derivation of the joint pdf of the magnitude and phase of the product of two independent complex Gaussian scalars is considered in [86], and the pdf corresponding to the sum of a complex Gaussian scalar and the product of two complex Gaussian scalars was derived in [87]. We extend the work in [86] by deriving the pdf of the product of a complex Gaussian vector and a complex Gaussian scalar. We also extend the work in [87] by deriving the pdf of the sum of a complex Gaussian vector and the product of a complex Gaussian scalar and a complex Gaussian vector [88].

Chapter 3

SIMO with single transmission

3.1 System Model and Problem Statement

3.1.1 System Model

We consider the system depicted in Figure 3.1 which is a single input multiple output (SIMO) system in which a single antenna transmitter communicates with a multiple antenna receiver in the presence of a single antenna proactive constant jammer. The number of receiver antennas is $R \geqslant 1$. The vector channel between the transmitter and the receiver is denoted by $\boldsymbol{H}$, and the vector channel between the jammer and the receiver is denoted by $\boldsymbol{G}$. The transmitted symbol is denoted by $\boldsymbol{x} \in \mathbb{C}$. The jamming signal sample is denoted by $\boldsymbol{v} \in \mathbb{C}$, and the additive noise vector is denoted by $\boldsymbol{Z} \in \mathbb{C}^R$. The corresponding received signal is denoted by $\boldsymbol{Y} \in \mathbb{C}^R$. Using this notation we have,

$$\boldsymbol{Y} = \boldsymbol{H}\boldsymbol{x} + \boldsymbol{G}\boldsymbol{v} + \boldsymbol{Z}. \tag{3.1}$$

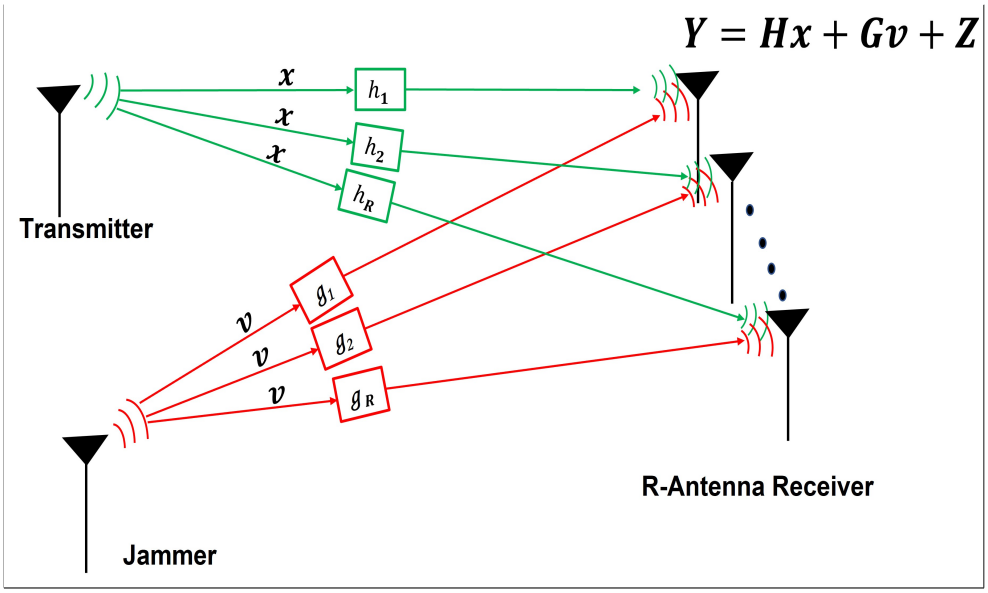

Figure 3.1: System Model.

The transmitter channel components are assumed to be *i.i.d.* as well as the components of the jammer channel. The i-th component of the transmitter channel, $\boldsymbol{h}_i$, and the l-th component of the jammer channel, $\boldsymbol{g}_l$, i and $l \in \{1, 2, \ldots, R\}$, are modeled as complex Gaussian random variables with means μ_h and μ_g, and variances σ_h^2 and σ_g^2 respectively, i.e., $\boldsymbol{h}_i \sim \mathcal{CN}(|\mu_h| e^{\jmath\theta_{h_i}}, \sigma_h^2)$ and $\boldsymbol{g}_l \sim \mathcal{CN}(|\mu_g| e^{\jmath\theta_{g_l}}, \sigma_g^2)$, where θ_{h_i} and θ_{g_l} are the phases of the means of $\boldsymbol{h}_i$ and $\boldsymbol{g}_l$. These phases are assumed to be *i.i.d.* uniformly distributed in $[0, 2\pi)$. Hence, $\boldsymbol{H} \sim \mathcal{CN}(\mu_h \mathbf{1}_R, \sigma_h^2 I_R)$ and $\boldsymbol{G} \sim \mathcal{CN}(\mu_g \mathbf{1}_R, \sigma_g^2 I_R)$. The jamming signal sample, $\boldsymbol{v}$, is assumed to be zero-mean, complex Gaussian random variable with known variance of σ_v^2; the covariance matrix of the additive white complex Gaussian noise is $\sigma_Z^2 I_R$ where σ_Z^2 is known, i.e., $\boldsymbol{v} \sim \mathcal{CN}(0, \sigma_v^2)$ and $\boldsymbol{Z} \sim \mathcal{CN}(0_R, \sigma_Z^2 I_R)$.

The transmitter, the jammer, and the receiver might be mobile or airborne, e.g., V2V and UAV communication systems. Hence, both $\boldsymbol{H}$ and $\boldsymbol{G}$ are assumed to subject to fading that is either Rayleigh or Rician process. The fading processes of $\boldsymbol{H}$ and $\boldsymbol{G}$ are statistically

independent. When the transmitter-receiver vector channel, $\boldsymbol{H}$, is Rayleigh fading, i.e., its mean is zero, we will consider the case where the receiver only knows the distribution of $\boldsymbol{H}$ (full CDI). When $\boldsymbol{H}$ is Rician fading, which can be the case when either the transmitter, the receiver, or both are airborne, we assume that the receiver knows σ_h and the relative strength of the LOS component of $\boldsymbol{H}$ which is given by $k_h = \frac{|\mu_h|}{\sigma_h}$, i.e., partial CDI.

For each of the two aforementioned cases, we consider two scenarios. In the first scenario, $\boldsymbol{G}$ has a zero mean, i.e., Rayleigh fading, and the receiver knows σ_g, and in the second scenario, $\boldsymbol{G}$ is Rician fading and the receiver knows both σ_g and $k_g = \frac{|\mu_g|}{\sigma_g}$. Hence, a total of four cases corresponding to four distinct scenarios are considered.

3.1.2 Problem Statement

This chapter aims to develop the ML detector for each of the four communication scenarios outlined above and repeated here for convenience.

1. *Statistical distribution of both $\boldsymbol{H}$ and $\boldsymbol{G}$ known:* The ML detector decides in favor of the constellation point $\hat{x}$ given by

$$\hat{x} = \arg\max_{x \in \mathcal{C}} p_{\boldsymbol{Y}|\boldsymbol{x}} \left(Y \middle| x; \sigma_h^2, \sigma_g^2 \right). \tag{3.2}$$

   In this case, the means of $\boldsymbol{H}$ and $\boldsymbol{G}$ components are zeros, i.e., neither the transmitter nor the jammer has an LOS component.

2. *Statistical distribution of $\boldsymbol{H}$ known and statistical distribution of $\boldsymbol{G}$ partially known:* The ML detector decides in favor of the constellation point $\hat{x}$ given by

$$\hat{x} = \arg\max_{x \in \mathcal{C}} p_{\boldsymbol{Y}|\boldsymbol{x}} \left(Y \middle| x; |\mu_g|, \sigma_g^2, \sigma_h^2 \right). \tag{3.3}$$

In this case, the means of $\boldsymbol{H}$ components are zeros, and the of phases of the means of $\boldsymbol{G}$ components are unknown and each component has an LOS.

3. *Statistical distribution of $\boldsymbol{H}$ partially known and statistical distribution of $\boldsymbol{G}$ known:* The ML detector decides in favor of the constellation point $\hat{x}$ given by

$$\hat{x} = \arg\max_{x \in \mathcal{C}} p_{\boldsymbol{Y}|\boldsymbol{x}} \left(Y \middle| x; |\mu_h|, \sigma_h^2, \sigma_g^2 \right). \tag{3.4}$$

Complementary to the previous case, in this case, the means of $\boldsymbol{G}$ components are zeros, and the of phases of the means of $\boldsymbol{H}$ components are unknown, and each component has an LOS.

4. *Statistical distribution of both $\boldsymbol{H}$ and $\boldsymbol{G}$ partially known:* The ML detector decides in favor of the constellation point $\hat{x}$ given by

$$\hat{x} = \arg\max_{x \in \mathcal{C}} p_{\boldsymbol{Y}|\boldsymbol{x}} \left(Y \middle| x; |\mu_h|, \sigma_h^2, |\mu_g|, \sigma_g^2 \right). \tag{3.5}$$

In this case, the phases of the means of $\boldsymbol{H}$ and $\boldsymbol{G}$ components are unknown, and every one of these components has an LOS component.

In the next section, we provide exact and approximate ML detection rules for each of the cases mentioned above.

3.2 Likelihood function expressions for the different CSI cases

To find the pdf of the received signal vector$Y$ given the transmitted symbol, $\boldsymbol{x}$, we notice that the received signal can be written as:

$$\boldsymbol{Y} = \boldsymbol{U} + \boldsymbol{J}. \tag{3.6}$$

where

$$\boldsymbol{U} = \boldsymbol{H}\boldsymbol{x} + \boldsymbol{Z}. \tag{3.7}$$

and

$$\boldsymbol{J} = \boldsymbol{G}\boldsymbol{v}. \tag{3.8}$$

From (3.6), and using the principles of probability, we have:

$$f_{\boldsymbol{Y}|\boldsymbol{x}}(Y|x) = f_{\boldsymbol{U}|\boldsymbol{x}}(Y|x) * f_{\boldsymbol{J}}(Y), \tag{3.9}$$

Where $*$ is the convolution operator, $f_{\boldsymbol{U}|\boldsymbol{x}}(Y|x)$ is the pdf of $\boldsymbol{U}$ given $\boldsymbol{x}$, and $f_{\boldsymbol{J}}(Y)$ is the pdf of $\boldsymbol{J}$. We note that because both the noise, $\boldsymbol{Z}$, and $\boldsymbol{H}$ are assumed Gaussian, the distribution of $\boldsymbol{U}$ conditioned on $\boldsymbol{x} = x$ is also Gaussian. However, since $\boldsymbol{J}$ comprises the product of the complex Gaussian scalar $\boldsymbol{v}$ and the complex Gaussian vector $\boldsymbol{G}$, its distribution is not Gaussian and depends on the information available at the receiver about jammer's channel $\boldsymbol{G}$. In particular, if $\boldsymbol{G}$ has a zero-mean, then, the pdf of $\boldsymbol{J}$ is given by (4.12), (here, the number of retransmissions, T, will be replaced by the number of receiver antennas, R); however, if $\boldsymbol{G}$ has a non-zero mean, we have the following theorem.

Theorem 3.1. *Let $\boldsymbol{J} = \boldsymbol{G}\boldsymbol{v}$, where $\boldsymbol{G} \in \mathbb{C}^R$ is a Gaussian vector, i.e., $\boldsymbol{G} \sim \mathcal{CN}(\mu_g \mathbf{1}_R, \sigma_g^2 I_R)$, and v is a zero-mean Gaussian scalar, i.e., $\boldsymbol{v} \sim \mathcal{CN}(0, \sigma_v^2)$, where σ_g and σ_v are known scalars, and I_R is the size R identity matrix. $\forall\ i$ and $l \in \{1, 2, \ldots, R\}$, $i \neq l$, let $|\mu_{g_i}| = |\mu_{g_l}|$ be known scalars, whereas $\angle\mu_{g_i}$ and $\angle\mu_{g_l}$ are i.i.d. uniformly distributed in $[0, 2\pi)$. Then, the pdf of $\boldsymbol{J}$ is given by:*

$$f_{\boldsymbol{J}}(J) = \frac{\exp\left(-k_g^2 R\right)}{\pi^R\ \sigma_g^{2R}\sigma_v^{2R}} \int_0^\infty \prod_{i=1}^{R} I_0\left(\frac{2k_g|J_i|}{\sigma_g\sigma_v\sqrt{t}}\right) \exp\left(-t - \frac{|J|^2}{\sigma_g^2\sigma_v^2 t}\right) \frac{dt}{t^R} \tag{3.10}$$

where $k_g = \dfrac{|\mu_g|}{\sigma_g^2}$.

Proof. See Appendix A.1. □

Using Theorems 3.1 and 4.1, we now consider the cases outlined in Section 3.1.2.

3.2.1 Statistical distribution of both $\boldsymbol{H}$ and $\boldsymbol{G}$ known:

In this case the receiver knows that $\boldsymbol{H} \sim \mathcal{CN}(\mathbf{0}_R, \sigma_h^2 I_R)$ and $\boldsymbol{G} \sim \mathcal{CN}(\mathbf{0}_R, \sigma_g^2 I_R)$ where σ_h^2 and σ_g^2 are known. The exact likely function for this case is given in the following theorem:

Theorem 3.2. *Let $\boldsymbol{U} = \boldsymbol{H}\boldsymbol{x} + \boldsymbol{Z}$ and $\boldsymbol{J} = \boldsymbol{G}\boldsymbol{v}$, where $\boldsymbol{H} \sim \mathcal{CN}(\mathbf{0}_R, \sigma_h^2 I_R)$, $\boldsymbol{G} \sim \mathcal{CN}(\mathbf{0}_R, \sigma_g^2 I_R)$, and $\boldsymbol{Z} \sim \mathcal{CN}(\mathbf{0}_R, \sigma_Z^2 I_R)$ are random vectors, whereas $\boldsymbol{v} \sim \mathcal{CN}(0, \sigma_v^2)$ and $\boldsymbol{x} \in \mathbb{C}$ are random scalars. The scalars σ_h, σ_g, σ_Z, and σ_v are known. The likelihood function of $\boldsymbol{Y} = \boldsymbol{U} + \boldsymbol{J}$ conditioned on $\boldsymbol{x}$ is given by:*

$$f_{\boldsymbol{Y}|\boldsymbol{x}}(Y|x) = \frac{1}{\pi^R} \int_0^\infty \frac{1}{(\sigma_h^2|x|^2 + \sigma_z^2 + \sigma_g^2\sigma_v^2 t)^R} \exp\left(-t - \frac{|Y|^2}{\sigma_h^2|x|^2 + \sigma_z^2 + \sigma_g^2\sigma_v^2 t}\right)\ dt. \tag{3.11}$$

Proof. See Appendix A.2. □

Gaussian Approximation (Case 1)

Assuming that the signal $\boldsymbol{J}$ resulting form the jammer transmission is zero-mean Gaussian with covariance $\mathrm{E}\{\boldsymbol{J}\boldsymbol{J}^{\dagger}\} = \sigma_g^2\sigma_v^2 I_R$, it can be readily shown that the likelihood function of $\boldsymbol{Y}$ conditioned on $\boldsymbol{x}$ is given by:

$$\hat{p}_{\boldsymbol{Y}|\boldsymbol{x}}(Y|x) = \frac{1}{\pi^R(\sigma_h^2|x|^2 + \sigma_g^2\sigma_v^2 + \sigma_Z^2)^R} \exp\left(\frac{-|Y|^2}{(\sigma_h^2|x|^2 + \sigma_g^2\sigma_v^2 + \sigma_Z^2)^R}\right), \tag{3.12}$$

3.2.2 Statistical distribution of $\boldsymbol{H}$ known and statistical distribution of $\boldsymbol{G}$ partially known:

As given by equation (3.6), the received signal vector, $\boldsymbol{Y}$, is the sum of the two vectors, $\boldsymbol{U}$ and $\boldsymbol{J}$, that are given by equations (3.7) and (3.8). However, now, the jammer's vector channel, $\boldsymbol{G}$, has specular components that result in non-zero mean vector whose l-th component, $l \in \{1, 2, \ldots, R\}$, is given by:

$$\mu_{g_l} = k_g\sigma_g e^{\jmath\theta_{g_l}}, \tag{3.13}$$

where the k-factor of the jammer's channel, k_g, is assumed to be known, while the phases of the mean vector components, θ_{g_l}, $l \in \{1, 2, \ldots, R\}$, are assumed to be *i.i.d.* random scalars uniformly distributed in $[0, 2\pi)$. The exact likely function for this case is given in the following theorem:

Theorem 3.3. *Let* $\boldsymbol{U} = \boldsymbol{H}\boldsymbol{x} + \boldsymbol{Z}$ *and* $\boldsymbol{J} = \boldsymbol{G}\boldsymbol{v}$, *where* $\boldsymbol{H} \sim \mathcal{CN}(\boldsymbol{0}_R, \sigma_h^2 I_R)$, $\boldsymbol{G} \sim \mathcal{CN}(|\mu_g|e^{\jmath\boldsymbol{\theta}_g}, \sigma_g^2 I_R)$[1], *and* $\boldsymbol{Z} \sim \mathcal{CN}(\boldsymbol{0}_R, \sigma_Z^2 I_R)$ *are random vectors, whereas* $\boldsymbol{v} \sim \mathcal{CN}(0, \sigma_v^2)$

[1]Throughout this chapter, we use $e^{\jmath\boldsymbol{\theta}_c}$, $c \in \{h, g\}$, to represent a column vector whose i-th component is equal to $e^{\jmath\boldsymbol{\theta}_{c_i}}$

and $\boldsymbol{x} \in \mathbb{C}$ *are random scalars. The scalars* $|\mu_g|$, σ_h, σ_g, σ_Z, *and* σ_v *are known.* $\boldsymbol{\theta}_g$ *is a vector whose components are assumed to be i.i.d. scalars uniformly distributed in* $[0, 2\pi)$. *The likelihood function of* $\boldsymbol{Y} = \boldsymbol{U} + \boldsymbol{J}$ *conditioned on* $\boldsymbol{x}$ *is given by:*

$$f_{\boldsymbol{Y}|\boldsymbol{x}}(Y|x) = \frac{\exp\left(-k_g^2 R\right)}{\pi^R} \exp\left(-\frac{|Y|^2}{\sigma_h^2|x|^2 + \sigma_z^2}\right) \int_0^\infty \frac{\exp(-t)}{(\sigma_h^2|x|^2 + \sigma_z^2 + \sigma_g^2\sigma_v^2 t)^R} \times$$
$$\prod_{i=1}^{R} \sum_{n=0}^{\infty} \left(\frac{k_g^2(\sigma_h^2|x|^2 + \sigma_z^2)}{\sigma_h^2|x|^2 + \sigma_z^2 + \sigma_g^2\sigma_v^2 t}\right)^n \frac{1}{n!}\, {}_1F_1\left(n+1, 1, \frac{\sigma_g^2\sigma_v^2|Y_i|^2\ t}{(\sigma_h^2|x|^2 + \sigma_z^2 + \sigma_g^2\sigma_v^2 t)(\sigma_h^2|x|^2 + \sigma_z^2)}\right)\, dt, \tag{3.14}$$

where $k_g = \dfrac{|\mu_g|}{\sigma_g^2}$, *and* ${}_1F_1(\cdot,\cdot,\cdot)$ *is the confluent hypergeometric function of the first kind.*

Proof. See Appendix A.3. □

Gaussian Approximation (Case 2)

Assuming that the signal $\boldsymbol{J}$ resulting form the jammer transmission is zero-mean Gaussian with covariance $\mathrm{E}\{\boldsymbol{J}\boldsymbol{J}^\dagger\} = \sigma_g^2\sigma_v^2 I_R$, it can be shown that the likelihood function of $\boldsymbol{Y}$ conditioned on $\boldsymbol{x}$ is identical that given by 3.12.

3.2.3 Statistical distribution of $\boldsymbol{H}$ partially known and statistical distribution of $\boldsymbol{G}$ known:

Complementary to the previous case, the transmitter's vector channel, $\boldsymbol{H}$, has specular components that result in non-zero mean vector whose i-th component, $i \in \{1, 2, \ldots, R\}$, is given by:

$$\mu_{h_i} = k_h \sigma_h e^{\jmath\theta_{h_i}}, \tag{3.15}$$

where the k-factor of the transmitter's channel, k_h, is assumed to be known, while the phases of the mean vector components, θ_{h_i}, $i \in \{1, 2, \ldots, R\}$, are assumed to be *i.i.d.* random scalars uniformly distributed in $[0, 2\pi)$. The exact likely function for this case is given in the following theorem:

Theorem 3.4. *Let $\boldsymbol{U} = \boldsymbol{H}\boldsymbol{x} + \boldsymbol{Z}$ and $\boldsymbol{J} = \boldsymbol{G}\boldsymbol{v}$, where $\boldsymbol{H} \sim \mathcal{CN}(|\mu_h| e^{\jmath \boldsymbol{\theta}_h}, \sigma_h^2 I_R)$, $\boldsymbol{G} \sim \mathcal{CN}(\boldsymbol{0}_R, \sigma_g^2 I_R)$, and $\boldsymbol{Z} \sim \mathcal{CN}(\boldsymbol{0}_R, \sigma_Z^2 I_R)$ are random vectors, whereas $\boldsymbol{v} \sim \mathcal{CN}(0, \sigma_v^2)$ and $\boldsymbol{x} \in \mathbb{C}$ are random scalars. The scalars $|\mu_h|$, σ_h, σ_g, σ_Z, and σ_v are known. $\boldsymbol{\theta}_h$ is a vector of i.i.d. scalars uniformly distributed in $[0, 2\pi)$. The likelihood function of $\boldsymbol{Y} = \boldsymbol{U} + \boldsymbol{J}$ conditioned on $\boldsymbol{x}$ is given by:*

$$f_{\boldsymbol{Y}|\boldsymbol{x}}(Y|x) = \frac{1}{\pi^R} \int_0^\infty \frac{1}{(\sigma_h^2 |x|^2 + \sigma_z^2 + \sigma_g^2 \sigma_v^2 t)^R} \exp\left(-t - \frac{k_h^2 \sigma_h^2 |x|^2 R + |Y|^2}{\sigma_h^2 |x|^2 + \sigma_z^2 + \sigma_g^2 \sigma_v^2 t}\right) \times \prod_{i=1}^{R} I_0\left(\frac{2 k_h \sigma_h |Y_i||x|}{\sigma_h^2 |x|^2 + \sigma_z^2 + \sigma_g^2 \sigma_v^2 t}\right) dt, \quad (3.16)$$

where $k_h = \dfrac{|\mu_h|}{\sigma_h^2}$.

Proof. See Appendix A.4. □

Gaussian Approximation (Case 3)

Assuming that the signal $\boldsymbol{J}$ resulting form the jammer transmission is zero-mean Gaussian with covariance $\mathrm{E}\{\boldsymbol{J}\boldsymbol{J}^\dagger\} = \sigma_g^2 \sigma_v^2 I_R$, yields the likelihood function in following lemma.

Lemma 3.1. *Let $\boldsymbol{U} = \boldsymbol{H}\boldsymbol{x} + \boldsymbol{Z}$ and $\boldsymbol{J} = \boldsymbol{G}\boldsymbol{v}$, where $\boldsymbol{H} \sim \mathcal{CN}(|\mu_h| e^{\jmath \boldsymbol{\theta}_h}, \sigma_h^2 I_R)$, $\boldsymbol{G} \sim \mathcal{CN}(\boldsymbol{0}_R, \sigma_g^2 I_R)$, and $\boldsymbol{Z} \sim \mathcal{CN}(\boldsymbol{0}_R, \sigma_Z^2 I_R)$ are random vectors, whereas $\boldsymbol{v} \sim \mathcal{CN}(0, \sigma_v^2)$ and $\boldsymbol{x} \in \mathbb{C}$ are random scalars. The scalars $|\mu_h|$, σ_h, σ_g, σ_Z, and σ_v are known. $\boldsymbol{\theta}_h$ is a vector*

of i.i.d. scalars uniformly distributed in $[0, 2\pi)$*. If* $\boldsymbol{J} \sim \mathcal{CN}(0, \sigma_g^2\sigma_v^2 I_R)$*, then the likelihood function of* $\boldsymbol{Y} = \boldsymbol{U} + \boldsymbol{J}$ *conditioned on* $\boldsymbol{x}$ *is given by:*

$$\hat{p}_{\boldsymbol{Y}|\boldsymbol{x}}(Y|x) = \frac{1}{\pi^R(\sigma_h^2|x|^2+\sigma_z^2+\sigma_g^2\sigma_v^2 t)^R} \exp\left(\frac{-|\boldsymbol{Y}|^2 - k_h^2\sigma_h^2|x|^2 R}{\sigma_h^2|x|^2 + \sigma_z^2 + \sigma_g^2\sigma_v^2}\right) \prod_{i=1}^{R} I_0\left(\frac{2k_h\sigma_h|x||Y_i|}{\sigma_h^2|x|^2 + \sigma_z^2 + \sigma_g^2\sigma_v^2}\right), \quad (3.17)$$

where $k_h = \dfrac{|\mu_h|}{\sigma_h^2}$.

Proof. See Appendix A.5. □

3.2.4 Statistical distribution of both $\boldsymbol{H}$ and $\boldsymbol{G}$ partially known:

In this case, the transmitter's vector channel, $\boldsymbol{H}$, and the jammer's vector channel, $\boldsymbol{G}$, have specular components that result in non-zero means for both channels. The means of the i-th component of $\boldsymbol{H}$ and l-th component of $\boldsymbol{G}$ are given by:

$$\mu_{h_i} = k_h\sigma_h e^{\jmath\theta_{h_i}}, \quad (3.18)$$

$$\mu_{g_l} = k_g\sigma_g e^{\jmath\theta_{g_l}}, \quad (3.19)$$

respectively, where θ_{h_i} and θ_{g_l} are assumed to be *i.i.d.* random variables uniformly distributed in $[0, 2\pi)$, i and $l \in \{1, 2, \ldots, R\}$. The k factors of both channels, i.e., k_h and k_g, are assumed to be known. The exact likely function for this case is given in the following theorem:

Theorem 3.5. *Let* $\boldsymbol{U} = \boldsymbol{H}\boldsymbol{x} + \boldsymbol{Z}$ *and* $\boldsymbol{J} = \boldsymbol{G}\boldsymbol{v}$*, where* $\boldsymbol{H} \sim \mathcal{CN}(|\mu_h|e^{\jmath\boldsymbol{\theta}_h}, \sigma_h^2 I_R)$*,* $\boldsymbol{G} \sim \mathcal{CN}(|\mu_g|e^{\jmath\boldsymbol{\theta}_g}, \sigma_g^2 I_R)$*, and* $\boldsymbol{Z} \sim \mathcal{CN}(\boldsymbol{0}_R, \sigma_Z^2 I_R)$ *are random vectors, whereas* $\boldsymbol{v} \sim \mathcal{CN}(0, \sigma_v^2)$ *and*

$\boldsymbol{x} \in \mathbb{C}$ are random scalars. The scalars $|\mu_h|$, σ_h, σ_g, σ_Z, and σ_v are known. $\boldsymbol{\theta}_h$ and $\boldsymbol{\theta}_g$ are vectors of i.i.d. scalars uniformly distributed in $[0, 2\pi)$. The likelihood function of $\boldsymbol{Y} = \boldsymbol{U} + \boldsymbol{J}$ conditioned on $\boldsymbol{x}$ is given by:

$$f_{\boldsymbol{Y}|\boldsymbol{x}}(Y|x) = \frac{1}{\pi^R} \exp\left(-k_g^2 R - \frac{|Y|^2 + k_h^2\sigma_h^2|x|^2 R}{\sigma_h^2|x|^2 + \sigma_z^2}\right) \int_0^\infty \frac{\exp(-t)}{(\sigma_h^2|x|^2 + \sigma_z^2 + \sigma_g^2\sigma_v^2 t)^R}$$
$$\times \prod_{i=1}^{R} \sum_{n=0}^{\infty} \sum_{m=0}^{\infty} \left(\frac{k_g^2(\sigma_h^2|x|^2 + \sigma_z^2)}{\sigma_h^2|x|^2 + \sigma_z^2 + \sigma_g^2\sigma_v^2 t}\right)^n \left(\frac{\sigma_g^2\sigma_v^2(|Y_i|^2 + k_h^2\sigma_h^2|x|^2)t}{(\sigma_h^2|x|^2 + \sigma_z^2 + \sigma_g^2\sigma_v^2 t)(\sigma_h^2|x|^2 + \sigma_z^2)}\right)^m \frac{(n+m)!}{(n!)^2(m!)}$$
$$\times \sum_{\ell=0}^{m} \frac{(\sigma_h^2|x|^2 + \sigma_z^2)^\ell}{(\ell!)\ (m-\ell)!(|Y_i|^2 + k_h^2\sigma_h^2|x|^2)^\ell} \Phi(x, Y_i)\ dt, \quad (3.20)$$

where

$$\Phi(x, Y_i) = \frac{((-c)^\ell + c^\ell)}{2} \Gamma\left(\frac{1+\ell}{2}\right) {}_1\tilde{F}_2\left(\frac{1+\ell}{2}; \frac{1}{2}, \frac{2+\ell}{2}; \frac{c^2}{4}\right)$$
$$+ \frac{c\ ((-c)^\ell - c^\ell)}{4} \Gamma\left(1 + \frac{\ell}{2}\right) {}_1\tilde{F}_2\left(\frac{2+\ell}{2}; \frac{3}{2}, \frac{3+\ell}{2}; \frac{c^2}{4}\right), \quad (3.21)$$

where $c = \dfrac{2k_h\sigma_h|x||Y_i|}{\sigma_h^2|x|^2 + \sigma_z^2}$, $\Gamma(\cdot)$ is the gamma function, and ${}_1\tilde{F}_2(\cdot;\cdot,\cdot;\cdot)$ is the regularized generalized hypergeomtric function.

Proof. See Appendix A.6. □

Gaussian Approximation (Case 4)

Assuming that the signal $\boldsymbol{J}$ resulting form the jammer transmission is zero-mean Gaussian with covariance $\mathrm{E}\{\boldsymbol{J}\boldsymbol{J}^\dagger\} = \sigma_g^2\sigma_v^2 I_R$, yields the likelihood function in (3.17).

3.3 Conclusion

This chapter considered a scenario in which a single-antenna transmitter communicates with a multiple-antenna receiver in the presence of a single-antenna continuous proactive jammer sending a zero-mean complex Gaussian signal over a complex Gaussian vector channel. The likelihood functions of the non-Gaussian signal induced at the receiver are derived for cases corresponding to whether the receiver has full CDI, or partial CDI of the transmitter's channel. The jammer's channel CDI is either fully or partially available at the receiver. Using the derived likelihood expressions, the optimal ML detector is developed along with the one based on the Gaussian approximation of the signal resulting form the jammer's transmission.

Chapter 4

SISO with multiple transmissions

4.1 System Model and Problem Statement

4.1.1 System Model

We consider the system depicted in Figure 4.1 which is a single input single output system in which a transmitter communicates with a receiver over a block fading channel in the presence of a proactive continuous jammer. The transmitter-receiver channel is denoted by $\boldsymbol{h}$, and the jammer-receiver channel is denoted by $\boldsymbol{g}$. Both channels are assumed to remain constant during the transmission of a block of T data symbols, and take independent realizations in subsequent blocks. The transmitted signal is denoted by $\boldsymbol{X} \in \mathbb{C}^T$ and is drawn from a T-dimensional constellation $\mathcal{C}$. The jammer's signal is denoted by $\boldsymbol{V} \in \mathbb{C}^T$, and the additive noise at the receiver is denoted by $\boldsymbol{Z} \in \mathbb{C}^T$. The corresponding received signal is denoted by $\boldsymbol{Y} \in \mathbb{C}^T$. Using this notation we have,

$$\boldsymbol{Y} = \boldsymbol{h}\boldsymbol{X} + \boldsymbol{g}\boldsymbol{V} + \boldsymbol{Z}. \tag{4.1}$$

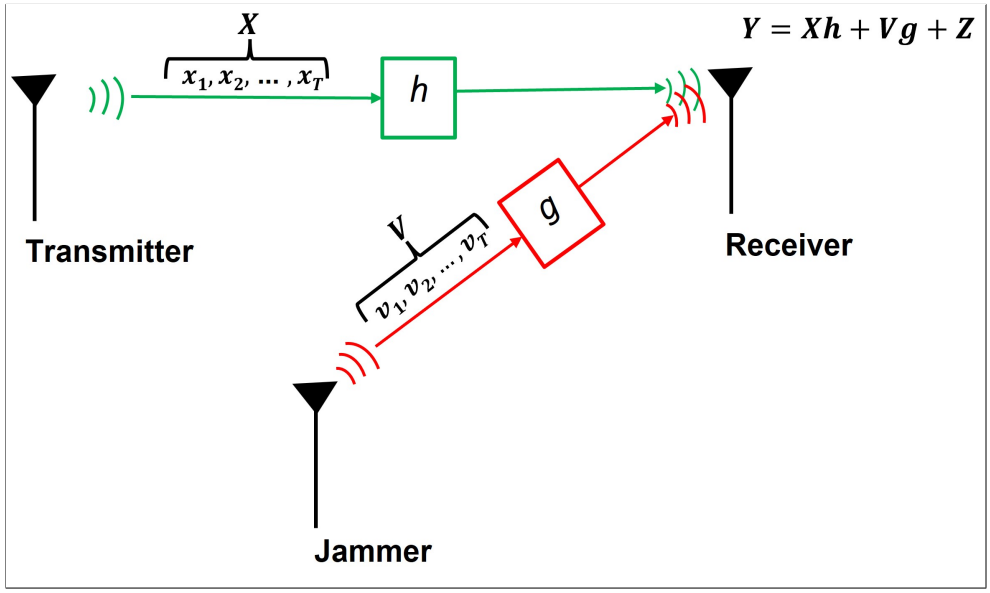

Figure 4.1: System Model.

The scalar channels $\boldsymbol{h}$ and $\boldsymbol{g}$ are modeled as independent complex Gaussian random variables with means μ_h and μ_g, and variances σ_h^2 and σ_g^2, respectively, i.e., $\boldsymbol{h} \sim \mathcal{CN}(\mu_h, \sigma_h^2)$ and $\boldsymbol{g} \sim \mathcal{CN}(\mu_g, \sigma_g^2)$. The independent Gaussian model of $\boldsymbol{h}$ and $\boldsymbol{g}$ implies that the magnitudes of $\boldsymbol{h}$ and $\boldsymbol{g}$, i.e., $|\boldsymbol{h}|$ and $|\boldsymbol{g}|$, are independent Rayleigh and/or Rician random variables depending whether their respective means are zeros or non-zeros [26]. The components of the jamming vector, $\boldsymbol{V}$, are assumed to be zero-mean, mutually independent complex Gaussian random variables with known variance of σ_V^2; the variance of the additive complex white Gaussian noise is σ_Z^2, i.e., $\boldsymbol{V} \sim \mathcal{CN}(0, \sigma_V^2 I_T)$ and $\boldsymbol{Z} \sim \mathcal{CN}(0, \sigma_Z^2 I_T)$, respectively.

The transmitter, the jammer, and the receiver might be mobile or airborne, which is the case in vehicle-to-vehicle (V2V) communications or when the transmitter and/or jammer are mounted on drones (UAVs). Hence, both $\boldsymbol{h}$ and $\boldsymbol{g}$ are assumed to subject to fading. The fading processes of $\boldsymbol{h}$ and $\boldsymbol{g}$ are statistically independent. When the transmitter-receiver channel, $\boldsymbol{h}$, is Rayleigh fading, i.e., $\mu_h = 0$, we consider two distinct cases: first,

that the receiver knows $\boldsymbol{h}$ perfectly (full CSI), and second, that the receiver only knows the distribution of $\boldsymbol{h}$ (full CDI). When the transmitter, the receiver, or both are UAVs, $\boldsymbol{h}$ is Rician fading [89]. In this case we assume that the receiver knows the relative strength of the line-of-sight (LOS), component of $\boldsymbol{h}$, which is given by its k factor, $k_h = \frac{|\mu_h|}{\sigma_h}$, i.e., partial CDI. For each of the three aforementioned cases, we consider two scenarios. In the first scenario, $\boldsymbol{g}$ is Rayleigh fading and the receiver knows σ_g, and in the second scenario, $\boldsymbol{g}$ is Rician fading and the receiver knows both σ_g and $k_g = \frac{|\mu_g|}{\sigma_g}$. Hence, a total of six cases corresponding to six distinct scenarios are considered.

4.1.2 Problem Statement

This chapter aims to develop the ML detector for each of the six communication scenarios outlined hereinabove. For two of these scenarios and for certain constellations, we will show that the ML detector is equivalent to a simplified detector that is significantly less complex to implement. The six cases we consider are the following:

1. *Realization of $\boldsymbol{h}$ known and statistical distribution of $\boldsymbol{g}$ partially known:* The ML detector decides in favor of the constellation point $\hat{X}$ given by

$$\hat{X} = \arg\max_{X \in \mathcal{C}} p_{\boldsymbol{Y}|\boldsymbol{X},\boldsymbol{h}} \left(Y \middle| X, h; |\mu_g|, \sigma_g^2 \right). \tag{4.2}$$

   In this case, the magnitude of the mean of the distribution of $\boldsymbol{g}$ is known, but not its phase. This case corresponds to the situation when the jammer channel has an LOS component.

2. *Realization of $\boldsymbol{h}$ and statistical distribution of $\boldsymbol{g}$ known:* The ML detector decides

in favor of the constellation point $\hat{X}$ given by

$$\hat{X} = \arg\max_{X \in \mathcal{C}} p_{\boldsymbol{Y}|\boldsymbol{X},\boldsymbol{h}} \left(Y \middle| X, h; \sigma_g^2\right), \tag{4.3}$$

where σ_g^2 is a known parameter and channel $\boldsymbol{g}$ is assumed to be zero mean. This case corresponds to the situation when the jammer channel has no LOS component.

3. *Statistical distribution of both $\boldsymbol{h}$ and $\boldsymbol{g}$ partially known:* The ML detector decides in favor of the constellation point $\hat{X}$ given by

$$\hat{X} = \arg\max_{X \in \mathcal{C}} p_{\boldsymbol{Y}|\boldsymbol{X}} \left(Y \middle| X; |\mu_h|, \sigma_h^2, |\mu_g|, \sigma_g^2\right). \tag{4.4}$$

In this case, the phases of the means of $\boldsymbol{h}$ and $\boldsymbol{g}$ are unknown, and both $\boldsymbol{h}$ and $\boldsymbol{g}$ have LOS components.

4. *Statistical distribution of $\boldsymbol{h}$ known and statistical distribution of $\boldsymbol{g}$ partially known:* The ML detector decides in favor of the constellation point $\hat{X}$ given by

$$\hat{X} = \arg\max_{X \in \mathcal{C}} p_{\boldsymbol{Y}|\boldsymbol{X}} \left(Y \middle| X; |\mu_g|, \sigma_g^2, \sigma_h^2\right). \tag{4.5}$$

In this case, the phase of the mean of $\boldsymbol{g}$ is not known, and the mean of $\boldsymbol{h}$ is zero. In this situation $\boldsymbol{g}$ has an LOS component but $\boldsymbol{h}$ does not.

5. *Statistical distribution of $\boldsymbol{h}$ partially known and statistical distribution of $\boldsymbol{g}$ known:* The ML detector decides in favor of the constellation point $\hat{X}$ given by

$$\hat{X} = \arg\max_{X \in \mathcal{C}} p_{\boldsymbol{Y}|\boldsymbol{X}} \left(Y \middle| X; |\mu_h|, \sigma_h^2, \sigma_g^2\right). \tag{4.6}$$

Complementary to the previous case, in this case the phase of the mean of $\boldsymbol{h}$ is not known and the mean of $\boldsymbol{g}$ is zero. Here, $\boldsymbol{h}$ has an LOS component but $\boldsymbol{g}$ does not.

6. *Statistical distribution of both $\boldsymbol{h}$ and $\boldsymbol{g}$ known:* The ML detector decides in favor of the constellation point $\hat{X}$ given by

$$\hat{X} = \arg\max_{X \in \mathcal{C}} p_{\boldsymbol{Y}|\boldsymbol{X}} \left(Y \middle| X; \sigma_h^2, \sigma_g^2 \right). \tag{4.7}$$

In this case both $\boldsymbol{h}$ and $\boldsymbol{g}$ are zero mean, i.e., neither the transmitter nor the jammer has an LOS component.

In the next section, we provide exact and approximate ML detection rules for each of the cases mentioned above.

4.2 Likelihood function expressions for the different CSI cases

In this section, the exact likelihood function expressions corresponding to the cases outlined in the previous section will be presented along with their approximate counterparts based on the Gaussian approximation of the non-Gaussian signal resulting from the jammer's transmissions. To derive the desired expressions, let

$$\boldsymbol{U} = \boldsymbol{h}\boldsymbol{X} + \boldsymbol{Z}, \tag{4.8}$$

and

$$\boldsymbol{J} = \boldsymbol{g}\boldsymbol{V}. \tag{4.9}$$

Hence, the received signal in (4.1) can be expressed as

$$\boldsymbol{Y} = \boldsymbol{U} + \boldsymbol{J}. \tag{4.10}$$

Noting that $\boldsymbol{U}$ and $\boldsymbol{J}$ are statistically independent, the likelihood function $p_{\boldsymbol{Y}|\boldsymbol{X}}(Y|X)$ corresponding to a received vector Y is given by:

$$p_{\boldsymbol{Y}|\boldsymbol{X}}(Y|X) = p_{\boldsymbol{U}|\boldsymbol{X}}(Y|X) * p_{\boldsymbol{J}}(Y), \tag{4.11}$$

where $*$ is the convolution operator, $p_{\boldsymbol{J}}(\cdot)$ is the joint *pdf* of the random vector $\boldsymbol{J}$ and $p_{\boldsymbol{U}|\boldsymbol{X}}(\cdot|X)$ is the joint *pdf* of the random vector $\boldsymbol{U}$ conditioned on the transmitted random symbol $\boldsymbol{X} = X$.

First, we note that, because both the noise, $\boldsymbol{Z}$, and the channel $\boldsymbol{h}$ are assumed Gaussian (except in Cases 1 and 2, wherein the channel is deterministic), the distribution of the vector $\boldsymbol{U}$ conditioned on $\boldsymbol{X} = X$ is also Gaussian. However, since $\boldsymbol{J}$ comprises the product of the complex Gaussian scalar $\boldsymbol{g}$ and the complex Gaussian vector $\boldsymbol{V}$, its distribution is not Gaussian and depends on the information available at the receiver about jammer's channel $\boldsymbol{g}$. In particular, we have the following theorem.

Theorem 4.1. *Let $\boldsymbol{J} = \boldsymbol{g}\boldsymbol{V}$, where $\boldsymbol{g} \sim \mathcal{CN}(0, \sigma_g^2)$ and $\boldsymbol{V} \in \mathbb{C}^T$ be Gaussian distributed, i.e., $\boldsymbol{V} \sim \mathcal{CN}(0, \sigma_V^2 I_T)$. Then, the pdf of $\boldsymbol{J}$ is given by:*

$$p_{\boldsymbol{J}}(J) = \frac{2K_{T-1}\left(\dfrac{2\|J\|}{\sigma_g \sigma_V}\right)}{\pi^T \sigma_g^{T+1} \sigma_V^{T+1} \|J\|^{T-1}}, \tag{4.12}$$

where $K_\nu(\cdot)$ is the modified Bessel function of the second kind of order ν.

Proof. See Appendix B.1. □

This *pdf* corresponds to a jammer's channel with zero mean and a known variance σ_g^2 and hence will be used to obtain the ML detector for cases 2, 5 and 6 outlined above. Next, we consider the case when the jammer's channel is non-zero mean.

Theorem 4.2. *Let $\boldsymbol{J} = \boldsymbol{g}\boldsymbol{V}$, where $\boldsymbol{g} \sim \mathcal{CN}(\mu_g, \sigma_g^2)$ and $\boldsymbol{V} \in \mathbb{C}^T$ is Gaussian distributed, i.e., $\boldsymbol{V} \sim \mathcal{CN}(0, \sigma_V^2 I_T)$. Let $k_g = \dfrac{|\mu_g|}{\sigma_g}$. Then, the pdf of $\boldsymbol{J}$ is given by:*

$$p_{\boldsymbol{J}}(J) = \frac{\exp\left(-k_g^2\right)}{\pi^T \sigma_g^{2T} \sigma_V^{2T}} \int_0^\infty I_0\left(2k_g\sqrt{t}\right) \exp\left(-t - \frac{\|J\|^2}{\sigma_g^2 \sigma_V^2 t}\right) \frac{dt}{t^T}. \tag{4.13}$$

where $I_0(\cdot)$ is the modified Bessel function of the first kind of order zero.

Proof. See Appendix B.2. □

To obtain this *pdf*, we assumed that $\mu_g = |\mu_g| e^{\jmath \boldsymbol{\theta_g}}$, where $\boldsymbol{\theta_g}$ is a random variable uniformly-distributed over $(0, 2\pi]$, and $|\mu_g|$ is known. Hence, this *pdf* corresponds to the case in which the strength of the LOS component of the jammer's channel is known as per cases 1, 3 and 4 outlined above.

Corollary 4.1. *When $\mu_g = 0$, the pdf in (4.13) reduces to the one in (4.12).*

Proof. The proof follows from the observation that $I_0(0) = 1$ and the fact that, for a complex scalar $z = |z| e^{\jmath \theta_z}$, the modified Bessel function of the second kind of order ν is given by [90]:

$$K_\nu(z) = \tfrac{1}{2}(\tfrac{1}{2}z)^\nu \int_0^\infty \exp\left(-t - \frac{z^2}{4t}\right) \frac{\mathrm{d}t}{t^{\nu+1}}, \quad |\theta_z| < \pi/4. \tag{4.14}$$

Since the right hand side of (4.13) is a function of $\|J\|$, which is real corresponding to

$\theta_z = 0$,

$$\int_0^\infty \exp\left(-t - \frac{\|J\|^2}{\sigma_g^2 \sigma_V^2 t}\right) \frac{dt}{t^T} = 2\, \frac{\sigma_g^{T+1}\sigma_V^{T+1}}{\|J\|^{T-1}}\, K_{T-1}\left(\frac{2\|J\|}{\sigma_g \sigma_V}\right),$$

which yields the statement of the corollary. □

Using Theorems 4.1 and 4.2, we are now ready to consider the cases outlined in Section 4.1.2.

4.2.1 Realization of $\boldsymbol{h}$ known and statistical distribution of $\boldsymbol{g}$ partially known

This section considers the case in which the receiver knows the current realization of $\boldsymbol{h}$ and knows that $\boldsymbol{g} \sim \mathcal{CN}(\mu_g, \sigma_g^2)$, where $|\mu_g|$ and σ_g^2 are known. The exact likelihood function for this case is given in the following theorem.

Theorem 4.3. *Let $\boldsymbol{U} = h\boldsymbol{X} + \boldsymbol{Z}$ and $\boldsymbol{J} = \boldsymbol{g}\boldsymbol{V}$, where $\boldsymbol{Z} \sim \mathcal{CN}(0, \sigma_Z^2 I_T)$, $\boldsymbol{V} \sim \mathcal{CN}(0, \sigma_V^2 I_T)$ and $\boldsymbol{X} \in \mathbb{C}^T$ are random vectors, $\boldsymbol{g} \sim \mathcal{CN}(|\mu_g| e^{\jmath \boldsymbol{\theta}_g}, \sigma_g^2)$ is a random scalar, h, $|\mu_g|$, σ_g, σ_Z, and σ_V are known deterministic scalars, and the phase $\boldsymbol{\theta}_g$ is a random scalar uniformly distributed over $[0, 2\pi)$. Let $k_g = \dfrac{|\mu_g|}{\sigma_g}$. Then, the likelihood function of $\boldsymbol{Y} = \boldsymbol{U} + \boldsymbol{J}$ conditioned on $\boldsymbol{X}$ and h is given by:*

$$p_{\boldsymbol{Y}|\boldsymbol{X},\boldsymbol{h}}(Y|X, h; |\mu_g|, \sigma_g^2) = \frac{\exp\left(-k_g^2\right)}{\pi^T} \int_0^\infty \frac{I_0\left(2k_g\sqrt{t}\right)}{\left(\sigma_Z^2 + \sigma_V^2 \sigma_g^2 t\right)^T} \exp\left(-t - \frac{\|Y - hX\|^2}{\sigma_Z^2 + \sigma_V^2 \sigma_g^2 t}\right) dt. \quad (4.15)$$

Proof. See Appendix B.3. □

Gaussian Approximation (Case 1)

The jamming signal, $\boldsymbol{J}$, observed at the receiver has been traditionally assumed to be zero-mean Gaussian with covariance $\mathrm{E}\{\boldsymbol{J}\boldsymbol{J}^{\dagger}\} = \sigma_g^2 \sigma_V^2 I_T$. Using this assumption, it can be readily verified that the approximate likelihood function is given by:

$$\hat{p}_{\boldsymbol{Y}|\boldsymbol{X},\boldsymbol{h}}(Y|X,h;|\mu_g|,\sigma_g^2) = \frac{1}{\pi^T \left(\sigma_Z^2 + \sigma_V^2 \sigma_g^2\right)^T} \exp\left(-\frac{\|Y - hX\|^2}{\sigma_Z^2 + \sigma_V^2 \sigma_g^2}\right). \tag{4.16}$$

Interestingly, the transmitter vector that maximizes (4.15) coincides with the one that maximizes (4.16); this fact is reinforced in the following result.

Corollary 4.2. *The vector of transmitted symbols, $\hat{X}$, that maximizes the exact likelihood function in* (4.15) *maximizes the approximate likelihood function given by* (4.16)*, i.e.,*

$$\arg\max_{X \in \mathcal{C}} p_{\boldsymbol{Y}|\boldsymbol{X},\boldsymbol{h}}(Y\big|X,h;|\mu_g|,\sigma_g^2) = \arg\max_{X \in \mathcal{C}} \hat{p}_{\boldsymbol{Y}|\boldsymbol{X},\boldsymbol{h}}(Y\big|X,h;|\mu_g|,\sigma_g^2)$$

Proof. The exact likelihood function $p_{\boldsymbol{Y}|\boldsymbol{X},\boldsymbol{h}}(Y\big|X,h;|\mu_g|,\sigma_g^2)$ is maximized by maximizing the integrand in (4.15) which is maximized by $\hat{X}$ that minimizes $\|Y_i - X_i\ h\|$. Minimizing this norm maximizes the exponential term in (4.16) and subsequently maximizes $\hat{p}_{\boldsymbol{Y}|\boldsymbol{X},\boldsymbol{h}}(Y\big|X,h;|\mu_g|,\sigma_g^2)$. □

4.2.2 Realization of $\boldsymbol{h}$ and statistical distribution of $\boldsymbol{g}$ known

In this case, the receiver knows the transmitter channel's current realization $\boldsymbol{h}$ and it knows that $\boldsymbol{g} \sim \mathcal{CN}(0, \sigma_g^2)$, where σ_g^2 is known. The exact likelihood function for this case is given in the following corollary.

Corollary 4.3. *Let* $\boldsymbol{U} = h\boldsymbol{X} + \boldsymbol{Z}$ *and* $\boldsymbol{J} = \boldsymbol{g}\boldsymbol{V}$*, where* $\boldsymbol{Z} \sim \mathcal{CN}(0, \sigma_Z^2 I_T)$*,* $\boldsymbol{V} \sim \mathcal{CN}(0, \sigma_V^2 I_T)$ *and* $\boldsymbol{X} \in \mathbb{C}^T$ *are random vectors ,* $\boldsymbol{g} \sim \mathcal{CN}(0, \sigma_g^2)$ *is a random scalar,* h*,* σ_Z*,* σ_g *and* σ_V *are known deterministic scalars. The likelihood function of* $\boldsymbol{Y} = \boldsymbol{U} + \boldsymbol{J}$ *conditioned on* $\boldsymbol{X}$ *and* h *is given by:*

$$p_{\boldsymbol{Y}|\boldsymbol{X},\boldsymbol{h}}(Y|X, h; \sigma_g^2) = \int_0^\infty \frac{1}{\pi^T \left(\sigma_Z^2 + \sigma_V^2 \sigma_g^2 t\right)^T} \exp\left(-t - \frac{\|Y - hX\|^2}{\sigma_Z^2 + \sigma_V^2 \sigma_g^2 t}\right) dt. \tag{4.17}$$

Corollary 4.4. *The likelihood function in Theorem 4.3 subsumes the one given in corollary 4.3.*

Proof. Setting k_g to zero in (4.15) and noticing that $I_0(0) = 1$ yield (4.17). □

Gaussian Approximation (Case 2)

Analogous to Case 1, assuming that the signal resulting form the jammer transmission, $\boldsymbol{J}$, is zero-mean Gaussian with covariance $\mathrm{E}\{\boldsymbol{J}\boldsymbol{J}^\dagger\} = \sigma_g^2 \sigma_V^2 I_T$ yields an approximate likelihood function identical to the one in (4.16). Since the exponent in (4.16) and the integrand in (4.17) both are maximized by the vector X that minimizes $\|Y - hX\|$, it follows that, in this case too, the Gaussian approximation of the jammer's signal yields identical performance to the ML detector based on the exact likelihood function albeit with a significant computation advantage; the Gaussian approximation does not require evaluating the integration in (4.17).

From Cases 1 and 2, it can be concluded that when the realization of $\boldsymbol{h}$ is known and the distribution of $\boldsymbol{g}$ is either partially or fully known, the detector that uses the Gaussian approximation of $\boldsymbol{J}$ achieves the same performance as the detector that uses its exact *pdf*. However, the former is computationally superior.

4.2.3 Statistical distribution of both $\boldsymbol{h}$ and $\boldsymbol{g}$ partially known

In this case the receiver knows that $\boldsymbol{h} \sim \mathcal{CN}(\mu_h, \sigma_h^2)$ and $\boldsymbol{g} \sim \mathcal{CN}(\mu_g, \sigma_g^2)$ where $|\mu_h|$, σ_h^2, $|\mu_g|$, and σ_g^2 are known. The exact likely function for this case is given in the following theorem:

Theorem 4.4. *Let $\boldsymbol{U} = \boldsymbol{h}\boldsymbol{X} + \boldsymbol{Z}$ and $\boldsymbol{J} = \boldsymbol{g}\boldsymbol{V}$, where $\boldsymbol{Z} \sim \mathcal{CN}(0, \sigma_Z^2 I_T)$, $\boldsymbol{V} \sim \mathcal{CN}(0, \sigma_V^2 I_T)$ and $\boldsymbol{X} \in \mathbb{C}^T$ are random vectors, and $\boldsymbol{g} \sim \mathcal{CN}(|\mu_g| e^{\jmath \boldsymbol{\theta}_g}, \sigma_g^2)$ and $\boldsymbol{h} \sim \mathcal{CN}(|\mu_h| e^{\jmath \boldsymbol{\theta}_h}, \sigma_h^2)$ are random scalars. The scalars σ_h, σ_g, $|\mu_h|$, $|\mu_g|$, σ_Z, and σ_V are known, and the phases $\boldsymbol{\theta}_h$ and $\boldsymbol{\theta}_g$ are independent and identically distributed (i.i.d.) random scalars uniformly distributed over $[0, 2\pi)$. Let $k_h = \dfrac{|\mu_h|}{\sigma_h}$ and $k_g = \dfrac{|\mu_g|}{\sigma_g}$. The likelihood function of $\boldsymbol{Y} = \boldsymbol{U} + \boldsymbol{J}$ conditioned on $\boldsymbol{X}$ is given by:*

$$p_{\boldsymbol{Y}|\boldsymbol{X}}(Y|X; |\mu_h|, \sigma_h^2, |\mu_g|, \sigma_g^2) = \frac{\exp\left(-k_g^2\right)}{\pi^T |\Sigma|} \times \int_0^\infty \frac{I_0\Big(2k_h\sigma_h|\hat{Y}^\dagger D(t)\hat{X}|\Big) I_0\left(2k_g\sqrt{t}\right)}{\prod_{i=1}^T \left(1 + \lambda_i \sigma_g^2 \sigma_V^2\ t\right)} \exp\Big(-t - \hat{Y}^\dagger D(t)\hat{Y} - k_h^2\sigma_h^2 \hat{X}^\dagger D(t)\hat{X}\Big) dt, \quad (4.18)$$

where $\Sigma = \mathrm{E}\{\boldsymbol{U}\boldsymbol{U}^\dagger | \boldsymbol{X}\}$, λ_i is the i-th eigenvalue of Σ^{-1}, $D(t)$ is a diagonal matrix whose i-th diagonal entry is given by $D_{ii} = \frac{\lambda_i}{1+\lambda_i\sigma_g^2\sigma_V^2 t}$, $\hat{Y} = Q^\dagger Y$ and $\hat{X} = Q^\dagger X$ where Q is the unitary matrix containing the eigenvectors of Σ^{-1}.

Proof. See Appendix B.4. □

Gaussian Approximation (Case 3)

Assuming that the signal $\boldsymbol{J}$ resulting form the jammer transmission is zero-mean Gaussian with covariance $\mathrm{E}\{\boldsymbol{J}\boldsymbol{J}^\dagger\} = \sigma_g^2 \sigma_V^2 I_T$ yields the likelihood function in the following lemma.

Lemma 4.1. *Let* $\boldsymbol{Y} = \boldsymbol{U} + \boldsymbol{J}$, $\boldsymbol{U} = \boldsymbol{h}\boldsymbol{X} + \boldsymbol{Z}$, *where* $\boldsymbol{Z} \sim \mathcal{CN}(0, \sigma_Z^2 I_T)$, *and* $\boldsymbol{X} \in \mathbb{C}^T$ *are random vectors, and* $\boldsymbol{h} \sim \mathcal{CN}(|\mu_h| e^{\jmath \boldsymbol{\theta}_h}, \sigma_h^2)$ *is a random scalar. The scalars* σ_h, $|\mu_h|$ *and* σ_Z *are known, and the phase* $\boldsymbol{\theta}_h$ *is a random scalar uniformly distributed over* $[0, 2\pi)$. *If* $\boldsymbol{J} \sim \mathcal{CN}(0, \sigma_g^2 \sigma_V^2 I_T)$, *where* σ_g *and* σ_V *are known scalars, then the likelihood function of* $\boldsymbol{Y} = \boldsymbol{U} + \boldsymbol{J}$ *conditioned on* $\boldsymbol{X}$ *is given by:*

$$\hat{p}_{\boldsymbol{Y}|\boldsymbol{X}}(Y|X) = \frac{1}{\pi^T |\Sigma_G|} \, I_0 \left(2 k_h \sigma_h |Y^\dagger \Sigma_G^{-1} X|\right) \exp\left(-Y^\dagger \Sigma_G^{-1} Y - k_h^2 \sigma_h^2 X^\dagger \Sigma_G^{-1} X\right), \tag{4.19}$$

where $\Sigma_G = \mathrm{E}\{\boldsymbol{Y}\boldsymbol{Y}^\dagger | \boldsymbol{X}\}$.

Proof. See Appendix B.5. □

Corollary 4.5. *if the constellation symbols satisfy* $\|\boldsymbol{X}_i\| = \|\boldsymbol{X}_j\|, \forall \boldsymbol{X}_i, \boldsymbol{X}_j \in \mathcal{C}, i \neq j$, *i.e., if the transmitted symbols have equal norms; then, the vector* $\hat{X} \in \mathcal{C}$ *that maximizes* $|Y^\dagger X|$ *maximizes both the exact likelihood function in* (4.18) *and the approximate likelihood function given by* (4.19), *i.e.,*

$$\arg\max_{X \in \mathcal{C}} p_{\boldsymbol{Y}|\boldsymbol{X}}(Y|X_j; |\mu_h|, \sigma_h^2, |\mu_g|, \sigma_g^2)\} = \arg\max_{X \in \mathcal{C}} \hat{p}_{\boldsymbol{Y}|\boldsymbol{X}}(Y|X_j; |\mu_h|, \sigma_h^2, |\mu_g|, \sigma_g^2)\}.$$

Proof. See Appendix B.6. □

Complementary to this corollary, we note that when the constellation vectors in $\mathcal{C}$ do not have identical norms, the ML detector based on the exact likelihood function in (4.18) yields a significant performance advantage over its counterpart that is based on the approximate likelihood function in (4.19), cf. Section 4.3.

Remark 1. *For every constellation symbol* X, *the ML detector assigns a partition,* D_X, *of the received signal space such that the detector decides in favor of* X *whenever it receives*

a signal $Y \in D_X$*. Knowing these regions and their boundaries facilitates detection and the computation of detection error probability. The decision boundary,* φ_{ij}*, between the symbols* X_i *and* X_j *is given by*

$$\varphi_{ij} = \{Y \in \mathbb{C}^T : \; p_{\boldsymbol{Y}|\boldsymbol{X}}(Y|X_i; |\mu_h|, \sigma_h^2, |\mu_g|, \sigma_g^2) = p_{\boldsymbol{Y}|\boldsymbol{X}}(Y|X_j; |\mu_h|, \sigma_h^2, |\mu_g|, \sigma_g^2)\}, \quad (4.20)$$

where $p_{\boldsymbol{Y}|\boldsymbol{X}}(Y|X_i; |\mu_h|, \sigma_h^2, |\mu_g|, \sigma_g^2)$ *is given by* (4.18)*. Finding* φ_{ij} *for the exact detector is intractable due to the integral nature of the equations involved. However, from Corollary 4.5, when the transmitted symbols have identical norms, the decision boundaries of the exact detector coincide with those of the Gaussian approximation one. Since the symbols have identical norms, it follows that*

$$\arg\max_{X \in \mathcal{C}} |Y^\dagger X| = \arg\min_{X \in \mathcal{C}} \|Y - X\|.$$

Hence, in this case, φ_{ij} *is a hyperplane that is equidistant from* X_i *and* X_j*, i.e.,*

$$\varphi_{ij} = \{Y \in \mathbb{C}^T : \|Y - X_i\| = \|Y - X_j\|\}. \quad (4.21)$$

□

4.2.4 Statistical distribution of $\boldsymbol{h}$ partially known and statistical distribution of $\boldsymbol{g}$ known

In this case, the receiver knows that $\boldsymbol{h} \sim \mathcal{CN}(\mu_h, \sigma_h^2)$ and $\boldsymbol{g} \sim \mathcal{CN}(0, \sigma_g^2)$, where σ_h^2, σ_g^2 and $|\mu_h|$ are known. The exact likelihood function for this case is given by the following corollary.

Corollary 4.6. *Let* $\boldsymbol{U} = \boldsymbol{h}\boldsymbol{X} + \boldsymbol{Z}$ *and* $\boldsymbol{J} = \boldsymbol{g}\boldsymbol{V}$*, where* $\boldsymbol{Z} \sim \mathcal{CN}(0, \sigma_Z^2 I_T)$*,* $\boldsymbol{V} \sim \mathcal{CN}(0, \sigma_V^2 I_T)$ *and* $\boldsymbol{X} \in \mathbb{C}^T$ *are random vectors,* $\boldsymbol{g} \sim \mathcal{CN}(0, \sigma_g^2)$ *and* $\boldsymbol{h} \sim \mathcal{CN}(|\mu_h| e^{\jmath \boldsymbol{\theta}_h}, \sigma_h^2)$ *are random scalars. The scalars* σ_h*,* σ_g*,* $|\mu_h|$*,* σ_Z*, and* σ_V *are known, and the phase* $\boldsymbol{\theta}_h$ *is a random scalar uniformly distributed over* $[0, 2\pi)$*. Let* $k_h = \dfrac{|\mu_h|}{\sigma_h}$*. The likelihood function of* $\boldsymbol{Y} = \boldsymbol{U} + \boldsymbol{J}$ *conditioned on* $\boldsymbol{X}$ *is given by:*

$$p_{\boldsymbol{Y}|\boldsymbol{X}}(Y|X; |\mu_h|, \sigma_h^2, \sigma_g^2) = \frac{1}{\pi^T |\Sigma|} \int_0^\infty \frac{I_0\left(2k_h \sigma_h |\hat{Y}^\dagger D(t) \hat{X}|\right)}{\prod_{i=1}^T \left(1 + \lambda_i \sigma_g^2 \sigma_V^2 t\right)} \times \exp\left(-t - \hat{Y}^\dagger D(t) \hat{Y} - k_h^2 \sigma_h^2 \hat{X}^\dagger D(t) \hat{X}\right) dt, \quad (4.22)$$

where $\Sigma = \mathrm{E}\{\boldsymbol{U}\boldsymbol{U}^\dagger | \boldsymbol{X}\}$*,* λ_i *is the i-th eigenvalue of* Σ^{-1}*,* $D(t)$ *is a diagonal matrix whose i-th diagonal entry is given by* $D_{ii} = \frac{\lambda_i}{1 + \lambda_i \sigma_g^2 \sigma_V^2 t}$*,* $\hat{Y} = Q^\dagger Y$ *and* $\hat{X} = Q^\dagger X$ *where* Q *is the unitary matrix containing the eigenvectors of* Σ^{-1}*.*

Proof. See Corollary 4.9 and Appendix B.4 below. □

Gaussian Approximation (Case 4)

Assuming that the signal $\boldsymbol{J}$ resulting form the jammer transmission is zero-mean Gaussian with covariance $\mathrm{E}\{\boldsymbol{J}\boldsymbol{J}^\dagger\} = \sigma_g^2 \sigma_V^2 I_T$ yields the likelihood function in (4.19).

4.2.5 Statistical distribution of $\boldsymbol{h}$ known and statistical distribution of $\boldsymbol{g}$ partially known

In this case, the receiver knows that $\boldsymbol{h} \sim \mathcal{CN}(0, \sigma_h^2)$ and $\boldsymbol{g} \sim \mathcal{CN}(\mu_g, \sigma_g^2)$, where σ_h^2, σ_g^2 and $|\mu_g|$ are known. The exact likely function for this case is given by the following corollary.

Corollary 4.7. *Let* $\boldsymbol{U} = \boldsymbol{h}\boldsymbol{X} + \boldsymbol{Z}$ *and* $\boldsymbol{J} = \boldsymbol{g}\boldsymbol{V}$*, where* $\boldsymbol{Z} \sim \mathcal{CN}(0, \sigma_Z^2 I_T)$*,* $\boldsymbol{V} \sim \mathcal{CN}(0, \sigma_V^2 I_T)$ *and* $\boldsymbol{X} \in \mathbb{C}^T$ *are random vectors, and* $\boldsymbol{g} \sim \mathcal{CN}(|\mu_g| e^{\jmath \boldsymbol{\theta}_g}, \sigma_g^2)$ *and* $\boldsymbol{h} \sim \mathcal{CN}(0, \sigma_h^2)$ *are random scalars. The scalars* σ_h*,* σ_g*,* $|\mu_g|$*,* σ_Z*, and* σ_V *are known, and the phase* $\boldsymbol{\theta}_g$ *is uniformly distributed over* $[0, 2\pi)$*. The likelihood function of* $\boldsymbol{Y} = \boldsymbol{U} + \boldsymbol{J}$ *conditioned on* $\boldsymbol{X}$ *is given by:*

$$p_{\boldsymbol{Y}|\boldsymbol{X}}(Y|X; \sigma_h^2, |\mu_g|, \sigma_g^2) = \frac{\exp\left(-k_g^2\right)}{\pi^T |\Sigma|} \times \int_0^\infty \frac{I_0\left(2k_g\sqrt{t}\right)}{\prod_{i=1}^T \left(1 + \lambda_i \sigma_g^2 \sigma_V^2 t\right)} \exp\left(-t - \sum_{i=1}^T \frac{\lambda_i\left(|Y_i|^2\right)}{1 + \lambda_i \sigma_g^2 \sigma_V^2 t}\right) dt, \quad (4.23)$$

where $k_g = \dfrac{|\mu_g|}{\sigma_g}$*,* $\Sigma = \mathrm{E}\{\boldsymbol{U}\boldsymbol{U}^\dagger | \boldsymbol{X}\}$*,* λ_i *is the* i*-th eigenvalue of* Σ^{-1}*,* $\hat{Y}_i$ *is the* i*-th component of* $\hat{Y} = Q^\dagger Y$*, where* Q *is the unitary matrix containing the eigenvectors of* Σ^{-1}*.*

Proof. See Corollary 4.9 and Appendix B.4 below. □

Gaussian Approximation (Case 5)

Assuming that the signal $\boldsymbol{J}$ resulting form the jammer transmission is zero-mean Gaussian with covariance $\mathrm{E}\{\boldsymbol{J}\boldsymbol{J}^\dagger\} = \sigma_g^2 \sigma_V^2 I_T$ yields the following likelihood function:

$$\hat{p}_{\boldsymbol{Y}|\boldsymbol{X}}(Y|X) = \frac{1}{\pi^T |\Sigma_G|} \exp\left(-Y^\dagger \Sigma_G^{-1} Y\right), \quad (4.24)$$

where $\Sigma_G = \mathrm{E}\{\boldsymbol{Y}\boldsymbol{Y}^\dagger | \mathbf{X}\}$, $\tilde{\lambda}_i$ is the i-th eigenvalue of Σ_G^{-1}, $\tilde{Y}_i$ is the i-th component of $\tilde{Y} = \tilde{Q}^\dagger Y$, where $\tilde{Q}$ is the unitary matrix containing the eigenvectors of Σ_G^{-1}.

4.2.6 Statistical distribution of both $\boldsymbol{h}$ and $\boldsymbol{g}$ known

In this case the receiver knows that $\boldsymbol{h} \sim \mathcal{CN}(0, \sigma_h^2)$ and $\boldsymbol{g} \sim \mathcal{CN}(0, \sigma_g^2)$, where σ_h^2 and σ_g^2 are known. The exact likelihood function for this case is given in the following corollary:

Corollary 4.8. *Let $\boldsymbol{U} = \boldsymbol{h}\boldsymbol{X} + \boldsymbol{Z}$ and $\boldsymbol{J} = \boldsymbol{g}\boldsymbol{V}$, where $\boldsymbol{Z} \sim \mathcal{CN}(0, \sigma_Z^2 I_T)$, $\boldsymbol{V} \sim \mathcal{CN}(0, \sigma_V^2 I_T)$ and $\boldsymbol{X} \in \mathbb{C}^T$ are random vectors. The variables $\boldsymbol{g} \sim \mathcal{CN}(0, \sigma_g^2)$ and $\boldsymbol{h} \sim \mathcal{CN}(0, \sigma_h^2)$ are random scalars, while σ_h, σ_g, σ_Z, and σ_V are known deterministic scalars. The likelihood function of $\boldsymbol{Y} = \boldsymbol{U} + \boldsymbol{J}$ conditioned on $\boldsymbol{X}$ is given by:*

$$p_{\boldsymbol{Y}|\boldsymbol{X}}(Y|X; \sigma_h^2, \sigma_g^2) = \frac{1}{\pi^T |\Sigma|} \int_0^\infty \frac{1}{\prod_{i=1}^T \left(1 + \lambda_i \sigma_V^2 \sigma_g^2 t\right)} \exp\left(-t - \sum_{i=1}^T \frac{\lambda_i |\hat{Y}_i|^2}{1 + \lambda_i \sigma_V^2 \sigma_g^2 t}\right) dt, \quad (4.25)$$

where $\Sigma = \mathrm{E}\{\boldsymbol{U}\boldsymbol{U}^\dagger | \boldsymbol{X}\}$, λ_i is the i-th eigenvalue of Σ^{-1}, $\hat{Y}_i$ is the i-th component of $\hat{Y} = Q^\dagger Y$, where Q is the unitary matrix containing the eigenvectors of Σ^{-1}.

Proof. See Corollary 4.9 and Appendix B.4. □

Gaussian Approximation (Case 6)

Assuming that the signal $\boldsymbol{J}$ resulting form the jammer transmission is zero-mean Gaussian with covariance $\mathrm{E}\{\boldsymbol{J}\boldsymbol{J}^\dagger\} = \sigma_g^2 \sigma_V^2 I_T$ yields the likelihood function in (4.24).

Corollary 4.9. *The likelihood function given in Theorem 4.4 is a general case for those given in Corollaries 4.6, 4.7, and 4.8.*

Proof. This result can be readily proven by setting k_h, k_g, or both to zero in (4.18) when the receiver knows the statistical distribution of the corresponding channel. Doing so yields the likelihood functions given in (4.22), (4.23), and (4.25). □

Remark 2. *if the constellation vectors are equal-norm, i.e.,* $\|\boldsymbol{X}_i\| = \|\boldsymbol{X}_j\|, \forall \boldsymbol{X}_i, \boldsymbol{X}_j \in \mathcal{C}, i \neq j$*; then, the result of Corollary 4.5 holds, i.e., the vector* $\hat{X} \in \mathcal{C}$ *that maximizes* $|Y^\dagger X|$ *maximizes each of the exact likelihood functions in* (4.22)*,* (4.23)*, and* (4.25) *along with their approximate counterparts given by* (4.19) *and* (4.24)*. However, when the constellation vectors in* $\mathcal{C}$ *do not have equal norms, the ML detectors based on the exact likelihood functions exhibit performance advantage over their counterparts that are based on the approximate likelihood functions, cf. Section 4.3.* □

4.3 Simulation Results

In this section, we will provide Simulation results to illustrate the advantage of the ML detection scheme based on the exact likelihood functions over the one based on the Gaussian approximation of the received signal component induced by the jammer. As mentioned in Section 4.2, this advantage only exists when either the receiver does not know the transmitter channel, $\boldsymbol{h}$, or when the transmitted symbols have different norms, cf. Sections 4.2.3, 4.2.4, 4.2.5, and 4.2.6. This advantage vanishes when $\boldsymbol{h}$ is known to the receiver, cf. Sections 4.2.1, and 4.2.2, or when the symbols have identical norms as shown analytically.For completeness, the latter is also shown by simulations.

To examine the aforementioned advantage of the exact ML detection scheme, we constructed symbol constellations based on the method in [91]. In particular, to generate a complex constellation $\mathcal{C}$ with 2^n T-dimensional symbols, we use the following procedure:

Constellation Design

1. Generate I random matrices of size $T \times 2^n$ from the standard complex Gaussian

distribution. For each matrix, compute the QR-decomposition, where Q is the unitary component of the matrix and R is its lower triangular component. Let Q_i be the Q-component of the i-th matrix, $i = 1, \ldots, I$. The set $\{Q_i\}$ is known to be asymptotically isotropically distributed on the unitary group of matrices [91].

2. Out of all the generated matrices, select the matrix whose Q component has the largest angular separation between its columns, that is, select the i^*'th matrix, where $i^* = \arg\min_i \max |(q_m^i)\dagger q_n^i|$, q_r^i is the r-th column of Q_i, $r = 1, \ldots, 2^n$.

3. Obtain the desired constellation, $\mathcal{C}$, by right multiplying Q_{i^*} by a $2^n \times 2^n$ diagonal matrix A, that is $\mathcal{C} = Q_{i^*}A$, where $A_{ii} = \sqrt{\frac{2i}{2^n+1}}$.

This method is proposed in [91] and is included here for completeness.

All simulations were conducted using MATLAB software Package [92]. In all simulations we set the noise variance to be $\sigma_Z^2 = 0.5$ and the jamming signal variance to be $\sigma_V^2 = 4.5$. These values were selected to have a 10 dB total power in the noise plus jamming signal. To ensure that the average channel power gain of both the transmitter channel and the jammer channel remain constant under different values of k_h and k_g, the transmitter channel variance, σ_h^2, and the jammer channel variance, σ_g^2, were set to $\sigma_h^2 = \dfrac{1}{k_h^2+1}$ and $\sigma_g^2 = \dfrac{1}{k_g^2+1}$, respectively. The Symbol Error Rate (SER) of each detector is evaluated at varying values of the signal to jamming plus noise ratio (SJNR). The SJNR in dB is calculated as follows:

$$SJNRindB = 10\log_{10}\left(\frac{\text{Average Transmitted Symbol Power}}{\text{Jamming Signal Power + Noise Power}}\right)$$

The symbol length, T, was set to either 2, 4, or 6. A 32-symbol constellation generated with the aforementioned technique is used in all simulations.

Example 1 In this example, we consider the case in which the k-factor of the jammer's channel, k_g, is equal to zero for various values of the k-factor of the transmitter's channel, k_h. This corresponds to the situation when the jammer has no LOS whereas the transmitter has an LOS (For completeness, the case when the transmitter has no LOS, i.e., $k_h = 0$ is also considered in this example). This might be the scenario where the transmitter is mobile and air-borne while the jammer is stationary, cf. Sections 4.2.4 and 4.2.6. Using these settings we obtained the symbol error rates (SERs) reported in Figure 4.2, for both the exact and approximate ML detectors.

From this figure, it can be seen that the exact ML detector always outperforms the approximate one. Furthermore, it can be seen that the advantage of the exact ML detector becomes more pronounced as k_h increases, i.e., when the LOS of the transmitter is strong.

Example 2 In Example 1, we investigated the effect of increasing the strength of the LOS component of the transmitter channel when the jammer channel has no LOS component for a symbol length $T = 4$. The greatest SER advantage of the exact detector over the approximate one was achieved when $k_h = 5$. Hence, in this example, we consider a complementary case in which the k-factor of the transmitter's channel is set to $k_h = 5$, corresponding to a scenario in which the transmitter has a strong LOS component which may be the case when the transmitter is static air-borne or highly-mounted. Various values of the symbol length T and the k-factor of the jammer's channel, k_g, are considered including the case with $k_g = 0$, cf. Sections 4.2.3 and 4.2.4. The SERs obtained in these cases are reported in Figures 4.3, 4.4, and 4.5 for both the exact and approximate ML

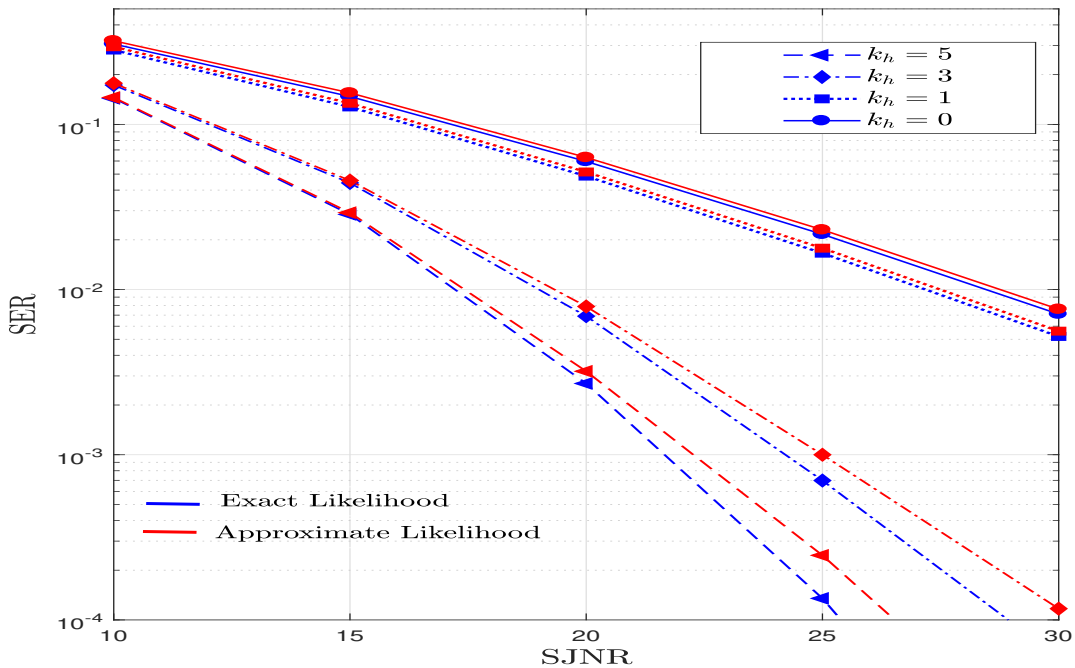

Figure 4.2: $T=4$, $k_g=0$ and various values of k_h.

detectors.

It can be seen from Figures 4.3, 4.4, and 4.5 that the exact ML detector significantly outperforms the approximate one for all values of K_g and T. Furthermore, it can be seen form these figures that increasing T yields a power gain for both detectors.

Example 3 In this example we consider the case in which the constellation symbols have equal norms. The k-factor of the transmitter's channel is set to $k_h = 5$, and the symbol length is set to $T = 4$. Various values of the k-factor of the jammer's channel, k_g, are considered including the case with $k_g = 0$. The SER curves obtained are reported in

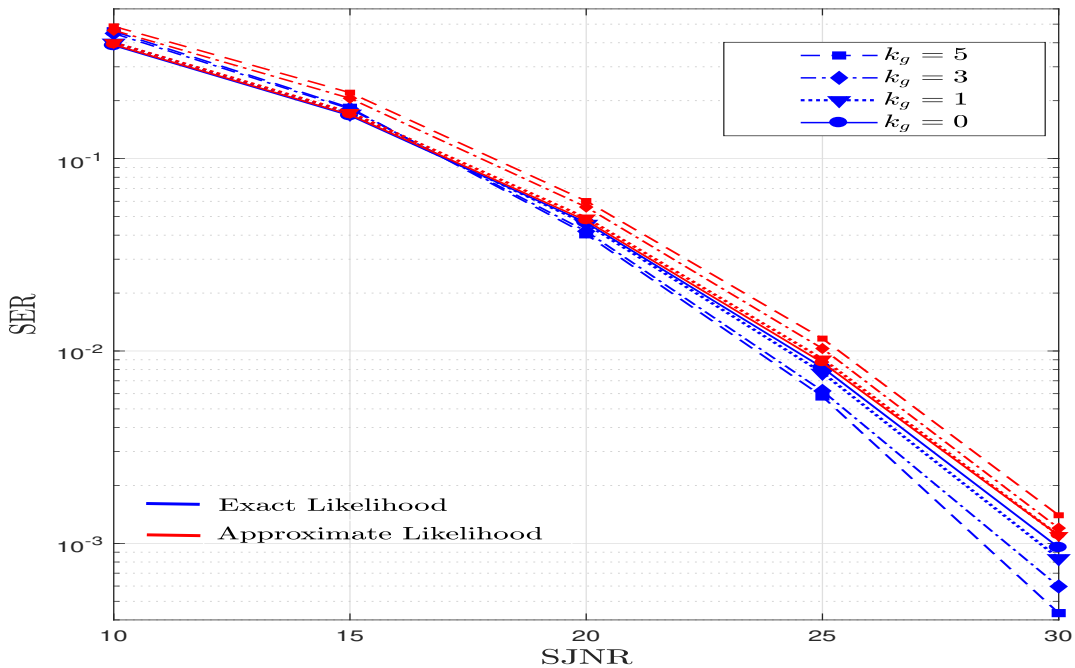

Figure 4.3: $T = 2$, $k_h = 5$ and various values of k_g.

Figure 4.6. It can be seen form this figure that the exact ML detector and the Gaussian approximate one yield identical performance in compliance with the analytic results.

Example 4 In this example we investigate the effect of the k-factors, k_h and k_g, on the performance of the exact ML detector. The symbol length is set to $T = 4$, the signal to jamming signal and noise ratio is SJNR $\in \{10, 20\}$ dB, while the k-factors k_h and $k_g \in \{0, 1, 2, 3, 4, 5\}$. The results obtained in this example are reported in Figures 4.7 and 4.8. It can be seen form Figure 4.7 that at SJNR $= 10$ dB, increasing k_g, i.e., intensifying the LOS component of the jammer's channel, increases the SER especially if the transmitter's channel has a weak LOS component ($k_h < 4$). On the contrary, it can be seen from Figure

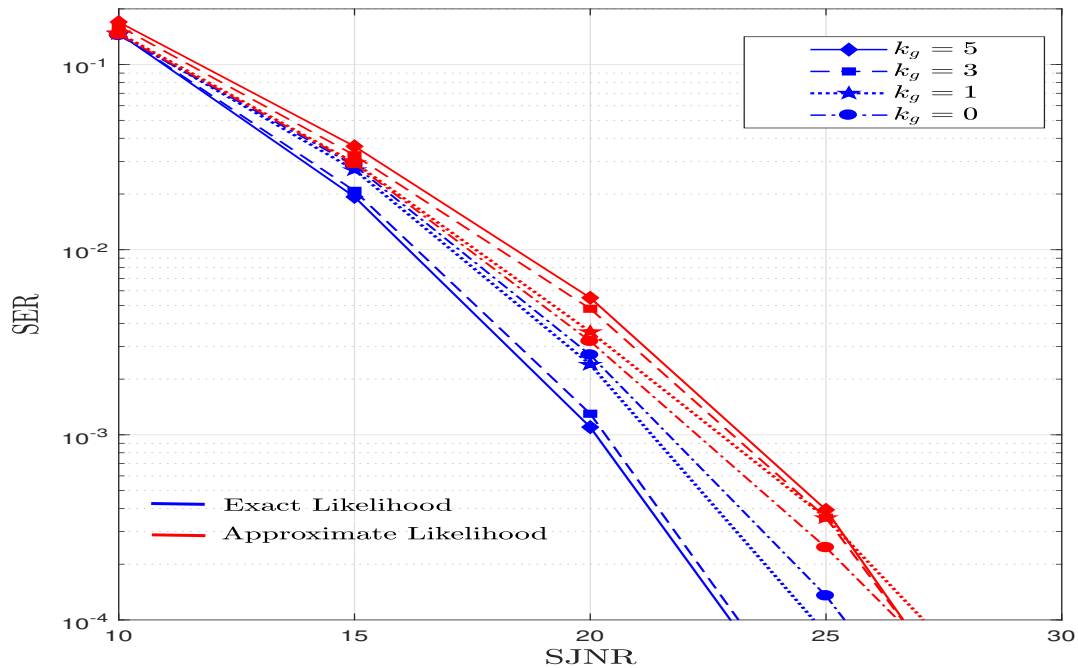

Figure 4.4: $T = 4$, $k_h = 5$ and various values of k_g.

4.8 that at SJNR $= 20$ dB, increasing k_g decreases the SER especially if the transmitter's channel has a strong LOS component ($k_h > 2$); however, if the transmitter's channel has a weak LOS component ($k_h \leq 2$), increasing k_g has a negligible effect on the SER.

To gain insight into the results reported in Figures 4.7 and 4.8, we observe that the integrand in (4.18) consists of two parts. The first part does not depend on the rotated received signal, $\hat{Y}$, or the rotated transmitted signal vector, $\hat{X}$, and hence does not depend on the SJNR. This part depends on k_g only and is given by $I_0\left(2k_g\sqrt{t}\right)$. The second part is given by the rest of the integrand in (4.18). This part depends on the SJNR through $\hat{Y}$, $\hat{X}$, the eigenvalues of Σ^{-1}, $\{\lambda_i\}_{i=1}^{T}$, and the values of k_h and k_g.

The decision making mechanism can be interpreted as follows: for every t, the second

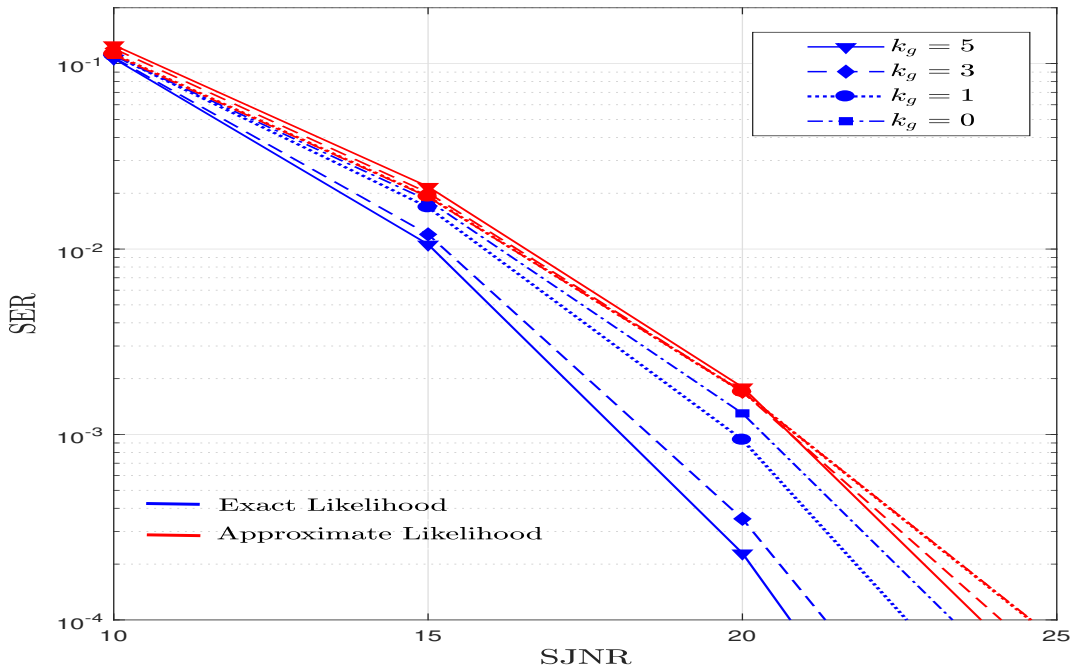

Figure 4.5: $T=6$, $k_h=5$ and various values of k_g.

part of the integrand in (4.18) yields a tentative decision on the symbol that has most likely been transmitted, whereas the first part, $I_0\left(2k_g\sqrt{t}\right)$, acts as weighting factor that reinforces this decision. Now, we notice that, for a given t, the function $I_0\left(2k_g\sqrt{t}\right)$ is monotonically increasing in k_g. Hence, at lower SJNRs, larger values of k_g tend to not only reduce the SJNR, but also to reinforce erroneous decisions, which are more likely to occur at those SJNRs, thereby increasing the symbol error rate. The opposite mechanism occurs at higher SJNRs. In particular, larger values of k_g tend to reinforce correct decisions, which are more likely to occur at those SJNRs, thereby reducing the symbol error rate.

Finally, it can be seen from Figures 4.7 and 4.8 that k_h has a more significant effect on the SER. Increasing k_h decreases the SER regardless of k_g.

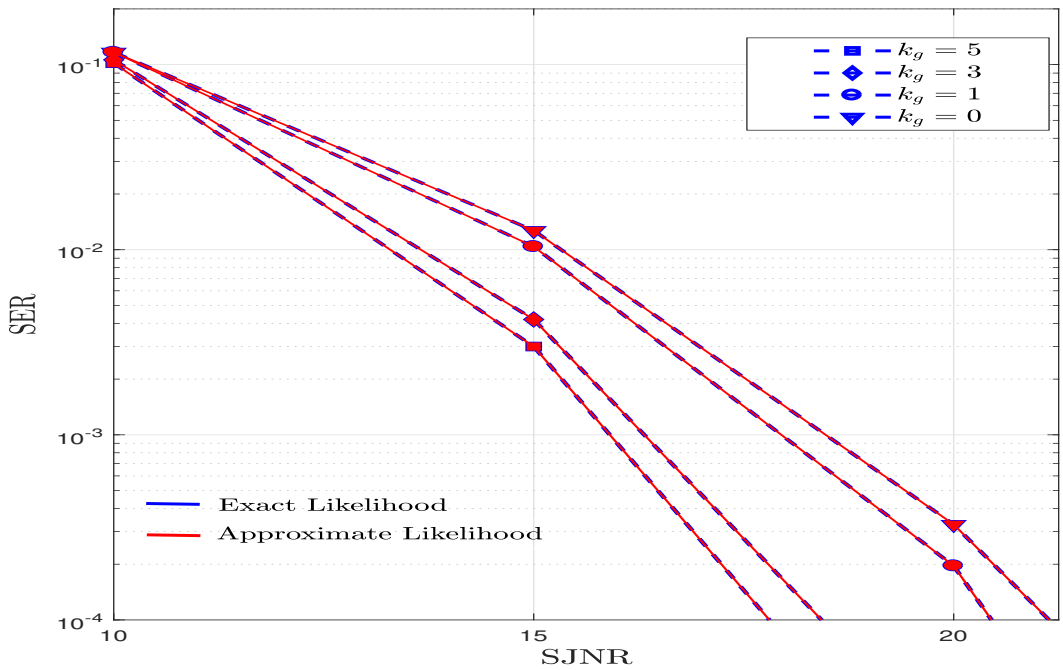

Figure 4.6: $T = 4$, $k_h = 5$ and various values of k_g.

4.4 Conclusion

This chapter considered a scenario in which a transmitter communicates with a receiver in the presence of a continuous proactive jammer sending a zero-mean complex Gaussian signal over a complex Gaussian channel. The likelihood functions of the non-Gaussian signal induced at the receiver are derived for cases corresponding to whether the receiver has full CSI, full CDI, or partial CDI of the transmitter's channel. The jammer's channel CDI is either fully or partially available at the receiver. Using the derived likelihood expressions,

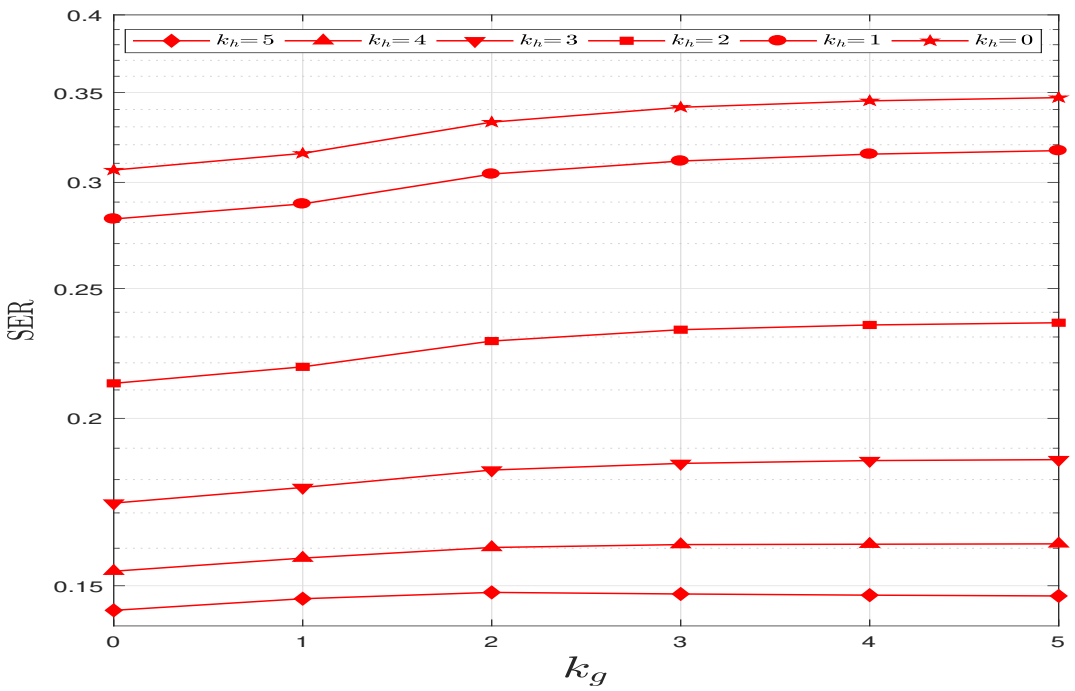

Figure 4.7: $T = 4$, SJNR = 10 dB and various values of k_g and k_h.

the optimal ML detector is developed. The cases in which the non-Gaussian signals resulting from the jammer's transmission can be approximated by Gaussian signals without affecting the efficacy of the ML detector are identified. For these cases, the equivalence of exact and approximated ML detectors is proved analytically and by simulations. Furthermore, cases in which the Gaussian approximation ML detector is not equivalent to the exact ML detector are identified. In these case, extensive simulations are conducted and the advantage of the exact ML detector over the Gaussian approximation is demonstrated.

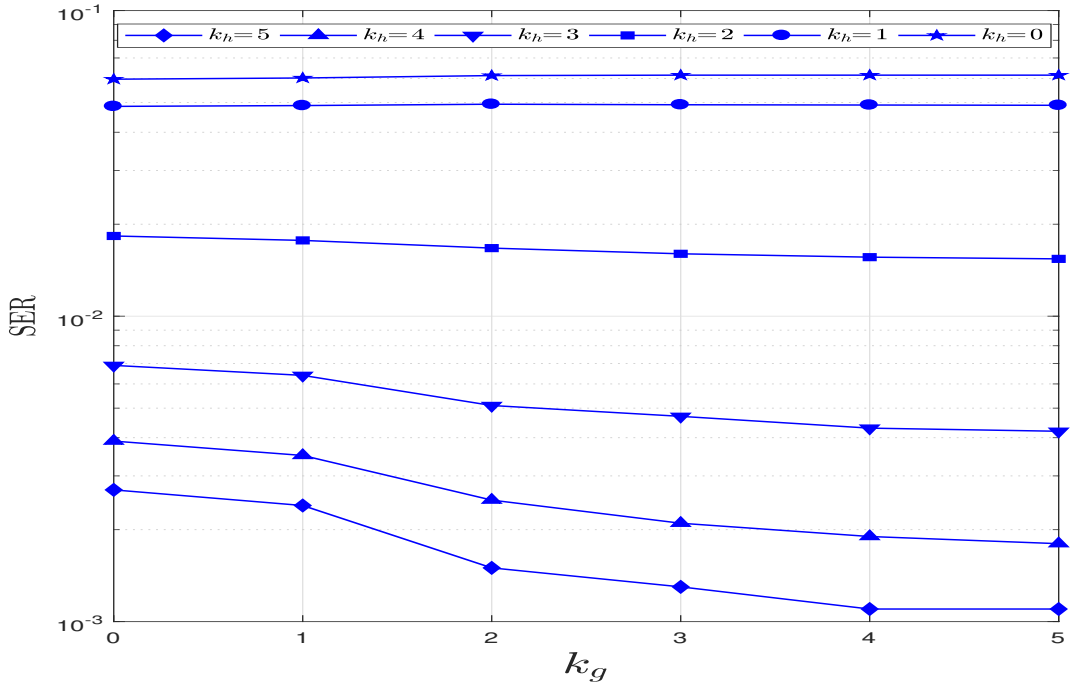

Figure 4.8: $T = 4$, SJNR = 20 dB and various values of k_g and k_h.

Chapter 5

SIDO with multiple transmissions

5.1 Introduction

In this chapter, we consider a scenario in which a single-antenna transmitter sends multi-dimensional complex symbols to a double-antenna receiver in the presence of a single-antenna barrage jammer. The transmitter-receiver and the jammer-receiver channels are assumed to be block fading independent Gaussian matrices with coherence time that is larger than the time required for transmitting the multi-dimensional symbol. The jammer's signal is represented by a vector of independent complex Gaussian random variables. Given the transmitted symbols, the received signal can be represented by the random vector resulting from adding a Gaussian vector to the product of a block diagonal Gaussian matrix and a Gaussian vector. We derive the conditional pdf of the received signal vector for the cases in which either full or partial channel distribution information (CDI) about the transmitter-receiver and jammer-receiver channels is available at the receiver. The block fading assumption along with the multiplication inherent in this model interweaves

the components of the received signal, thereby complicating the derivation of the required conditional pdf and rendering it intractable for receivers with more than two antennas. To the best of our knowledge, the scenario considered herein was not considered in the literature and, in a sense, complements the results reported in [86], [87], and in Chapter 4.

This chapter is organized as follows. In Section 5.2 we present the system model and the problem statement for four different cases. Expressions for the likelihood functions corresponding to each of these cases are presented in Section 5.3. This section also presents expressions for the likelihood function obtained by treating the jammer's component of the received signal as if it were Gaussian distributed. In Section 5.4 we present simulation results and Section 5.5 concludes the chapter. For ease of flow, most derivations are relegated to the appendices.

5.2 System Model and Problem Statement

We consider the system depicted in Figure 5.1, i.e., a system composed of a single-antenna transmitter communicating with a double-antenna receiver in the presence of a single-antenna barrage jammer. The transmitter-receiver channel, $\boldsymbol{H} \in \mathbb{C}^{2\times 1}$, and the jammer-receiver channel, $\boldsymbol{G} \in \mathbb{C}^{2\times 1}$, are assumed to be block fading vector channels, i.e., they remain constant during the transmission of any data symbol and take independent realizations for subsequent symbols. Unlike their scalar counterparts, the block fading vector channels considered herein interweave the components of the received signal, rendering the derivation of the likelihood function intractable for more than two receive antennas.

Both $\boldsymbol{H}$ and $\boldsymbol{G}$ are modeled as independent proper complex Gaussian random vectors with mean vectors $\boldsymbol{\mu}_H$ and $\boldsymbol{\mu}_G$, and covariance matrices $\sigma_h^2 I_2$ and $\sigma_g^2 I_2$, respectively, where σ_h and σ_g are known scalars, i.e., $\boldsymbol{H} \sim \mathcal{CN}(\boldsymbol{\mu}_H, \sigma_h^2 I_2)$ and $\boldsymbol{G} \sim \mathcal{CN}(\boldsymbol{\mu}_G, \sigma_g^2 I_2)$. The

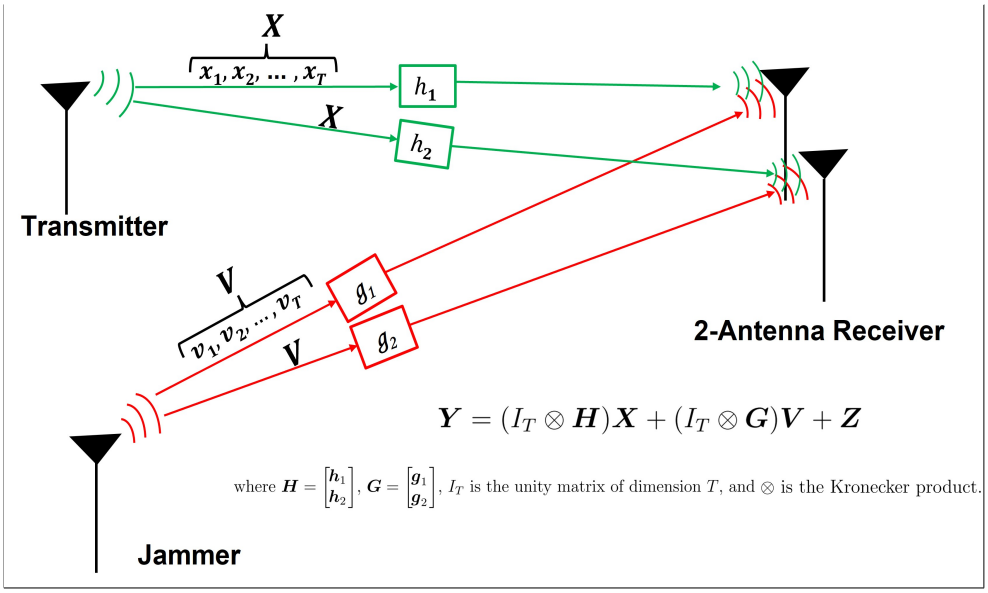

Figure 5.1: System Model.

transmitter-receiver and the jammer-receiver distances are assumed to be much larger than the receiver's inter-antenna spacing, this assumption allows us to express the mean vectors of $\boldsymbol{H}$ and $\boldsymbol{G}$ as $\boldsymbol{\mu}_H = |\boldsymbol{\mu}_h|[e^{-\jmath\boldsymbol{\theta}_{h_1}} \;\; e^{-\jmath\boldsymbol{\theta}_{h_2}}]^\dagger$ and $\boldsymbol{\mu}_G = |\boldsymbol{\mu}_g|[e^{-\jmath\boldsymbol{\theta}_{g_1}} \;\; e^{-\jmath\boldsymbol{\theta}_{g_2}}]^\dagger$, where $|\boldsymbol{\mu}_h|$ are $|\boldsymbol{\mu}_g|$ are known scalars, whereas $\boldsymbol{\theta}_{h_1}, \boldsymbol{\theta}_{h_2}, \boldsymbol{\theta}_{g_1}$, and $\boldsymbol{\theta}_{g_2}$ are $i.i.d$ random scalars uniformly distributed in $[0, 2\pi)$. The transmitter, the jammer, and the receiver can be mobile or airborne, which is the case in vehicle-to-vehicle (V2V) and unmanned aerial vehicle (UAVs) communications. Hence, both channels, $\boldsymbol{H}$ and $\boldsymbol{G}$, are assumed to be subject to independent fading processes. Both channels can be Rayleigh or Rician fading depending on whether their respective means, $\boldsymbol{\mu}_H$ and $\boldsymbol{\mu}_G$, are zero or non-zero vectors [26]. For the case in which the transmitter-receiver channel, $\boldsymbol{H}$, is Rayleigh fading, i.e., $|\boldsymbol{\mu}_h| = 0$, we assume that the receiver has full CDI about $\boldsymbol{H}$. On the other hand, for the case in which $\boldsymbol{H}$ is Rician fading, e.g., the case when either the transmitter and/or the receiver is a UAV [89], we assume that the receiver has a partial CDI about $\boldsymbol{H}$ represented by the

relative strength of its line-of-sight (LOS) components given by its k-factor, $k_h = \frac{|\boldsymbol{\mu}_h|}{\sigma_h}$. Analogously, $\boldsymbol{G}$ is either Rayleigh fading and the receiver knows σ_g, or $\boldsymbol{G}$ is Rician fading and the receiver knows σ_g and $k_g = \frac{|\boldsymbol{\mu}_g|}{\sigma_g}$.

The transmitted symbol, the jamming signal, and the additive noise at the receiver are denoted by $\boldsymbol{X} \in \mathbb{C}^T$, $\boldsymbol{V} \in \mathbb{C}^T$, and $\bar{\boldsymbol{Z}} \in \mathbb{C}^{2\times T}$, respectively. The jamming vector, $\boldsymbol{V}$, and the vectorized additive white Gaussian noise, $\boldsymbol{Z} = \text{vec}(\bar{\boldsymbol{Z}})$, are assumed to be independent circularly symmetric complex Gaussian random vectors, i.e., $\boldsymbol{V} \sim \mathcal{CN}(\boldsymbol{0}, \sigma_V^2 I_T)$ and $\boldsymbol{Z} \sim \mathcal{CN}(\boldsymbol{0}, \sigma_Z^2 I_{2T})$, where σ_V and σ_Z are known scalars. The received signal is denoted by $\bar{\boldsymbol{Y}} \in \mathbb{C}^{2\times T}$ and is given by:

$$\bar{\boldsymbol{Y}} = \boldsymbol{H}(\boldsymbol{X}^*)^\dagger + \boldsymbol{G}(\boldsymbol{V}^*)^\dagger + \bar{\boldsymbol{Z}}. \tag{5.1}$$

It can be shown that the vectorized version of (5.1) is given by:

$$\boldsymbol{Y} = (I_T \otimes \boldsymbol{H})\boldsymbol{X} + (I_T \otimes \boldsymbol{G})\boldsymbol{V} + \boldsymbol{Z}, \tag{5.2}$$

where $\boldsymbol{Y} \in \mathbb{C}^{2T}$ and $\otimes$ denotes the Kronecker product operator.

This chapter aims at developing the ML detector for each of the four cases outlined hereinabove. For all these cases, we show that the ML detector outperforms the detector based on the Gaussian approximation of the signal induced at the receiver by the jammer transmission. This contrasts with the case in which the receiver has a single antenna. In that case, the exact detector and the Gaussian approximation detector coincide when the constellation symbols have unit norm.

The four cases considered herein are the following.

1. *Statistical distribution of both $\boldsymbol{H}$ and $\boldsymbol{G}$ partially known:* The ML detector decides

in favor of the constellation point $\hat{X}$ given by

$$\hat{X} = \arg\max_{X \in \mathcal{C}} p_{\boldsymbol{Y}|\boldsymbol{X}} \left(Y \middle| X; |\boldsymbol{\mu}_h|, \sigma_h^2, |\boldsymbol{\mu}_g|, \sigma_g^2 \right). \tag{5.3}$$

In this case, the phases of the mean vectors of $\boldsymbol{H}$ and $\boldsymbol{G}$, i.e., $\boldsymbol{\theta}_{\mu_{h_1}}$, $\boldsymbol{\theta}_{\mu_{h_2}}$, $\boldsymbol{\theta}_{\mu_{g_1}}$, and $\boldsymbol{\theta}_{\mu_{g_2}}$ are random and unknown. This situation arises when both the transmitter and the jammer channels have LOS components.

2. *Statistical distribution of $\boldsymbol{H}$ partially known and statistical distribution of $\boldsymbol{G}$ known:* The ML detector decides in favor of the constellation point $\hat{X}$ given by

$$\hat{X} = \arg\max_{X \in \mathcal{C}} p_{\boldsymbol{Y}|\boldsymbol{X}} \left(Y \middle| X; |\boldsymbol{\mu}_h|, \sigma_h^2, \sigma_g^2 \right). \tag{5.4}$$

In this case the phases of the mean vector of $\boldsymbol{H}$, i.e., $\boldsymbol{\theta}_{\mu_{h_1}}$ and $\boldsymbol{\theta}_{\mu_{h_2}}$, are random and unknown while the mean vector of $\boldsymbol{G}$ is zero. This situation arises when the transmitter channel has an LOS component but the jammer channel does not.

3. *Statistical distribution of $\boldsymbol{H}$ known and statistical distribution of $\boldsymbol{G}$ partially known:* The ML detector decides in favor of the constellation point $\hat{X}$ given by

$$\hat{X} = \arg\max_{X \in \mathcal{C}} p_{\boldsymbol{Y}|\boldsymbol{X}} \left(Y \middle| X; |\boldsymbol{\mu}_g|, \sigma_g^2, \sigma_h^2 \right). \tag{5.5}$$

Complementary to the previous case, the phases of the mean vector of $\boldsymbol{G}$, i.e., $\boldsymbol{\theta}_{\mu_{g_1}}$ and $\boldsymbol{\theta}_{\mu_{g_2}}$, are random and unknown while the mean vector of $\boldsymbol{H}$ is zero. In this situation the jammer channel has an LOS component but the transmitter channel does not.

4. *Statistical distribution of both* $\boldsymbol{H}$ *and* $\boldsymbol{G}$ *known:* The ML detector decides in favor of the constellation point $\hat{X}$ given by

$$\hat{X} = \arg\max_{X \in \mathcal{C}} p_{\boldsymbol{Y}|\boldsymbol{X}} \left(Y \middle| X; \sigma_h^2, \sigma_g^2 \right). \tag{5.6}$$

In this case both $\boldsymbol{H}$ and $\boldsymbol{G}$ have zero mean vectors, i.e., neither the transmitter channel nor the jammer channel has an LOS component.

In the next section, we will provide exact and approximate ML detection rules for each of the aforementioned cases.

5.3 Likelihood function expressions for the different CSI cases

In this section, we present the exact likelihood function expressions for the cases outlined in the previous section along with the likelihood expressions based on the Gaussian approximation of the non-Gaussian signal resulting from the jammer's transmissions.

5.3.1 Statistical distribution of both $\boldsymbol{H}$ and $\boldsymbol{G}$ partially known:

In this case the transmitter channel and the jammer channel have LOS components. This might be the case when the jammer and the transmitter are airborne, or when the receiver is airborne or highly mounted.

The exact likelihood function

The exact likelihood function for this case is given in the following theorem:

Theorem 5.1. *Let* $\boldsymbol{Y} = (I_T \otimes \boldsymbol{H})\boldsymbol{X} + (I_T \otimes \boldsymbol{G})\boldsymbol{V} + \boldsymbol{Z}$, *where* $\boldsymbol{X} \in \mathbb{C}^T$, $\boldsymbol{V} \sim \mathcal{CN}(\boldsymbol{0}, \sigma_V^2 I_T)$, $\boldsymbol{Z} \sim \mathcal{CN}(\boldsymbol{0}, \sigma_Z^2 I_{2T})$, $\boldsymbol{H} \sim \mathcal{CN}\left(|\boldsymbol{\mu}_h|[e^{-\jmath\boldsymbol{\theta}_{\mu_{h_1}}} \;\; e^{-\jmath\boldsymbol{\theta}_{\mu_{h_2}}}]^\dagger, \sigma_h^2 I_T\right)$ *and* $\boldsymbol{G} \sim \mathcal{CN}\left(|\boldsymbol{\mu}_g|[e^{-\jmath\boldsymbol{\theta}_{\mu_{g_1}}} \;\; e^{-\jmath\boldsymbol{\theta}_{\mu_{g_2}}}]^\dagger, \sigma_g^2 I_T\right)$. *The scalars* $|\boldsymbol{\mu}_h|$, $|\boldsymbol{\mu}_g|$, σ_h, σ_g, σ_Z, *and* σ_V *are known, and the phases* $\boldsymbol{\theta}_{\mu_{h_1}}$, $\boldsymbol{\theta}_{\mu_{h_2}}$, $\boldsymbol{\theta}_{\mu_{g_1}}$, *and* $\boldsymbol{\theta}_{\mu_{g_2}}$ *are i.i.d. random scalars uniformly distributed over* $[0, 2\pi)$. *Let* $k_h = \dfrac{|\boldsymbol{\mu}_h|}{\sigma_h}$ *and* $k_g = \dfrac{|\boldsymbol{\mu}_g|}{\sigma_g}$. *The likelihood function of* $\boldsymbol{Y}$ *conditioned on* $\boldsymbol{X} = X$ *is given by:*

$$f_{\boldsymbol{Y}|\boldsymbol{X}}(Y|X) = \frac{\exp\left(-2k_g^2\right)}{4\pi^{2T+2}\sigma_g^4\sigma_v^4|\Sigma|^2} \int_0^{2\pi}\int_0^{2\pi} \exp\Big(-(Y_o - k_h\sigma_h e^{\jmath\theta_{\mu_{h_1}}} X)^\dagger \Sigma^{-1} (Y_o - k_h\sigma_h e^{\jmath\theta_{\mu_{h_1}}} X)\Big)$$
$$\times \exp\left(-(Y_e - k_h\sigma_h e^{\jmath\theta_{\mu_{h_2}}} X)^\dagger \; \Sigma^{-1} (Y_e - k_h\sigma_h e^{\jmath\theta_{\mu_{h_2}}} X)\right) \Psi_{X,Y,k_h}(\theta_{\mu_{h_1}}, \theta_{\mu_{h_2}}) \; d\theta_{\mu_{h_1}} d\theta_{\mu_{h_2}}, \quad (5.7)$$

where $\Sigma = \sigma_h^2 X X^\dagger + \sigma_z^2 I_T$, *and*

$$\Psi_{X,Y,k_h}(\theta_{\mu_{h_1}}, \theta_{\mu_{h_2}}) =$$
$$\int_0^1\int_0^1 \frac{t \; (\; \bar{t} \;)^{T-3}}{|\Lambda t + \bar{t} \; I_T|} \exp\left(\frac{-t}{\sigma_g^2\sigma_v^2\bar{t}}\right) \exp\Big(\bar{u}(Y_o - k_h\sigma_h e^{\jmath\theta_{\mu_{h_1}}} X)^\dagger \Upsilon(\Sigma, t)(Y_o - k_h\sigma_h e^{\jmath\theta_{\mu_{h_1}}} X)\Big)$$
$$\times \exp\Big(u(Y_e - k_h\sigma_h e^{\jmath\theta_{\mu_{h_2}}} X)^\dagger \Upsilon(\Sigma, t)(Y_e - k_h\sigma_h e^{\jmath\theta_{\mu_{h_2}}} X)\Big) \; I_0\left(\frac{2k_g}{\sigma_g\sigma_v}\sqrt{\frac{\bar{u} \; t}{\bar{t}}}\right) I_0\left(\frac{2k_g}{\sigma_g\sigma_v}\sqrt{\frac{u \; t}{\bar{t}}}\right)$$
$$\times \; I_0\Big(4u\bar{u}t|(Y_o - k_h\sigma_h e^{\jmath\theta_{\mu_{h_1}}} X)^\dagger \Upsilon(\Sigma, t)(Y_e - k_h\sigma_h e^{\jmath\theta_{\mu_{h_2}}} X)|\Big) \; du \; dt, \quad (5.8)$$

where $Y_o = [Y_1^*, \ldots, Y_{2i-1}^*, \ldots, Y_{2T-1}^*]^\dagger$, $Y_e = [Y_2^*, \ldots, Y_{2i}^*, \ldots, Y_{2T}^*]^\dagger$, $\bar{t} = 1 - t$, $\bar{u} = 1 - u$, Λ *is the matrix of eigenvalues of* Σ^{-1}, *and* $\Upsilon(\Sigma, t) = \Sigma\left(I_T + \frac{\bar{t}}{t}\Sigma^{-1}\right)^{-1}$.

Proof. See Appendix C.1. □

We note that $\boldsymbol{Y}_o$ and $\boldsymbol{Y}_e$ are the outputs of the first and second receive antennas. We also note the symmetry of the expressions in (5.7) and (5.8) in $\boldsymbol{Y}_o$ and $\boldsymbol{Y}_e$, which reflects the symmetry of the channels observed by the two antennas. The computation of (5.8) is compounded by the fact that a term of the integrand in (5.8), namely, $I_0\Big(4u\bar{u}\ t|(Y_o - k_h\sigma_h e^{\jmath\theta_{\mu_{h_1}}}X)^\dagger \Upsilon(\Sigma, t)(Y_e - k_h\sigma_h e^{\jmath\theta_{\mu_{h_2}}}X)|\Big)$, contains the inner product of the output of the first and second receive antennas. This portends the difficulties that are likely to be encountered if the proposed technique were to be used to obtain the likelihood function for the case with more than two receive antennas.

Gaussian Approximation

Due to mathematical tractability, the signal induced by the jammer at the receiver has been commonly assumed to be Gaussian distributed, see, e.g., [43, 70, 73, 76–78]. In this chapter, we investigate this assumption for all considered cases.

Approximating the signal resulting form the jammer transmission at the i-th receive antenna, $i \in \{1, 2\}$, by a Gaussian vector $\boldsymbol{J}_i = \boldsymbol{g}_i\boldsymbol{V}$, where $\boldsymbol{J}_i \sim \mathcal{CN}\left(\boldsymbol{0}_T, \sigma_g^2\sigma_v^2 I_T\right)$ yields the likelihood function in the following lemma.

Lemma 5.1. *Let $\boldsymbol{Y}$, $\boldsymbol{X}$, $\boldsymbol{V}$, $\boldsymbol{Z}$, $\boldsymbol{H}$, $\boldsymbol{G}$, k_h and k_g be as defined in Theorem 5.1, and let $\boldsymbol{J} = \boldsymbol{g}_i\boldsymbol{V}$ where $i \in \{1, 2\}$. Assume that $\boldsymbol{J} \sim \mathcal{CN}(\boldsymbol{0}_T, \sigma_g^2\sigma_V^2 I_T)$, then the likelihood function of $\boldsymbol{Y}$ conditioned on $\boldsymbol{X} = X$ is given by:*

$$f_{\boldsymbol{Y}|\boldsymbol{X}}(Y|X) = \frac{1}{\pi^{2T}|\Sigma_N|^2}\exp\left(-Y_o^\dagger\Sigma_N^{-1}Y_o - Y_e^\dagger\Sigma_N^{-1}Y_e - 2k_h^2\sigma_h^2X^\dagger\Sigma_N^{-1}X\right)$$
$$\times I_0\left(2k_h\sigma_h|Y_o^\dagger\ \Sigma_N^{-1}X|\right) I_0\left(2k_h\sigma_h|Y_e^\dagger\ \Sigma_N^{-1}X|\right), \tag{5.9}$$

where $\Sigma_N = \sigma_h^2XX^\dagger + (\sigma_g^2\sigma_v^2 + \sigma_Z^2)I_T$, and Y_o and Y_e are defined in Theorem 5.1.

Proof. See Appendix C.2. □

It can be noticed from (5.9) that in this case, and in the other cases as will be seen later, the likelihood function based on the Gaussian approximation does not incorporate the k-factor of the jammer's channel, k_g. Not incorporating this information renders the performance of the detector based on this likelihood function inferior to the one based on the exact one, cf. Section 5.4 below.

5.3.2 Statistical distribution of $\boldsymbol{H}$ partially known and statistical distribution of $\boldsymbol{G}$ known:

The conditional statistical distribution of the received signal for this case is required for optimal detection when the jammer-receiver channel does not have an LOS component, whereas the transmitter-receiver channel has an LOS component with a known k-factor. Such a scenario may arise when both the jammer and the receiver are ground-based and the transmitter is airborne or highly mounted.

The exact likelihood function

The exact likelihood function for this case is given in the following corollary.

Corollary 5.1. *Let $\boldsymbol{Y}$, $\boldsymbol{X}$, $\boldsymbol{V}$, $\boldsymbol{Z}$, $\boldsymbol{H}$, Σ, $\boldsymbol{\theta}_{\mu_{h_1}}$, $\boldsymbol{\theta}_{\mu_{h_2}}$ and k_h be as defined in Theorem 5.1, and let $\boldsymbol{G} \sim \mathcal{CN}\left(\mathbf{0}_T, \sigma_g^2 I_2\right)$ where σ_g is a known scalar. The likelihood function of $\boldsymbol{Y}$*

conditioned on $\boldsymbol{X} = X$ *is given by:*

$$f_{\boldsymbol{Y}|\boldsymbol{X}}(Y|X) = \frac{1}{4\pi^{2T+2}\sigma_g^4\sigma_v^4|\Sigma|^2}\int_0^{2\pi}\int_0^{2\pi}\exp\Big(-(Y_o - k_h\sigma_h e^{\jmath\theta_{\mu_{h_1}}}X)^\dagger\Sigma^{-1}(Y_o - k_h\sigma_h e^{\jmath\theta_{\mu_{h_1}}}X)\Big)$$
$$\times\exp\Big(-(Y_e - k_h\sigma_h e^{\jmath\theta_{\mu_{h_2}}}X)^\dagger\ \Sigma^{-1}(Y_e - k_h\sigma_h e^{\jmath\theta_{\mu_{h_2}}}X)\Big)\ \Phi_{X,Y,k_h}(\theta_{\mu_{h_1}},\theta_{\mu_{h_2}})\ d\theta_{\mu_{h_1}}d\theta_{\mu_{h_2}}, \tag{5.10}$$

where

$$\Phi_{X,Y,k_h}(\theta_{\mu_{h_1}},\theta_{\mu_{h_2}}) = \int_0^1\int_0^1 \frac{t\ (\ \bar{t}\ )^{T-3}}{|\Lambda t + \bar{t}\ I_T|}\exp\left(\frac{-t}{\sigma_g^2\sigma_v^2\bar{t}}\right)$$
$$\times\exp\Big(\bar{u}(Y_o - k_h\sigma_h e^{\jmath\theta_{\mu_{h_1}}}X)^\dagger\Upsilon(\Sigma,t)(Y_o - k_h\sigma_h e^{\jmath\theta_{\mu_{h_1}}}X)\Big)$$
$$\times\exp\Big(u(Y_e - k_h\sigma_h e^{\jmath\theta_{\mu_{h_2}}}X)^\dagger\Upsilon(\Sigma,t)(Y_e - k_h\sigma_h e^{\jmath\theta_{\mu_{h_2}}}X)\Big)$$
$$\times I_0\Big(4u\bar{u}t|(Y_o - k_h\sigma_h e^{\jmath\theta_{\mu_{h_1}}}X)^\dagger\Upsilon(\Sigma,t)(Y_e - k_h\sigma_h e^{\jmath\theta_{\mu_{h_2}}}X)|\Big)\ du\ dt, \tag{5.11}$$

where Λ, $\bar{t}$, Y_o, Y_e, $\Upsilon(\Sigma,t)$, *and* $\bar{u}$ *are defined in Theorem 5.1.*

Proof. Setting k_g to zero in (5.7) and (5.8) and noticing that $I_0(0) = 1$ yields (5.10) and (5.11), respectively. □

It can be noticed that the role of the function $\Phi_{X,Y,k_h}(\theta_{\mu_{h_1}},\theta_{\mu_{h_2}})$ in (5.10) is similar to the role of the function $\Psi_{X,Y,k_h}(\theta_{\mu_{h_1}},\theta_{\mu_{h_2}})$ in (5.7). In particular, both functions render the outputs of both antennas inseparable, which compounds the evaluation of the respective likelihood functions. However, in comparison with $\Psi_{X,Y,k_h}(\theta_{\mu_{h_1}},\theta_{\mu_{h_2}})$ in (5.8), the computation of $\Phi_{X,Y,k_h}(\theta_{\mu_{h_1}},\theta_{\mu_{h_2}})$ in (5.11) is less demanding because it does not contain the Bessel functions involving k_g.

Gaussian Approximation

From Lemma 5.1, it can be seen that the likelihood function based on the Gaussian approximation does not incorporate the k-factor of the jammer's channel, k_g. Hence, it can be readily verified that approximating the received signal components corresponding to the jammer's transmission by Gaussian vectors as in Section 5.3.1 yields the same likelihood function given in (5.9).

5.3.3 Statistical distribution of $\boldsymbol{H}$ known and statistical distribution of $\boldsymbol{G}$ partially known:

Complementary to the previous case, in this case the jammer-receiver channel has an LOS component with a known k-factor, whereas the transmitter-receiver channel has no LOS component. Such a case arises when the jammer is airborne or highly mounted whereas both the transmitter and the receiver are ground-based.

The exact likelihood function

The exact likelihood function in this case is given in the following corollary.

Corollary 5.2. *Let $\boldsymbol{Y}$, $\boldsymbol{X}$, $\boldsymbol{V}$, $\boldsymbol{Z}$, $\boldsymbol{G}$, Σ and k_g be as defined in Theorem 5.1, and let $\boldsymbol{H} \sim \mathcal{CN}\left(\mathbf{0}_T, \sigma_h^2 I_T\right)$ where σ_h is a known scalar. The likelihood function of $\boldsymbol{Y}$ conditioned on $\boldsymbol{X} = X$ is given by:*

$$f_{\boldsymbol{Y}|\boldsymbol{X}}(Y|X) = \frac{\exp\left(-2k_g^2\right)}{\pi^{2T}\sigma_g^4\sigma_v^4|\Sigma|^2} \exp\left(-\left(Y_o^\dagger\ \Sigma^{-1}\ Y_o\right) - \left(Y_e^\dagger\ \Sigma^{-1} Y_e\right)\right) \Omega_{X,Y,k_h}, \tag{5.12}$$

where

$$\Omega_{X,Y,k_h} = \int_0^1 \int_0^1 \frac{t\ (\ \bar{t}\ )^{T-3}}{|\Lambda t + \bar{t}\ I_T|} \exp\left(-\frac{t}{\sigma_g^2 \sigma_v^2 \bar{t}}\right) \exp\left(\bar{u} Y_o^\dagger \Upsilon(\Sigma, t) Y_o + u Y_e^\dagger \Upsilon(\Sigma, t) Y_e\right)$$
$$\times I_0\left(\frac{2k_g}{\sigma_g \sigma_v}\sqrt{\frac{\bar{u}\ t}{\bar{t}}}\right) I_0\left(\frac{2k_g}{\sigma_g \sigma_v}\sqrt{\frac{u\ t}{\bar{t}}}\right) I_0\left(4u\bar{u}t|Y_o^\dagger\ \Upsilon(\Sigma, t) Y_e|\right) dudt, \quad (5.13)$$

where Λ, $\bar{t}$, Y_o, Y_e, $\Upsilon(\Sigma, t)$, *and* $\bar{u}$ *are defined in Theorem 5.1.*

Proof. Setting k_h to zero in (5.7) and (5.8) and noticing that $(2\pi)^{-2} \int_0^{2\pi} \int_0^{2\pi} d\theta_{\mu_{h_1}} d\theta_{\mu_{h_2}} = 1$, and $I_0(0) = 1$ yields (5.12) and (5.13), respectively. □

Comparing (5.12) with (5.7) and (5.10), we notice that (5.12) does not involve integration over $\theta_{\mu_{h_1}}$ and $\theta_{\mu_{h_2}}$. This is due to the fact that $\boldsymbol{H}$ is zero mean, which renders the computation of the expression in (5.12) much less demanding than its counterparts in (5.7) and (5.10).

Gaussian Approximation

Approximating the signal resulting form the jammer transmission at the i-th receive antenna, $i \in \{1, 2\}$, by a Gaussian vector $\boldsymbol{J}_i = \boldsymbol{g}_i \boldsymbol{V}$, where $\boldsymbol{J}_i \sim \mathcal{CN}\left(\boldsymbol{0}_T, \sigma_g^2 \sigma_v^2 I_T\right)$ yields the likelihood function in the following lemma.

Lemma 5.2. *Let* $\boldsymbol{Y}$, $\boldsymbol{X}$, $\boldsymbol{V}$, $\boldsymbol{Z}$, $\boldsymbol{G}$, Σ *and* k_g *be as defined in Theorem 5.1, and let* $\boldsymbol{H} \sim \mathcal{CN}\left(\boldsymbol{0}_T, \sigma_h^2 I_T\right)$ *where* σ_h *is a known scalar. Let* $\boldsymbol{J} = \boldsymbol{g}_i \boldsymbol{V}$ *where* $i \in \{1, 2\}$. *Assume that* $\boldsymbol{J} \sim \mathcal{CN}(\boldsymbol{0}_T, \sigma_g^2 \sigma_V^2 I_T)$, *then the likelihood function of* $\boldsymbol{Y}$ *conditioned on* $\boldsymbol{X} = X$ *is given by:*

$$f_{\boldsymbol{Y}|\boldsymbol{X}}(Y|X) = \frac{1}{\pi^{2T}|\Sigma_N|^2} \exp\left(-\left(Y_o^\dagger \Sigma_N^{-1} Y_o + Y_e^\dagger \Sigma_N^{-1} Y_e\right)\right), \quad (5.14)$$

where $\Sigma_N = \sigma_h^2 X X^\dagger + (\sigma_g^2 \sigma_v^2 + \sigma_Z^2) I_T$ *, and* Y_o *and* Y_e *are defined in Theorem 5.1.*

Proof. Setting k_h to zero in (5.9) and noticing that $I_0(0) = 1$ yields (5.14). □

As in Lemma 5.1, it can be seen form (5.14) that the likelihood function based on the Gaussian approximation does not incorporate the k-factor of the jammer's channel, k_g. Moreover, in comparison with (5.9), we notice that the computation of likelihood function in (5.14) is less demanding because it does not contain the Bessel functions involving k_h.

5.3.4 Statistical distribution of both $\boldsymbol{H}$ and $\boldsymbol{G}$ known:

In this case, neither the transmitter-receiver channel nor the jammer-receiver channel has an LOS component. This might be the case when all parties are ground-based.

The exact likelihood function

The exact likelihood function in this case is given in the following corollary:

Corollary 5.3. *Let* $\boldsymbol{Y}$*,* $\boldsymbol{X}$*,* $\boldsymbol{V}$*,* $\boldsymbol{Z}$ *and* Σ *be as defined in Theorem 5.1, and let* $\boldsymbol{H} \sim \mathcal{CN}\left(\mathbf{0}_T, \sigma_h^2 I_T\right)$ *and* $\boldsymbol{G} \sim \mathcal{CN}\left(\mathbf{0}_T, \sigma_g^2 I_T\right)$*, where* σ_h *and* σ_g *are known scalars. Then, the likelihood function of* $\boldsymbol{Y}$ *conditioned on* $\boldsymbol{X} = X$ *is given by:*

$$f_{\boldsymbol{Y}|\boldsymbol{X}}(Y|X) = \frac{1}{\pi^{2T}\sigma_g^4\sigma_v^4|\Sigma|^2} \exp\left(-\left(Y_o^\dagger\ \Sigma^{-1}\ Y_o\right) - \left(Y_e^\dagger\ \Sigma^{-1} Y_e\right)\right) \Gamma_{X,Y,k_h}, \tag{5.15}$$

where

$$\Gamma_{X,Y,k_h} = \int_0^1 \int_0^1 \frac{t\ (\ \bar{t}\ )^{T-3}}{|\Lambda t + \bar{t}\ I_T|} \exp\left(\bar{u}\ Y_o^\dagger\ \Upsilon(\Sigma, t)\ Y_o + u\ Y_e^\dagger\ \Upsilon(\Sigma, t)\ Y_e - \frac{t}{\sigma_g^2 \sigma_v^2 \bar{t}} \right)$$
$$\times\ I_0\left(4\ u\ \bar{u}\ t\ |Y_o^\dagger\ \Upsilon(\Sigma, t)\ Y_e|\right) du\ dt, \quad (5.16)$$

where Λ, $\bar{t}$, Y_o, Y_e, $\Upsilon(\Sigma, t)$ *and* $\bar{u}$ *are defined in Theorem 5.1.*

Proof. Setting k_h and k_g to zeros in (5.7) and (5.8) and noticing that $\frac{1}{(2\pi)^2} \int_0^{2\pi} \int_0^{2\pi} d\theta_{\mu_{h_1}} d\theta_{\mu_{h_2}} = 1$, and $I_0(0) = 1$ yields (5.15) and (5.16), respectively. □

The fact that (5.15) does not involve the double integration over $\theta_{\mu_{h_1}}$ and $\theta_{\mu_{h_2}}$, and that Γ_{X,Y,k_h} in (5.16) does not include the two Bessel functions involving k_g that were present in (5.13) makes the exact likelihood function of this case the least computationally demanding among all considered cases.

Gaussian Approximation

Due to the fact that the likelihood function based on the Gaussian approximation does not incorporate the jammer's channel k-factor, k_g, cf. Lemma 5.1 and Lemma 5.2, approximating the signal resulting form the jammer's transmission at the receiver by Gaussian vectors as in Sections 5.3.1 and 5.3.3 yields a likelihood expression identical to the one in (5.14).

5.4 Simulation Results

In this section, we compare the performance of the ML detector based on the exact likelihood functions provided hereinabove with that of the approximate ML detector based on the Gaussian assumption of the signals received due to the jammer's transmissions. Moreover, we examine the performance gain achieved by using double instead of a single receive antenna in addition to the impact of the symbol length, T, on performance.

All simulations were conducted by using MATLAB software Package [92]. In all simulations, we used constellations of unit norm symbols constructed with the method proposed in [91]. In particular, to generate a complex constellation $\mathcal{C}$ with 2^n T-dimensional symbols, we follow the same steps outlined in Chapter 4; however, we omit the final step of that procedure since in this chapter we used a unity norm constellation.

To facilitate the presentation of results, we fix the total power of the noise plus jamming signal to 10 dB. To do so, in all simulations, we set the noise variance to $\sigma_Z^2 = 0.5$ and the jamming signal variance to $\sigma_V^2 = 4.5$. To maintain a constant average channel power gain for the transmitter and jammer channels under different values of k_h and k_g, the transmitter channel variance, σ_h^2, and the jammer channel variance, σ_g^2, are set to $\sigma_h^2 = \dfrac{1}{k_h^2+1}$ and $\sigma_g^2 = \dfrac{1}{k_g^2+1}$, respectively. In all forthcoming examples, except Example 4, the symbol length is set to $T = 4$, and the data rate is set to 0.75 bits per channel use (bpcu).

Example 1 In this example, we set the k-factor of the jammer's channel, k_g, to zero for various values of the k-factor of the transmitter's channel, k_h. This scenario arises when the transmitter is highly mounted or airborne while the jammer and the receiver are ground-based, cf. Section 5.3.1. Using these settings, we obtained the symbol error rates (SERs) reported in Figure 5.2 for both the exact and approximate ML detectors. The

superiority of the exact ML detector over the approximate one is apparent in Figure 5.2. Furthermore, it can be seen that the performance of both detectors improves when k_h increases, i.e., when the LOS of the transmitter's channel becomes stronger. For instance, at a signal-to-jamming-plus-noise ratio (SJNR) of 10 dB, increasing the k-factor of the transmitter channel from $k_h = 1$ to $k_h = 3$ reduces the SER from around 9×10^{-3} to about 2×10^{-3} for the exact ML detector and form about 2×10^{-2} to 9×10^{-3} for the approximate one. However, the advantage of the exact ML detector is more pronounced at lower values of k_h. For instance, at an SER of 10^{-3}, the exact ML detector exhibits an advantage of 3 dB when $k_h = 1$ and 2 dB when $k_h = 3$.

This figure illustrates the sharp contrast between the behaviour of the exact and approximate ML detectors for the cases of single and double receive antennas. In particular, as shown in [93], the performance of these detectors coincides when the signalling constellation has a unit norm and the receiver has one antenna. However, the exact ML detector offers a significant performance advantage over its approximate counterpart when the receiver has two antennas, albeit with a higher computational cost. □

Example 2 In this example, we consider a case complementary to that considered in Example 1. In particular, in this example, the k-factor of the transmitter's channel was set to $k_h = 0$, and various values were used for the k-factor of the jammer's channel, k_g. This scenario arises when the jammer is highly mounted or airborne while the transmitter and the receiver are ground-based, cf. Section 5.3.3.

The SER curves obtained in this example are reported in Figure 5.3 for both the exact and approximate ML detectors. It can be seen from Figure 5.3 that, as in the cases considered in Example 1, the exact ML detector significantly outperforms the approximate one. For instance, at an SER of 1×10^{-2}, the exact ML detector has an advantage of

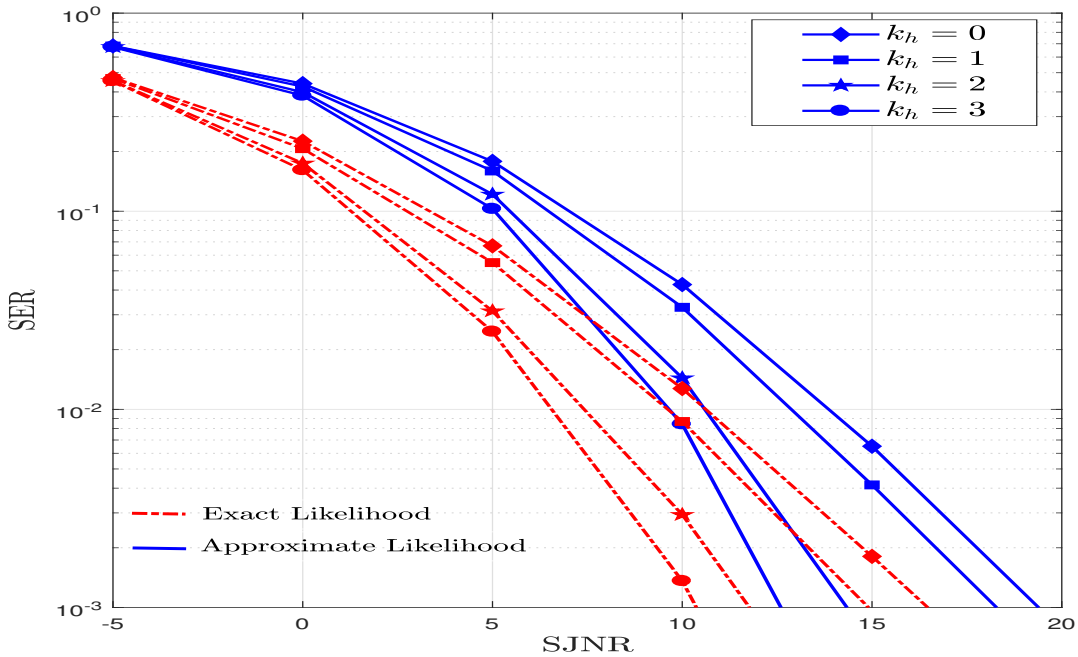

Figure 5.2: $T = 4$, $k_g = 0$ and various values of k_h.

3 dB at $k_g = 0$ and 3.25 dB at $k_g = 8$. Furthermore, it can be noticed that, although the detection performance of both detectors is not highly sensitive to the changes in k_g, the detection performance of the exact ML detector improves with the strength of the jammer's LOS component, i.e., increasing k_g decreases the SER. For instance, at an SJNR of 10 dB, the SER drops form 1.4×10^{-2} at $k_g = 0$ to 1×10^{-2} at $k_g = 8$.

This example suggests that a receiver with an intense LOS component to the jammer is more resilient to jamming. In a complementary fashion, it is more effective for the jammer to be occluded from, than for it to have an LOS component to, the receiver.

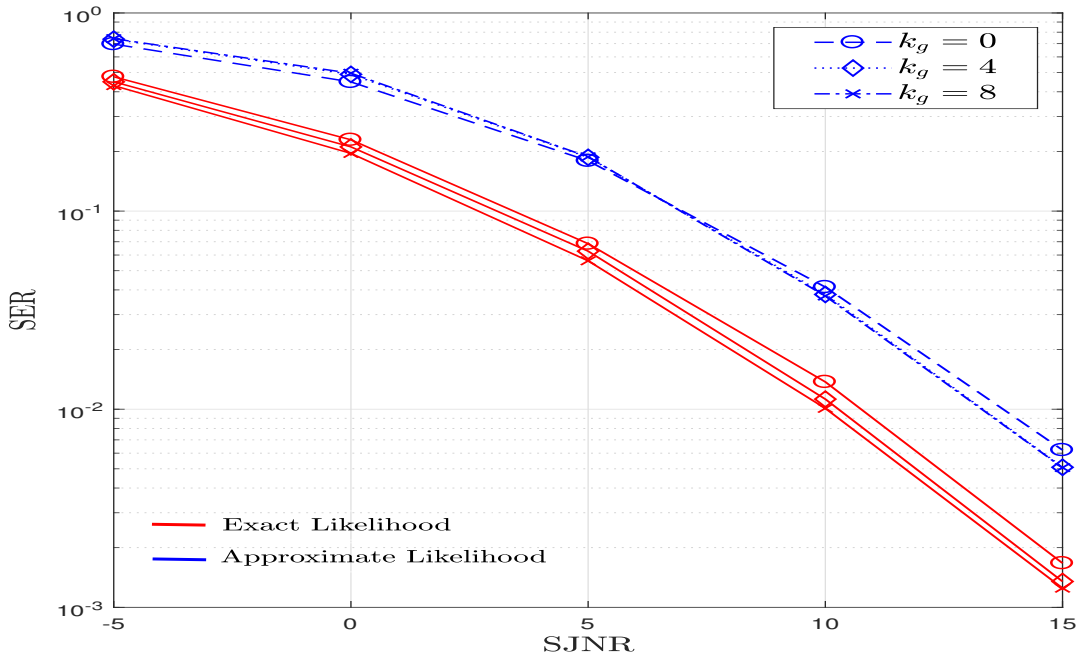

Figure 5.3: $T = 4$, $k_h = 0$ and various values of k_g.

Example 3 In this example, we compare the performance achieved by a double-antenna receiver with that achieved by a single-antenna one for various values of k_h and k_g. The SER curves obtained in this example are presented in Figure 5.4. This figure illustrates the robustness of double-antenna receivers to jamming. For instance, at an SER of 3.3×10^{-3}, the exact ML detector yielded a gain of 11 dB when $k_h = k_g = 2$, a gain of 6 dB when $k_h = k_g = 0$, and a gain of 9.5 dB when $k_h = 2$ and $k_g = 0$.

This example suggests that equipping the receiver with more antennas will likely offer significant jamming resilience. Unfortunately, however, as previously pointed out in Section 4.2, deriving the optimal ML detector for cases with more than two receive antennas seems daunting. Furthermore, performing optimal detection with a large number of re-

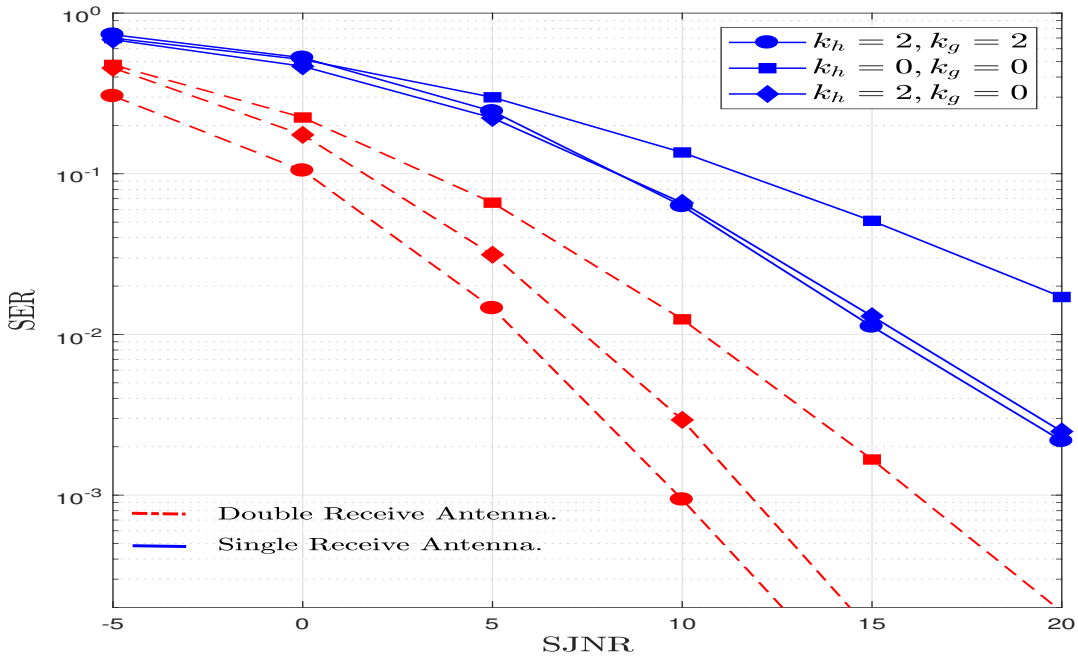

Figure 5.4: Detection performance of double receive antenna vs. single receive antenna for $T = 4$ and various values of k_h and k_g.

ceive antennas is likely to be computationally extensive unless closed-form expressions are obtained for the respective likelihood functions.

Example 4 In this example, we investigate the effect of the symbol length, T, on the performance of the exact and the Gaussian approximation-based ML detectors. Two values of T were considered, namely, $T = 2$ and $T = 4$. For each value of T, performance is evaluated at three transmission rates, namely, 0.5, 1, and 2 bpcu. The k-factors of both channels are chosen to be zero, i.e., $k_h = k_g = 0$. The results obtained in this example are presented in Figure 5.5. It can be noticed from this figure that using larger symbol lengths yields better performance.

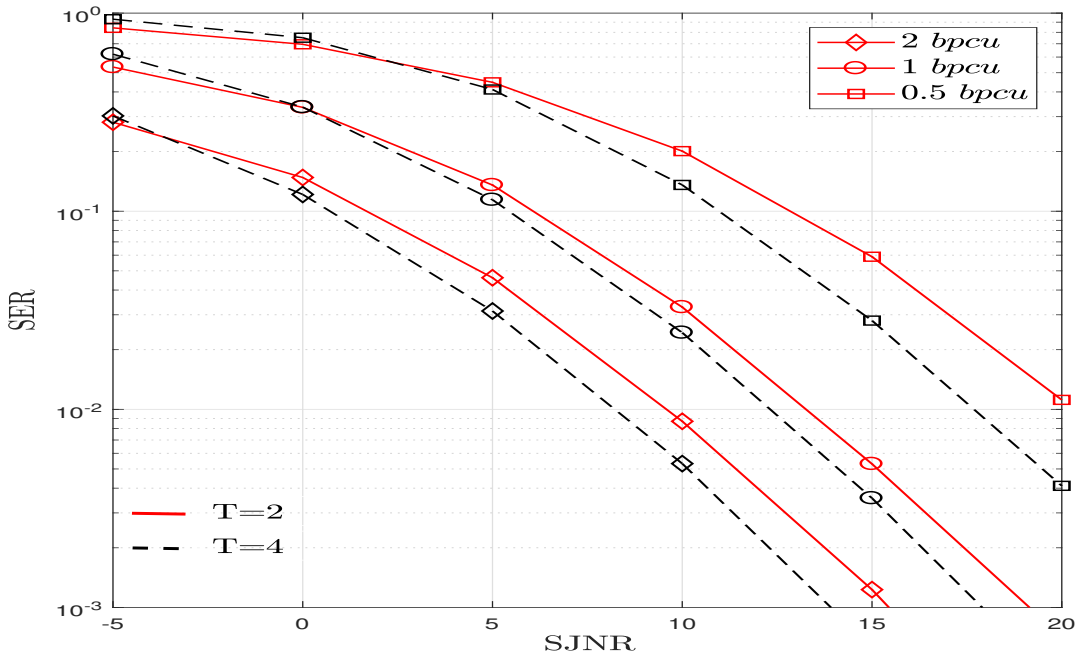

Figure 5.5: Detection performance for different data rates and various values of T, $k_h = 0$ and $k_g = 0$.

For instance, at an SER of 1×10^{-2}, using $T = 4$ has an SJNR advantage of 1.5 dB when the data rate is 0.5 bpcu and 2.5 dB when the data rate is 2 bpcu over the case of $T = 2$.

5.5 Conclusion

We considered a scenario in which a single-antenna transmitter communicates with a double-antenna receiver in the presence of a continuous proactive single-antenna jammer. The jammer's transmitted signal, the transmitter-receiver, and the jammer-receiver channels are assumed to be Gaussian, thereby inducing a non-Gaussian jamming signal at the

receiver. For this scenario, the likelihood functions of the received signals are derived for the cases in which the receiver has full or partial CDI about the transmitter's channel and the jammer's channel. These likelihood functions are used to develop the optimal ML detector. Furthermore, the likelihood functions based on the Gaussian approximation of the signal component resulting from the jammer's transmission are derived, and the corresponding detector is developed. The detection performance of both detectors is tested through numerical simulations. These simulations revealed the superiority of the ML detector based on the exact likelihood functions over the one based on Gaussian approximations for the case of unit-norm constellations. This is in sharp contrast with the single antenna case wherein the two detectors are equivalent for this type of constellations [93]. Simulation results showed the significant power advantage of the exact ML detector, especially when the transmitter has a strong LOS component. Furthermore, these results showed that a double-antenna receiver with strong LOS components to the transmitter and the jammer is more resilient to proactive barrage jamming than its single-antenna counterpart. Extending these results to receivers with more than two antennas seems daunting and computationally extensive, but it will likely yield valuable performance gains.

Chapter 6

Conclusions and Future Work

This thesis considered scenarios in which a a single-antenna transmitter communicates with a single-antenna, double-antenna, or multiple-antenna receiver over an unknown complex Gaussian scalar or vector channel. This communication is attacked by a single-antenna proactive, continuous jammer sending a zero-mean complex Gaussian signal over a complex Gaussian scalar or vector channel. The transmitter uses a multi-dimensional complex constellation for the single-antenna and the double-antenna receiver, whereas for the multiple antenna receiver, the transmitter uses a one-dimensional complex constellation. The likelihood functions of the non-Gaussian signal induced at the receiver are derived for cases corresponding to whether the receiver has full CSI, full CDI, or partial CDI of the transmitter's channel. The jammer's channel CDI is either fully or partially available at the receiver. Using the derived likelihood expressions, the exact ML detectors along with detectors based on the Gaussian approximation of the signal resulting form the jammer's transmission are developed. The detection performance of both types of detectors receivers is investigated using MATLAB simulations. The results of these simulations show that:

- For the single-antenna receiver,

  1. If the receiver knows the realization of the transmitter's channel, or if the constellation symbols have equal powers, the exact ML detector and the Gaussian approximation-based ML detector make the same detection decision for every received sample.
  2. If the receiver does not know realization of the transmitter's channel, or if the constellation symbols have different powers, the exact ML detector is superior to the Gaussian approximation-based one.
  3. The superiority of the exact ML detector becomes more pronounced with the increase of the intensity of the LOS component of the transmitter's channel, or the increase in constellation symbols length.
  4. At high SJNR values (SJNR $\geqslant$ 20 dB), increasing the intensity of the LOS of the jammer's channel improves the SER performance of the exact ML detector.
  5. At low SJNR values (SJNR $\geqslant$ 10 dB), decreasing the intensity of the LOS of the jammer's channel improves the SER performance of the exact ML detector.

- For the double-antenna receiver,

  1. The exact ML detector has a superiority over the Gaussian approximation-based one for the case of equal-power constellations. This is in sharp contrast with the single antenna case wherein the two detectors are equivalent for this type of constellations.
  2. The exact ML detector has a significant power advantage, especially when the transmitter has a strong LOS component.

3. The double-antenna receiver with strong LOS components to the transmitter and the jammer is more resilient to proactive barrage jamming than its single-antenna counterpart.

Future Work

The work presented in this thesis could be extended in the following directions:

- The likelihood values provided by the developed detectors could be used to make soft detection decisions. Studying the detection performance based on soft detection is a possible extension of this thesis.
- A given number of receive antennas could be grouped into groups of double-antenna receivers. The decisions of these receivers can be combined using sensor fusion techniques, e.g., majority voting, Dempster-Shafer theory [94], etc.
- For a multiple-antenna receiver and multi-dimensional constellation, a method might be developed for combining the detection decisions for each component of the transmitted symbol (developed in Chapter 3) with the decisions of each single antenna for the whole transmitted symbol (developed in Chapter 4). Combining the detection decisions over space and time will surely enhance the system immunity against jamming.

Appendix A

Proofs for chaper 3

A.1 Proof of Theorem 3.1

From (3.8), it can be seen that given the jamming signal sample, $\boldsymbol{v}$, and the phases vector of the jammer channel's mean vector, $\boldsymbol{\theta_g}$, the signals resulting form the jammer transmission at the receiver antennas are independent Complex Gaussian signals whose joint pdf is given by:

$$f_{\boldsymbol{J}|\boldsymbol{v},\boldsymbol{\theta_g}}(J|v,\theta_g) = \prod_{i=1}^{R} f_{\boldsymbol{j}_i|\boldsymbol{v},\boldsymbol{\theta_g}_i}(j_i|v,\theta_{g_i}) \tag{A.1}$$

where

$$f_{\boldsymbol{j_i}|\boldsymbol{v},\boldsymbol{\theta_g}_i}(j_i|v,\theta_{g_i}) = \frac{1}{\pi\ |v|^2\sigma_g^2}\exp\left\{\left(\frac{-|j_i - k_g\sigma_g v e^{j\theta_{g_i}}|^2}{\sigma_g^2|v|^2}\right)\right\}. \tag{A.2}$$

Since the pdf $f_{\boldsymbol{\theta_g}_i|\boldsymbol{v}}(\theta_{g_i}|v) = \dfrac{1}{2\pi}$, then

$$f_{\boldsymbol{j_i},\boldsymbol{\theta_{g_i}}|\boldsymbol{v}}(j_i,\theta_{g_i}|v) = \frac{1}{2\pi^2\ |v|^2\sigma_g^2}\exp\left\{\left(\frac{-|j_i - k_g\sigma_g v e^{\jmath\theta_{g_i}}|^2}{\sigma_g^2|v|^2}\right)\right\}, \tag{A.3}$$

$$= \frac{\exp\left(-k_g^2\right)}{2\pi^2\ |v|^2\sigma_g^2}\exp\left\{\left(\frac{-|j_i|^2}{\sigma_g^2|v|^2} + \frac{2k_g|j_i|\cos(\theta_{g_i}+\alpha_i)}{\sigma_g|v|}\right)\right\}, \tag{A.4}$$

where $\alpha_i = \angle v - \angle j_i$.

Integrating (A.4) over all possible realizations of θ_{g_i} yields:

$$f_{\boldsymbol{j_i}|\boldsymbol{v}}(j_i|v) = \frac{\exp\left(-k_g^2\right)}{\pi\ |v|^2\sigma_g^2} I_0\left(\frac{2k_g|j_i|}{\sigma_g|v|}\right)\exp\left\{\left(\frac{-|j_i|^2}{\sigma_g^2|v|^2}\right)\right\},$$

$$= \frac{\exp\left(-k_g^2\right)}{\pi\ |v|^2\sigma_g^2}\sum_{\ell=0}^{\infty}\left(\frac{k_g|j_i|}{\sigma_g|v|}\right)^{2\ell}\left(\frac{1}{\ell!}\right)^2\exp\left\{\left(\frac{-|j_i|^2}{\sigma_g^2|v|^2}\right)\right\}, \tag{A.5}$$

where $I_0(\cdot)$ is the modified Bessel function of the first kind of order zero.

From (A.5), we get:

$$f_{\boldsymbol{J}|\boldsymbol{v}}(J|v) = \frac{\exp\left(-k_g^2 R\right)}{\pi^R\ |v|^{2R}\sigma_g^{2R}}\prod_{i=1}^{R}\sum_{\ell_i=0}^{\infty}\left(\frac{k_g|j_i|}{\sigma_g|v|}\right)^{2\ell_i}\left(\frac{1}{\ell_i!}\right)^2\exp\left\{\left(\frac{-|J|^2}{\sigma_g^2|v|^2}\right)\right\}, \tag{A.6}$$

Multiplying (A.6) by the pdf of $\boldsymbol{v}$, $f_{\boldsymbol{v}}(v) = \dfrac{1}{\pi\sigma_v^2}\exp\left\{\left(\dfrac{-|v|^2}{\sigma_v^2}\right)\right\}$, yields:

$$f_{\boldsymbol{J},\boldsymbol{v}}(J,v) = \frac{\exp\left(-k_g^2 R\right)}{\pi^{R+1}\ \sigma_g^{2R}\sigma_v^2}\sum_{\ell_1,\ldots,\ell_R=0}^{\infty}\left(\frac{k_g^2}{\sigma_g^2}\right)^{\sum_{i=1}^{R}\ell_i}\prod_{i=1}^{R}\frac{|j_i|^{2\ell_i}}{(\ell_i!)^2}\ \frac{1}{|v|^{2\sum_{i=1}^{R}\ell_i+2R}}$$
$$\times\exp\left\{\left(\frac{-|J|^2}{\sigma_g^2|v|^2} - \frac{|v|^2}{\sigma_v^2}\right)\right\}. \tag{A.7}$$

Integrating (A.7) over all possible realizations of $\boldsymbol{v}$ yields:

$$f_{\boldsymbol{J}}(J) = \frac{\exp\left(-k_g^2 R\right)}{\pi^{R+1}\ \sigma_g^{2R}\sigma_v^2} \sum_{\ell_1,\ldots,\ell_R=0}^{\infty} \left(\frac{k_g^2}{\sigma_g^2}\right)^{\sum_{i=1}^{R}\ell_i} \prod_{i=1}^{R} \frac{|j_i|^{2\ell_i}}{(\ell_i!)^2} \times \int_v \frac{1}{|v|^{2\sum_{i=1}^{R}\ell_i+2R}} \exp\left\{\left(\frac{-|J|^2}{\sigma_g^2|v|^2} - \frac{|v|^2}{\sigma_v^2}\right) d_v\right\} \quad \text{(A.8)}$$

Let $\mathcal{I}$ be the integration part of (A.8), moving to the polar coordinates system where $|v| = r$ and $d_v = r d_r d_\theta$, where $\theta = \angle v$, $\mathcal{I}$ becomes:

$$\begin{aligned}\mathcal{I} &= \int_0^{2\pi}\int_0^{\infty} \frac{1}{r^{2\sum_{i=1}^{R}\ell_i+2R}} \exp\left\{\left(\frac{-|J|^2}{\sigma_g^2 r^2} - \frac{r^2}{\sigma_v^2}\right) r d_r d_\theta\right\} \\ &= 2\pi \int_0^{\infty} \frac{1}{r^{2\sum_{i=1}^{R}\ell_i+2R}} \exp\left\{\left(\frac{-|J|^2}{\sigma_g^2 r^2} - \frac{r^2}{\sigma_v^2}\right) r d_r\right\} \end{aligned} \quad \text{(A.9)}$$

Using the change of variables $u = \ln\left(\frac{\sigma_g r^2}{\sigma_v |J|}\right)$ yields:

$$\begin{aligned}\mathcal{I} &= \pi \int_{-\infty}^{\infty} \left(\frac{\sigma_g}{\sigma_v|J|}\right)^{\sum_{i=1}^{R}\ell_i+R-1} \exp\left\{\left(\frac{-2|J|}{\sigma_g\sigma_v}\left(\frac{e^u+e^{-u}}{2}\right) - (\sum_{i=1}^{R}\ell_i + R - 1)u\right) du\right\} \\ &= 2\pi \left(\frac{\sigma_g}{\sigma_v|J|}\right)^{\ell_1+\ldots+\ell_R+R-1} K_{\ell_1+\ldots+\ell_R+R-1}\left(\frac{2|J|}{\sigma_g\sigma_v}\right) \end{aligned} \quad \text{(A.10)}$$

where $K_\nu(\cdot)$ is the modified Bessel function of second kind of order ν. Using the integral representation of $K_\nu(\cdot)$ yields:

$$\mathcal{I} = \pi \left(\frac{1}{\sigma_v}\right)^{2(\ell_1+\ldots+\ell_R+R-1)} \int_0^{\infty} \exp\left(-t - \frac{|J|^2}{\sigma_g^2\sigma_v^2 t}\right) \frac{dt}{t^{\ell_1+\ldots+\ell_R+R}}. \quad \text{(A.11)}$$

Substituting for $\mathcal{I}$ in (A.8) yields:

$$f_{\boldsymbol{J}}(J) = \frac{\exp\left(-k_g^2 R\right)}{\pi^R \ \sigma_g^{2R}\sigma_v^{2R}} \int_0^\infty \prod_{i=1}^{R} \sum_{\ell_i}^{\infty} \left(\frac{k_g|j_i|}{\sigma_g\sigma_v\sqrt{t}}\right)^{2\ell_i} \frac{1}{(\ell_i!)^2} \exp\left(-t - \frac{|J|^2}{\sigma_g^2\sigma_v^2 t}\right) \frac{dt}{t^R},$$
$$= \frac{\exp\left(-k_g^2 R\right)}{\pi^R \ \sigma_g^{2R}\sigma_v^{2R}} \int_0^\infty \prod_{i=1}^{R} I_0\left(\frac{2k_g|j_i|}{\sigma_g\sigma_v\sqrt{t}}\right) \exp\left(-t - \frac{|J|^2}{\sigma_g^2\sigma_v^2 t}\right) \frac{dt}{t^R} \tag{A.12}$$

A.2 Proof of Theorem 3.2

It is apparent form (3.7) that given the transmitted symbol $\boldsymbol{x} = x$, $\boldsymbol{U}$ is a complex Gaussian vector whose pdf is the following:

$$f_{\boldsymbol{U}|\boldsymbol{x}}(U|x) = \frac{1}{\pi^R(\sigma_h^2|x|^2 + \sigma_z^2)^R} \exp\left\{\left(\frac{|U|^2}{(\sigma_h^2|x|^2 + \sigma_z^2)}\right)\right\} \tag{A.13}$$

From (3.9) we have:

$$f_{\boldsymbol{Y}|\boldsymbol{x}}(Y|x) = \int_S f_{\boldsymbol{U}|\boldsymbol{x}}(Y - S|x) f_{\boldsymbol{J}}(S) dS$$
$$= \frac{1}{\left(\pi^2\sigma_g^2\sigma_v^2(\sigma_h^2|x|^2 + \sigma_z^2)\right)^R} \int_0^\infty \exp(-t) \times$$
$$\prod_{i=1}^{R} \int_{S_i} \exp\left\{\left(\frac{-|Y_i - S_i|^2}{\sigma_h^2|x|^2 + \sigma_z^2}\right)\right\} \exp\left(-\frac{|S_i|^2}{\sigma_g^2\sigma_v^2 t}\right) d_{S_i} \frac{dt}{t^R} \tag{A.14}$$

noticing that

$$|Y_i - S_i|^2 = |Y_i|^2 + |S_i|^2 - 2|Y_i||S_i|\cos(\theta_{S_i} - \beta_i),$$

where $\theta_{S_i} = \angle S_i$ and $\beta_i = \angle Y_i$, yields:

$$f_{\boldsymbol{Y}|\boldsymbol{x}}(Y|x) = \frac{1}{\left(\pi^2\sigma_g^2\sigma_v^2(\sigma_h^2|x|^2+\sigma_z^2)\right)^R} \exp\left\{\left(\frac{-|Y|^2}{\sigma_h^2|x|^2+\sigma_z^2}\right)\right\} \int_0^\infty \exp(-t)\times$$
$$\prod_{i=1}^{R} \int_{S_i} \exp\left\{\left(\frac{-|S_i|^2+2|Y_i||S_i|\cos(\theta_{S_i}-\beta_i)}{\sigma_h^2|x|^2+\sigma_z^2}\right)\right\} \exp\left(-\frac{|S_i|^2}{\sigma_g^2\sigma_v^2 t}\right) d_{S_i}\frac{dt}{t^R}. \quad \text{(A.15)}$$

Let II be the inner integration in (A.15), i.e.,:

$$II = \int_{S_i} \exp\left(-\gamma|S_i|^2\right)\exp\left(\frac{2|Y_i||S_i|\cos(\theta_{S_i}-\beta_i)}{\sigma_h^2|x|^2+\sigma_z^2}\right) d_{S_i}, \quad \text{(A.16)}$$

where $\gamma = \dfrac{1}{\sigma_h^2|x|^2+\sigma_z^2} + \dfrac{1}{\sigma_g^2\sigma_v^2 t}$.

Moving to the polar coordinate system where $|S_i| = r$ and $d_{s_i} = r d_r d_{\theta_{S_i}}$, equation (A.16) becomes:

$$II = \int_0^\infty r\ \exp\left\{\left(-\gamma r^2\right)\right\} \int_0^{2\pi} \exp\left\{\left(\frac{2|Y_i|r\cos(\theta_{S_i}-\beta_i)}{\sigma_h^2|x|^2+\sigma_z^2}\right)\right\} d\theta_{S_i} r d_r, \quad \text{(A.17)}$$

the inner integration in (A.17) is equal to

$$2\pi\ I_0\left(\frac{2|Y_i|r}{\sigma_h^2|x|^2+\sigma_z^2}\right) = 2\pi \sum_{m=0}^{\infty}\left(\frac{|Y_i|^2 r^2}{(\sigma_h^2|x|^2+\sigma_z^2)^2}\right)^m \frac{1}{(m!)^2}, \quad \text{(A.18)}$$

Substituting from (A.18) in (A.17) yields:

$$II = 2\pi \sum_{m=0}^{\infty}\left(\frac{|Y_i|^2}{(\sigma_h^2|x|^2+\sigma_z^2)^2}\right)^m \frac{1}{(m!)^2} \int_0^\infty r^{2m}\ \exp\left\{\left(-\gamma r^2\right)\right\} r d_r, \quad \text{(A.19)}$$

Let $\gamma r^2 = u \Rightarrow 2rdr = \dfrac{du}{\gamma}$, substituting in (A.19) we get:

$$
\begin{aligned}
II &= \pi \sum_{m=0}^{\infty} \left(\frac{|Y_i|^2}{(\sigma_h^2|x|^2 + \sigma_z^2)^2} \right)^m \frac{1}{m!} \frac{1}{\gamma^{m+1}} \\
&= \pi \left(\frac{\sigma_g^2 \sigma_v^2 (\sigma_h^2|x|^2 + \sigma_z^2)t}{\sigma_h^2|x|^2 + \sigma_z^2 + \sigma_g^2\sigma_v^2 t} \right) \sum_{m=0}^{\infty} \left(\frac{\sigma_g^2\sigma_v^2|Y_i|^2\ t}{(\sigma_h^2|x|^2 + \sigma_z^2 + \sigma_g^2\sigma_v^2 t)(\sigma_h^2|x|^2 + \sigma_z^2)} \right)^m \frac{1}{m!}, \\
&= \pi \left(\frac{\sigma_g^2 \sigma_v^2 (\sigma_h^2|x|^2 + \sigma_z^2)t}{\sigma_h^2|x|^2 + \sigma_z^2 + \sigma_g^2\sigma_v^2 t} \right) \exp\left(\frac{\sigma_g\sigma_v|Y_i|^2 t}{(\sigma_h^2|x|^2 + \sigma_z^2 + \sigma_g^2\sigma_v^2 t)(\sigma_h^2|x|^2 + \sigma_z^2)} \right), \\
&= \pi \left(\frac{\sigma_g^2 \sigma_v^2 (\sigma_h^2|x|^2 + \sigma_z^2)t}{\sigma_h^2|x|^2 + \sigma_z^2 + \sigma_g^2\sigma_v^2 t} \right) \exp\left(\frac{|Y_i|^2}{(\sigma_h^2|x|^2 + \sigma_z^2)} - \frac{|Y_i|^2}{(\sigma_h^2|x|^2 + \sigma_z^2 + \sigma_g^2\sigma_v^2 t)} \right). \qquad \text{(A.20)}
\end{aligned}
$$

Substituting for II from (A.20) in (A.15) yields:

$$
f_{\boldsymbol{Y}|\boldsymbol{x}}(Y|x) = \frac{1}{\pi^R} \int_0^{\infty} \frac{1}{(\sigma_h^2|x|^2 + \sigma_z^2 + \sigma_g^2\sigma_v^2 t)^R} \exp\left(-t - \frac{|Y|^2}{\sigma_h^2|x|^2 + \sigma_z^2 + \sigma_g^2\sigma_v^2 t} \right) dt. \qquad \text{(A.21)}
$$

A.3 Proof of Theorem 3.3

First of all, we start by noticing that the pdf of $f_{\boldsymbol{U}|\boldsymbol{x}}(U|x)$ for this case is identical to that given by (A.13). From (3.9) we have:

$$
\begin{aligned}
f_{\boldsymbol{Y}|\boldsymbol{x}}(Y|x) &= \int_S f_{\boldsymbol{U}|\boldsymbol{x}}(Y - S|x) f_{\boldsymbol{J}}(S) dS, \\
&= \frac{\exp\left(-k_g^2 R\right)}{\left(\pi^2\sigma_g^2\sigma_v^2(\sigma_h^2|x|^2 + \sigma_z^2)\right)^R} \int_0^{\infty} \exp(-t) \times \qquad \text{(A.22)} \\
&\prod_{i=1}^{R} \int_{S_i} \exp\left(\frac{-|Y_i - S_i|^2}{(\sigma_h^2|x|^2 + \sigma_z^2)} \right) I_0\left(\frac{2k_g|S_i|}{\sigma_g\sigma_v\sqrt{t}} \right) \exp\left(-\frac{|S_i|^2}{\sigma_g^2\sigma_v^2 t} \right) d_{S_i} \frac{dt}{t^R},
\end{aligned}
$$

noticing that

$$|Y_i - S_i|^2 = |Y_i|^2 + |S_i|^2 - 2|Y_i||S_i|\cos(\theta_{S_i} - \beta_i),$$

where $\theta_{S_i} = \angle S_i$ and $\beta_i = \angle Y_i$, yields:

$$f_{\boldsymbol{Y}|\boldsymbol{x}}(Y|x) = \frac{\exp\left(-k_g^2 R\right)}{\left(\pi^2\sigma_g^2\sigma_v^2(\sigma_h^2|x|^2+\sigma_z^2)\right)^R}\exp\left(\frac{-|Y|^2}{(\sigma_h^2|x|^2+\sigma_z^2)}\right)\int_0^\infty \exp(-t)\times$$
$$\prod_{i=1}^{R}\int_{S_i}\exp\left\{\left(\frac{-|S_i|^2+2|Y_i||S_i|\cos(\theta_{S_i}-\beta_i)}{(\sigma_h^2|x|^2+\sigma_z^2)}\right)\right\}I_0\left(\frac{2k_g|S_i|}{\sigma_g\sigma_v\sqrt{t}}\right)\exp\left(-\frac{|S_i|^2}{\sigma_g^2\sigma_v^2 t}\right)d_{S_i}\frac{dt}{t^R}. \tag{A.23}$$

Let II be the inner integration in (A.23), using the series expansion of $I_0(\cdot)$ yields:

$$II = \sum_{n=0}^{\infty}\left(\frac{k_g^2}{\sigma_g^2\sigma_v^2 t}\right)^n\frac{1}{(n!)^2}\int_{S_i}|S_i|^{2n}\exp\left(-\gamma|S_i|^2\right)\exp\left(\frac{2|Y_i||S_i|\cos(\theta_{S_i}-\beta_i)}{\sigma_h^2|x|^2+\sigma_z^2}\right)d_{S_i}, \tag{A.24}$$

where $\gamma = \dfrac{1}{\sigma_h^2|x|^2+\sigma_z^2} + \dfrac{1}{\sigma_g^2\sigma_v^2 t}$.

Moving to the polar coordinate system where $|S_i| = r$ and $d_{s_i} = r d_r d_{\theta_{S_i}}$, equation (A.24) becomes:

$$II = \sum_{n=0}^{\infty}\left(\frac{k_g^2}{\sigma_g^2\sigma_v^2 t}\right)^n\frac{1}{(n!)^2}\int_0^\infty r^{2n}\exp\left\{\left(-\gamma r^2\right)\right\}\int_0^{2\pi}\exp\left(\frac{2|Y_i|r\cos(\theta_{S_i}-\beta_i)}{\sigma_h^2|x|^2+\sigma_z^2}\right)d\theta_{S_i} r d_r, \tag{A.25}$$

the inner integration in (A.25) is equal to

$$2\pi\ I_0\left(\frac{2|Y_i|r}{\sigma_h^2|x|^2+\sigma_z^2}\right) = 2\pi\sum_{m=0}^{\infty}\left(\frac{|Y_i|^2 r^2}{(\sigma_h^2|x|^2+\sigma_z^2)^2}\right)^m\frac{1}{(m!)^2}, \tag{A.26}$$

Substituting from (A.26) in (A.25) yields:

$$II = 2\pi \sum_{n,m=0}^{\infty} \left(\frac{k_g^2}{\sigma_g^2\sigma_v^2 t}\right)^n \frac{1}{(n!)^2} \left(\frac{|Y_i|^2}{(\sigma_h^2|x|^2+\sigma_z^2)^2}\right)^m \frac{1}{(m!)^2} \int_0^{\infty} r^{2(n+m)} \exp\{\left(-\gamma r^2\right)\} r d_r, \tag{A.27}$$

Let $\gamma r^2 = u \Rightarrow 2rdr = \dfrac{du}{\gamma}$, substituting in (A.27) we get:

$$\begin{aligned}
II =& \pi \sum_{n,m=0}^{\infty} \left(\frac{k_g^2}{\sigma_g^2\sigma_v^2 t}\right)^n \left(\frac{|Y_i|^2}{(\sigma_h^2|x|^2+\sigma_z^2)^2}\right)^m \frac{(n+m)!}{(n!)^2(m!)^2} \frac{1}{\gamma^{n+m+1}} \\
&= \pi \left(\frac{\sigma_g^2\sigma_v^2(\sigma_h^2|x|^2+\sigma_z^2)t}{\sigma_h^2|x|^2+\sigma_z^2+\sigma_g^2\sigma_v^2 t}\right) \sum_{n=0}^{\infty} \left(\frac{k_g^2(\sigma_h^2|x|^2+\sigma_z^2)}{\sigma_h^2|x|^2+\sigma_z^2+\sigma_g^2\sigma_v^2 t}\right)^n \times \\
&\sum_{m=0}^{\infty} \left(\frac{\sigma_g^2\sigma_v^2|Y_i|^2\ t}{(\sigma_h^2|x|^2+\sigma_z^2+\sigma_g^2\sigma_v^2 t)(\sigma_h^2|x|^2+\sigma_z^2)}\right)^m \frac{(n+m)!}{(n!)^2(m!)^2}, \\
&= \pi \left(\frac{\sigma_g^2\sigma_v^2(\sigma_h^2|x|^2+\sigma_z^2)t}{\sigma_h^2|x|^2+\sigma_z^2+\sigma_g^2\sigma_v^2 t}\right) \sum_{n=0}^{\infty} \left(\frac{k_g^2(\sigma_h^2|x|^2+\sigma_z^2)}{\sigma_h^2|x|^2+\sigma_z^2+\sigma_g^2\sigma_v^2 t}\right)^n \frac{1}{n!} \times \\
&{}_1F_1\left(n+1, 1, \frac{\sigma_g^2\sigma_v^2|Y_i|^2\ t}{(\sigma_h^2|x|^2+\sigma_z^2+\sigma_g^2\sigma_v^2 t)(\sigma_h^2|x|^2+\sigma_z^2)}\right),
\end{aligned} \tag{A.28}$$

where ${}_1F_1(\cdot,\cdot,\cdot)$ is the confluent hypergeometric function of the first kind [95]. Substituting for II from (A.28) in (A.23) completes the proof.

A.4 Proof of Theorem 3.4

It is apparent form (3.7) that given the transmitted symbol $\boldsymbol{x} = x$, $\boldsymbol{U}$ is Complex Gaussian vector. Given the phases of the channel mean vector components $\boldsymbol{\theta}_h = \theta_h$, it can be shown

that the pdf of $\boldsymbol{U}$ conditioned on $\boldsymbol{\theta}_h$ and x is given by:

$$f_{\boldsymbol{U}|\boldsymbol{x},\theta_h}(U|x,\theta_h) = \frac{1}{\pi^R(\sigma_h^2|x|^2+\sigma_z^2)^R}\exp\left(\frac{-\sum_{i=0}^{R}|U_i - k_h\sigma_h x e^{\jmath\theta_{h_i}}|^2}{\sigma_h^2|x|^2+\sigma_z^2}\right). \tag{A.29}$$

From (3.9) we have:

$$\begin{aligned} f_{\boldsymbol{Y}|\boldsymbol{x},\theta_h}(Y|x,\theta_h) &= \int_S f_{\boldsymbol{U}|\boldsymbol{x},\theta_h}(Y-S|x,\theta_h) f_{\boldsymbol{J}}(S)dS \\ &= \frac{1}{\left(\pi^2\sigma_g^2\sigma_v^2(\sigma_h^2|x|^2+\sigma_z^2)\right)^R}\int_0^\infty \exp(-t)\times \\ &\prod_{i=1}^{R}\int_{S_i}\exp\left(\frac{-|Y_i - k_h\sigma_h x e^{\jmath\theta_{h_i}} - S_i|^2}{\sigma_h^2|x|^2+\sigma_z^2}\right)\exp\left(-\frac{|S_i|^2}{\sigma_g^2\sigma_v^2 t}\right)d_{S_i}\frac{dt}{t^R}, \end{aligned} \tag{A.30}$$

noticing that

$$|Y_i - k_h\sigma_h x e^{\jmath\theta_{h_i}} - S_i|^2 = |Y_i - k_h\sigma_h x e^{\jmath\theta_{h_i}}|^2 + |S_i|^2 - 2|Y_i - k_h\sigma_h x e^{\jmath\theta_{h_i}}||S_i|\cos(\theta_{S_i}-\beta_i),$$

where $\theta_{S_i} = \angle S_i$ and $\beta_i = \angle(Y_i - k_h\sigma_h x e^{\jmath\theta_{h_i}})$, yields:

$$\begin{aligned} f_{\boldsymbol{Y}|\boldsymbol{x},\theta_h}(Y|x,\theta_h) = &\frac{1}{\left(\pi^2\sigma_g^2\sigma_v^2(\sigma_h^2|x|^2+\sigma_z^2)\right)^R}\int_0^\infty \exp(-t)\prod_{i=1}^{R}\exp\left(\frac{-|Y_i - k_h\sigma_h x e^{\jmath\theta_{h_i}}|^2}{\sigma_h^2|x|^2+\sigma_z^2}\right) \\ &\times\int_{S_i}\exp\left(\frac{-|S_i|^2 + 2|Y_i - k_h\sigma_h x e^{\jmath\theta_{h_i}}||S_i|\cos(\theta_{S_i}-\beta_i)}{\sigma_h^2|x|^2+\sigma_z^2}\right)\exp\left(-\frac{|S_i|^2}{\sigma_g^2\sigma_v^2 t}\right)d_{S_i}\frac{dt}{t^R}. \end{aligned} \tag{A.31}$$

Let II be the inner integration in (A.31), using the series expansion of $I_0(\cdot)$ yields:

$$II = \int_{S_i}\exp\left(-\gamma|S_i|^2\right)\exp\left(\frac{2|Y_i - k_h\sigma_h x e^{\jmath\theta_{h_i}}||S_i|\cos(\theta_{S_i}-\beta_i)}{\sigma_h^2|x|^2+\sigma_z^2}\right)d_{S_i}, \tag{A.32}$$

where $\gamma = \dfrac{1}{\sigma_h^2|x|^2+\sigma_z^2} + \dfrac{1}{\sigma_g^2\sigma_v^2 t}$.

Moving to the polar coordinate system where $|S_i| = r$ and $d_{s_i} = rd_r d_{\theta_{S_i}}$, equation (A.32) becomes:

$$II = \int_0^\infty \exp\left(\left(-\gamma r^2\right)\right) \int_0^{2\pi} \exp\left(\frac{2|Y_i - k_h\sigma_h x e^{\jmath\theta_{h_i}}|r\cos(\theta_{S_i}-\beta_i)}{\sigma_h^2|x|^2+\sigma_z^2}\right) d\theta_{S_i} r d_r, \tag{A.33}$$

the inner integration in (A.33) is equal to

$$2\pi\ I_0\left(\frac{2|Y_i - k_h\sigma_h x e^{\jmath\theta_{h_i}}|r}{\sigma_h^2|x|^2+\sigma_z^2}\right) = 2\pi\sum_{m=0}^{\infty}\left(\frac{|Y_i - k_h\sigma_h x e^{\jmath\theta_{h_i}}|^2 r^2}{(\sigma_h^2|x|^2+\sigma_z^2)^2}\right)^m \frac{1}{(m!)^2}, \tag{A.34}$$

Substituting from (A.34) in (A.33) yields:

$$II = 2\pi\sum_{m=0}^{\infty}\left(\frac{|Y_i - k_h\sigma_h x e^{\jmath\theta_{h_i}}|^2}{(\sigma_h^2|x|^2+\sigma_z^2)^2}\right)^m \frac{1}{(m!)^2}\int_0^\infty r^{2m}\ \exp\left(-\gamma r^2\right) r d_r, \tag{A.35}$$

Let $\gamma r^2 = u \Rightarrow 2rdr = \dfrac{du}{\gamma}$, substituting in (A.35) we get:

$$\begin{aligned} II &= \pi\sum_{m=0}^{\infty}\left(\frac{|Y_i - k_h\sigma_h x e^{\jmath\theta_{h_i}}|^2}{(\sigma_h^2|x|^2+\sigma_z^2)^2}\right)^m \frac{1}{m!}\frac{1}{\gamma^{m+1}} \\ &= \pi\left(\frac{\sigma_g^2\sigma_v^2(\sigma_h^2|x|^2+\sigma_z^2)t}{\sigma_h^2|x|^2+\sigma_z^2+\sigma_g^2\sigma_v^2 t}\right)\sum_{m=0}^{\infty}\left(\frac{\sigma_g^2\sigma_v^2|Y_i - k_h\sigma_h x e^{\jmath\theta_{h_i}}|^2 t}{(\sigma_h^2|x|^2+\sigma_z^2+\sigma_g^2\sigma_v^2 t)(\sigma_h^2|x|^2+\sigma_z^2)}\right)^m \frac{1}{m!} \\ &= \pi\left(\frac{\sigma_g^2\sigma_v^2(\sigma_h^2|x|^2+\sigma_z^2)t}{\sigma_h^2|x|^2+\sigma_z^2+\sigma_g^2\sigma_v^2 t}\right)\exp\left(\frac{\sigma_g^2\sigma_v^2|Y_i - k_h\sigma_h x e^{\jmath\theta_{h_i}}|^2 t}{(\sigma_h^2|x|^2+\sigma_z^2+\sigma_g^2\sigma_v^2 t)(\sigma_h^2|x|^2+\sigma_z^2)}\right) \end{aligned} \tag{A.36}$$

Substituting for II from (A.36) in (A.31) yields:

$$
\begin{aligned}
f_{\boldsymbol{Y}|\boldsymbol{x},\theta_h}(Y|x,\theta_h) &= \frac{1}{\pi^R}\int_0^\infty \frac{\exp(-t)}{(\sigma_h^2|x|^2+\sigma_z^2+\sigma_g^2\sigma_v^2 t)^R}\prod_{i=1}^{R}\exp\left(-\frac{|Y_i-k_h\sigma_h x e^{\jmath\theta_{h_i}}|^2}{\sigma_h^2|x|^2+\sigma_z^2}\right)\\
&\quad\times\exp\left(\frac{\sigma_g^2\sigma_v^2|Y_i-k_h\sigma_h x e^{\jmath\theta_{h_i}}|^2 t}{(\sigma_h^2|x|^2+\sigma_z^2+\sigma_g^2\sigma_v^2 t)(\sigma_h^2|x|^2+\sigma_z^2)}\right)\,dt,\\
&= \frac{1}{\pi^R}\int_0^\infty \frac{\exp(-t)}{(\sigma_h^2|x|^2+\sigma_z^2+\sigma_g^2\sigma_v^2 t)^R}\prod_{i=1}^{R}\exp\left(-\frac{|Y_i-k_h\sigma_h x e^{\jmath\theta_{h_i}}|^2}{\sigma_h^2|x|^2+\sigma_z^2+\sigma_g^2\sigma_v^2 t}\right)\,dt,
\end{aligned}
$$

noticing that

$$
|Y_i-k_h\sigma_h x e^{\jmath\theta_{h_i}}|^2 = |Y_i|^2+k_h^2\sigma_h^2|x|^2-2k_h\sigma_h|Y_i||x|\cos(\theta_{h_i}-\phi_i), \tag{A.37}
$$

yields:

$$
\begin{aligned}
f_{\boldsymbol{Y}|\boldsymbol{x},\theta_h}(Y|x,\theta_h) &= \frac{1}{\pi^R}\int_0^\infty \frac{1}{(\sigma_h^2|x|^2+\sigma_z^2+\sigma_g^2\sigma_v^2 t)^R}\exp\left(-t-\frac{k_h^2\sigma_h^2|x|^2R+|Y|^2}{\sigma_h^2|x|^2+\sigma_z^2+\sigma_g^2\sigma_v^2 t}\right)\\
&\quad\times\prod_{i=1}^{R}\exp\left(\frac{2k_h\sigma_h|Y_i||x|\cos(\theta_{h_i}-\phi_i)}{\sigma_h^2|x|^2+\sigma_z^2+\sigma_g^2\sigma_v^2 t}\right)\,dt.
\end{aligned} \tag{A.38}
$$

Multiplying (A.38) by the pdf of $\theta_h = \dfrac{1}{(2\pi)^R}$ and integrating the result over all possible

values of θ_h yields:

$$
\begin{aligned}
f_{\boldsymbol{Y}|\boldsymbol{x}}(Y|x) &= \frac{1}{\pi^R}\int_0^\infty \frac{1}{(\sigma_h^2|x|^2+\sigma_z^2+\sigma_g^2\sigma_v^2 t)^R}\exp\left(-t-\frac{k_h^2\sigma_h^2|x|^2R+|Y|^2}{\sigma_h^2|x|^2+\sigma_z^2+\sigma_g^2\sigma_v^2 t}\right)\\
&\qquad\times\prod_{i=1}^R\int_0^{2\pi}\exp\left(\frac{2k_h\sigma_h|Y_i||x|\cos(\theta_{h_i}-\phi_i)}{\sigma_h^2|x|^2+\sigma_z^2+\sigma_g^2\sigma_v^2 t}\right)\frac{1}{2\pi}\,d_{\theta_{h_i}}\,dt,\\
&= \frac{1}{\pi^R}\int_0^\infty \frac{1}{(\sigma_h^2|x|^2+\sigma_z^2+\sigma_g^2\sigma_v^2 t)^R}\exp\left(-t-\frac{k_h^2\sigma_h^2|x|^2R+|Y|^2}{\sigma_h^2|x|^2+\sigma_z^2+\sigma_g^2\sigma_v^2 t}\right)\\
&\qquad\times\prod_{i=1}^R I_0\left(\frac{2k_h\sigma_h|Y_i||x|}{\sigma_h^2|x|^2+\sigma_z^2+\sigma_g^2\sigma_v^2 t}\right)\,dt.
\end{aligned}
$$

A.5 Proof of Lemma 3.1

Given the transmitted symbol $\boldsymbol{x}=x$, and the phases of the mean vector components $\boldsymbol{\theta_h}=\theta_h$, it can be seen that the received signal vector, $\boldsymbol{Y}$, is a complex Gaussian random vector whose components are independent. The i-th component of $\boldsymbol{Y}$ has a mean $\mu_{Y_i|x,\theta_{h_i}}=k_h\sigma_h x e^{\jmath\theta_{h_i}}$, and a variance $\sigma_{Y_i}^2=\sigma_h^2|x|^2+\sigma_z^2+\sigma_g^2\sigma_v^2$, $i\in\{1,\cdots,R\}$. The pdf of $\boldsymbol{Y_i}$ conditioned on $\boldsymbol{x}$ and $\boldsymbol{\theta_{h}}_i$ is given by:

$$
\begin{aligned}
\hat{p}_{\boldsymbol{Y_i}|\boldsymbol{x},\boldsymbol{\theta_h}_i}(Y_i|x,\theta_{h_i}) &= \frac{1}{\pi(\sigma_h^2|x|^2+\sigma_z^2+\sigma_g^2\sigma_v^2)}\exp\left(\frac{-Y_i-k_h\sigma_h x e^{\jmath\theta_{h_i}}|^2}{\sigma_h^2|x|^2+\sigma_z^2+\sigma_g^2\sigma_v^2}\right),\\
&= \frac{\exp\left(\frac{-|Y_i|^2-k_h^2\sigma_h^2|x|^2}{\sigma_h^2|x|^2+\sigma_z^2+\sigma_g^2\sigma_v^2}\right)}{\pi(\sigma_h^2|x|^2+\sigma_z^2+\sigma_g^2\sigma_v^2)}\exp\left(\frac{2k_h\sigma_h|Y_i||x|\cos(\theta_{h_i})}{\sigma_h^2|x|^2+\sigma_z^2+\sigma_g^2\sigma_v^2}\right).
\end{aligned}
\tag{A.39}
$$

Multiplying (A.39) by the pdf of $\boldsymbol{\theta_{h_i}}$, $p_{\boldsymbol{\theta_{h_i}}}(\theta_{h_i}) = \dfrac{1}{2\pi}$ and integrating over all possible values of θ_{h_i} yields:

$$\begin{aligned}\hat{p}_{\boldsymbol{Y_i}|\boldsymbol{x}}(Y_i|x) &= \frac{\exp\left(\dfrac{-|Y_i|^2 - k_h^2\sigma_h^2|x|^2}{\sigma_h^2|x|^2+\sigma_z^2+\sigma_g^2\sigma_v^2}\right)}{\pi(\sigma_h^2|x|^2+\sigma_z^2+\sigma_g^2\sigma_v^2)}\int_0^{2\pi}\exp\left(\frac{2k_h\sigma_h|Y_i||x|\cos(\theta_{h_i})}{\sigma_h^2|x|^2+\sigma_z^2+\sigma_g^2\sigma_v^2}\right)\frac{d_{\theta_{h_i}}}{2\pi}\\ &= \frac{\exp\left(\dfrac{-|Y_i|^2 - k_h^2\sigma_h^2|x|^2}{\sigma_h^2|x|^2+\sigma_z^2+\sigma_g^2\sigma_v^2}\right)}{\pi(\sigma_h^2|x|^2+\sigma_z^2+\sigma_g^2\sigma_v^2)}I_0\left(\frac{2k_h\sigma_h|Y_i||x|\cos(\theta_{h_i})}{\sigma_h^2|x|^2+\sigma_z^2+\sigma_g^2\sigma_v^2}\right).\end{aligned} \tag{A.40}$$

Using (A.40) in $\hat{p}_{\boldsymbol{Y}|\boldsymbol{x}}(Y|x) = \prod_{i=1}^{R}\hat{p}_{\boldsymbol{Y_i}|\boldsymbol{x}}(Y_i|x)$ completes the proof.

A.6 Proof of Theorem 3.5

From (3.9) we have:

$$\begin{aligned}f_{\boldsymbol{Y}|\boldsymbol{x},\theta_h}(Y|x,\theta_h) &= \int_S f_{\boldsymbol{U}|\boldsymbol{x},\theta_h}(Y-S|x,\theta_h)f_{\boldsymbol{J}}(S)dS\\ &= \frac{\exp\left(-k_g^2R\right)}{\left(\pi^2\sigma_g^2\sigma_v^2(\sigma_h^2|x|^2+\sigma_z^2)\right)^R}\int_0^\infty \exp(-t)\times\\ &\prod_{i=1}^{R}\int_{S_i}\exp\left\{\left(\frac{-|Y_i-k_h\sigma_h x e^{\jmath\theta_{h_i}}-S_i|^2}{(\sigma_h^2|x|^2+\sigma_z^2)}\right)\right\}I_0\left(\frac{2k_g|S_i|}{\sigma_g\sigma_v\sqrt{t}}\right)\exp\left(-\frac{|S_i|^2}{\sigma_g^2\sigma_v^2 t}\right)d_{S_i}\frac{dt}{t^R}\end{aligned} \tag{A.41}$$

noticing that

$$|Y_i - k_h\sigma_h x e^{\jmath\theta_{h_i}} - S_i|^2 = |Y_i - k_h\sigma_h x e^{\jmath\theta_{h_i}}|^2 + |S_i|^2 - 2|Y_i - k_h\sigma_h x e^{\jmath\theta_{h_i}}||S_i|\cos(\theta_{S_i}-\beta_i),$$

where $\theta_{S_i} = \angle(S_i)$ and $\beta_i = \angle(Y_i - k_h\sigma_h x e^{\jmath\theta_{h_i}})$, yields:

$$f_{\boldsymbol{Y}|\boldsymbol{x},\theta_h}(Y|x,\theta_h) = \frac{\exp\left(-k_g^2 R\right)}{\left(\pi^2\sigma_g^2\sigma_v^2(\sigma_h^2|x|^2+\sigma_z^2)\right)^R}\int_0^\infty \exp(-t)\prod_{i=1}^{R}\exp\left\{\left(\frac{-|Y_i - k_h\sigma_h x e^{\jmath\theta_{h_i}}|^2}{(\sigma_h^2|x|^2+\sigma_z^2)}\right)\right\}\times$$
$$\int_{S_i}\exp\left\{\left(\frac{-|S_i|^2 + 2|Y_i - k_h\sigma_h x e^{\jmath\theta_{h_i}}||S_i|\cos(\theta_{S_i}-\beta_i)}{(\sigma_h^2|x|^2+\sigma_z^2)}\right)\right\} I_0\left(\frac{2k_g|S_i|}{\sigma_g\sigma_v\sqrt{t}}\right)\times$$
$$\exp\left(-\frac{|S_i|^2}{\sigma_g^2\sigma_v^2 t}\right) d_{S_i}\frac{dt}{t^R}. \tag{A.42}$$

Let II be the inner integration in (A.42), using the series expansion of $I_0(\cdot)$ yields:

$$II = \sum_{n=0}^{\infty}\left(\frac{k_g^2}{\sigma_g^2\sigma_v^2 t}\right)^n \frac{1}{(n!)^2}\int_{S_i}|S_i|^{2n}\exp\left(-\gamma|S_i|^2\right)\exp\left(\frac{2|Y_i - k_h\sigma_h x e^{\jmath\theta_{h_i}}||S_i|\cos(\theta_{S_i}-\beta_i)}{\sigma_h^2|x|^2+\sigma_z^2}\right)d_{S_i}, \tag{A.43}$$

where $\gamma = \dfrac{1}{\sigma_h^2|x|^2+\sigma_z^2} + \dfrac{1}{\sigma_g^2\sigma_v^2 t}$.

Moving to the polar coordinate system where $|S_i| = r$ and $d_{s_i} = r d_r d_{\theta_{S_i}}$, equation (A.43) becomes:

$$II = \sum_{n=0}^{\infty}\left(\frac{k_g^2}{\sigma_g^2\sigma_v^2 t}\right)^n \frac{1}{(n!)^2}$$
$$\times\int_0^\infty r^{2n}\exp\left\{\left(-\gamma r^2\right)\right\}\int_0^{2\pi}\exp\left\{\left(\frac{2|Y_i - k_h\sigma_h x e^{\jmath\theta_{h_i}}|r\cos(\theta_{S_i}-\beta_i)}{\sigma_h^2|x|^2+\sigma_z^2}\right)\right\}d\theta_{S_i} r d_r, \tag{A.44}$$

the inner integration in (A.44) is equal to

$$2\pi\ I_0\left(\frac{2|Y_i - k_h\sigma_h x e^{\jmath\theta_{h_i}}|r}{\sigma_h^2|x|^2+\sigma_z^2}\right) = 2\pi\sum_{m=0}^{\infty}\left(\frac{|Y_i - k_h\sigma_h x e^{\jmath\theta_{h_i}}|^2 r^2}{(\sigma_h^2|x|^2+\sigma_z^2)^2}\right)^m \frac{1}{(m!)^2}, \tag{A.45}$$

Substituting from (A.45) in (A.44) yields:

$$II = 2\pi \sum_{n,m=0}^{\infty} \left(\frac{k_g^2}{\sigma_g^2\sigma_v^2 t}\right)^n \frac{1}{(n!)^2} \left(\frac{|Y_i - k_h\sigma_h x e^{\jmath\theta_{h_i}}|^2}{(\sigma_h^2|x|^2+\sigma_z^2)^2}\right)^m \frac{1}{(m!)^2} \int_0^{\infty} r^{2(n+m)} \exp\{(-\gamma r^2)\} r d_r, \tag{A.46}$$

Let $\gamma r^2 = u \Rightarrow 2rdr = \dfrac{du}{\gamma}$, substituting in (A.46) we get:

$$\begin{aligned} II =& \pi \sum_{n,m=0}^{\infty} \left(\frac{k_g^2}{\sigma_g^2\sigma_v^2 t}\right)^n \left(\frac{|Y_i - k_h\sigma_h x e^{\jmath\theta_{h_i}}|^2}{(\sigma_h^2|x|^2+\sigma_z^2)^2}\right)^m \frac{(n+m)!}{(n!)^2(m!)^2} \frac{1}{\gamma^{n+m+1}} \\ =& \pi \left(\frac{\sigma_g^2\sigma_v^2 t(\sigma_h^2|x|^2+\sigma_z^2)}{\sigma_h^2|x|^2+\sigma_z^2+\sigma_g^2\sigma_v^2 t}\right) \sum_{n=0}^{\infty} \left(\frac{k_g^2(\sigma_h^2|x|^2+\sigma_z^2)}{\sigma_h^2|x|^2+\sigma_z^2+\sigma_g^2\sigma_v^2 t}\right)^n \\ & \times \sum_{m=0}^{\infty} \left(\frac{\sigma_g^2\sigma_v^2 t|Y_i - k_h\sigma_h x e^{\jmath\theta_{h_i}}|^2}{(\sigma_h^2|x|^2+\sigma_z^2+\sigma_g^2\sigma_v^2 t)(\sigma_h^2|x|^2+\sigma_z^2)}\right)^m \frac{(n+m)!}{(n!)^2(m!)^2}. \end{aligned} \tag{A.47}$$

Substituting for II from (A.47) in (A.41) yields:

$$\begin{aligned} f_{\boldsymbol{Y}|\boldsymbol{x},\theta_h}(Y|x,\theta_h) =& \frac{\exp(-k_g^2 R)}{\pi^R} \int_0^{\infty} \frac{\exp(-t)}{(\sigma_h^2|x|^2+\sigma_z^2+\sigma_g^2\sigma_v^2 t)^R} \prod_{i=1}^{R} \exp\left\{\left(-\frac{|Y_i - k_h\sigma_h x e^{\jmath\theta_{h_i}}|^2}{\sigma_h^2|x|^2+\sigma_z^2}\right)\right\} \\ \times& \sum_{n=0}^{\infty} \left(\frac{k_g^2(\sigma_h^2|x|^2+\sigma_z^2)}{\sigma_h^2|x|^2+\sigma_z^2+\sigma_g^2\sigma_v^2 t}\right)^n \frac{1}{(n!)^2} \sum_{m=0}^{\infty} \left(\frac{\sigma_g^2\sigma_v^2 t|Y_i - k_h\sigma_h x e^{\jmath\theta_{h_i}}|^2}{(\sigma_h^2|x|^2+\sigma_z^2+\sigma_g^2\sigma_v^2 t)(\sigma_h^2|x|^2+\sigma_z^2)}\right)^m \frac{(n+m)!}{(m!)^2} dt, \end{aligned} \tag{A.48}$$

Using the following substitution $|Y_i - k_h\sigma_h x e^{\jmath\theta_{h_i}}|^2 = |Y_i|^2 + k_h^2\sigma_h^2|x|^2 - 2k_h\sigma_h|Y_i||x|\cos(\theta_{h_i} - \phi_i)$ in (A.48) yields:

$$f_{\boldsymbol{Y}|\boldsymbol{x},\theta_h}(Y|x,\theta_h) = \frac{1}{\pi^R}\exp\big(-k_g^2 R\big)$$
$$\times \exp\left(-\frac{|Y|^2 + k_h^2\sigma_h^2|x|^2 R}{\sigma_h^2|x|^2+\sigma_z^2}\right)\int_0^\infty \frac{\exp(-t)}{(\sigma_h^2|x|^2+\sigma_z^2+\sigma_g^2\sigma_v^2 t)^R}\prod_{i=1}^{R}\exp\left(\frac{2k_h\sigma_h|x||Y_i|}{\sigma_h^2|x|^2+\sigma_z^2}\cos(\theta_{h_i}-\phi_i)\right)$$
$$\times\sum_{n=0}^{\infty}\left(\frac{k_g^2(\sigma_h^2|x|^2+\sigma_z^2)}{\sigma_h^2|x|^2+\sigma_z^2+\sigma_g^2\sigma_v^2 t}\right)^n\frac{1}{(n!)^2}\sum_{m=0}^{\infty}\left(\frac{\sigma_g^2\sigma_v^2 t(|Y_i|^2+k_h^2\sigma_h^2|x|^2-2k_h\sigma_h|Y_i||x|\cos(\theta_{h_i}-\phi_i)}{(\sigma_h^2|x|^2+\sigma_z^2+\sigma_g^2\sigma_v^2 t)(\sigma_h^2|x|^2+\sigma_z^2)}\right)^m$$
$$\times\frac{(n+m)!}{(m!)^2}\,dt, \quad \text{(A.49)}$$

Multiplying (A.49) by the pdf of $\theta_h = \dfrac{1}{(2\pi)^R}$ and integrating the result over all possible values of θ_h yields:

$$f_{\boldsymbol{Y}|\boldsymbol{x},\theta_h}(Y|x,\theta_h) = \frac{1}{\pi^R}\exp\left(-k_g^2 R - \frac{|Y|^2+k_h^2\sigma_h^2|x|^2 R}{\sigma_h^2|x|^2+\sigma_z^2}\right)\int_0^\infty\frac{\exp(-t)}{(\sigma_h^2|x|^2+\sigma_z^2+\sigma_g^2\sigma_v^2 t)^R}$$
$$\times\prod_{i=1}^{R}\sum_{n=0}^{\infty}\left(\frac{k_g^2(\sigma_h^2|x|^2+\sigma_z^2)}{\sigma_h^2|x|^2+\sigma_z^2+\sigma_g^2\sigma_v^2 t}\right)^n\frac{1}{(n!)^2}\sum_{m=0}^{\infty}\left(\frac{\sigma_g^2\sigma_v^2 t}{\sigma_h^2|x|^2+\sigma_z^2+\sigma_g^2\sigma_v^2 t}\right)^m\frac{(n+m)!}{(m!)^2}$$
$$\times\int_0^{2\pi}\left(\frac{|Y_i|^2+k_h^2\sigma_h^2|x|^2-2k_h\sigma_h|Y_i||x|\cos(\theta_{h_i}-\phi_i)}{\sigma_h^2|x|^2+\sigma_z^2}\right)^m\exp\left(\frac{2k_h\sigma_h|x||Y_i|}{\sigma_h^2|x|^2+\sigma_z^2}\cos(\theta_{h_i}-\phi_i)\right)$$
$$\times\frac{1}{2\pi}\,d_{\theta_{h_i}}\,dt, \quad \text{(A.50)}$$

Denote the inner integration in (A.50) by $\Phi(x, Y_i)$. Using the binomial expansion, $(a+b)^m = \sum_{\ell=0}^{m}\dfrac{m!\;a^\ell\;b^{m-\ell}}{\ell!\;(m-\ell)!}$, where $a = -2k_h\sigma_h|Y_i||x|\cos(\theta_{h_i}-\phi_i)$ and $b = |Y_i|^2+k_h^2\sigma_h^2|x|^2$, yields:

$$\Phi(x, Y_i) = \sum_{\ell=0}^{m} \frac{(m!)(|Y_i|^2 + k_h^2\sigma_h^2|x|^2)^{m-\ell}}{(\ell!)\ (m-\ell)!(\sigma_h^2|x|^2 + \sigma_z^2)^{m-\ell}}$$
$$\times \int_0^{2\pi} \left(\frac{-2k_h\sigma_h|x||Y_i|}{\sigma_h^2|x|^2 + \sigma_z^2}\right)^{\ell} (\cos(\theta_{h_i} - \phi_i))^{\ell} \exp\left(\frac{2k_h\sigma_h|x||Y_i|}{\sigma_h^2|x|^2 + \sigma_z^2}\cos(\theta_{h_i} - \phi_i)\right) \frac{d_{\theta_{h_i}}}{2\pi}, \quad \text{(A.51)}$$

The integration in (A.51) is given by:

$$\Phi(x, Y_i) = \frac{((-c)^{\ell} + c^{\ell})}{2}\Gamma\left(\frac{1+\ell}{2}\right) {}_1\tilde{F}_2\left(\frac{1+\ell}{2}; \frac{1}{2}, \frac{2+\ell}{2}; \frac{c^2}{4}\right)$$
$$+ \frac{c\ ((-c)^{\ell} - c^{\ell})}{4}\Gamma\left(1 + \frac{\ell}{2}\right) {}_1\tilde{F}_2\left(\frac{2+\ell}{2}; \frac{3}{2}, \frac{3+\ell}{2}; \frac{c^2}{4}\right), \quad \text{(A.52)}$$

where $c = \dfrac{2k_h\sigma_h|x||Y_i|}{\sigma_h^2|x|^2 + \sigma_z^2}$, $\Gamma(\cdot)$ is the gamma function, and ${}_1\tilde{F}_2(\cdot;\cdot,\cdot;\cdot)$ is the regularized generalized hypergeomtric function [96].

Substituting for $\Phi(x, Y_i)$ from (A.51) into (A.50) yields:

$$f_{\boldsymbol{Y}|\boldsymbol{x}}(Y|x) = \frac{1}{\pi^R}\exp\left(-k_g^2 R - \frac{|Y|^2 + k_h^2\sigma_h^2|x|^2 R}{\sigma_h^2|x|^2 + \sigma_z^2}\right)\int_0^{\infty} \frac{\exp(-t)}{(\sigma_h^2|x|^2 + \sigma_z^2 + \sigma_g^2\sigma_v^2 t)^R}$$
$$\times \prod_{i=1}^{R}\sum_{n=0}^{\infty}\sum_{m=0}^{\infty}\left(\frac{k_g^2(\sigma_h^2|x|^2 + \sigma_z^2)}{\sigma_h^2|x|^2 + \sigma_z^2 + \sigma_g^2\sigma_v^2 t}\right)^n \left(\frac{\sigma_g^2\sigma_v^2(|Y_i|^2 + k_h^2\sigma_h^2|x|^2)t}{(\sigma_h^2|x|^2 + \sigma_z^2 + \sigma_g^2\sigma_v^2 t)(\sigma_h^2|x|^2 + \sigma_z^2)}\right)^m \frac{(n+m)!}{(n!)^2(m!)}$$
$$\times \sum_{\ell=0}^{m} \frac{(\sigma_h^2|x|^2 + \sigma_z^2)^{\ell}}{(\ell!)\ (m-\ell)!(|Y_i|^2 + k_h^2\sigma_h^2|x|^2)^{\ell}}\Phi(x, Y_i)\ dt, \quad \text{(A.53)}$$

Appendix B

Proofs for chaper 4

B.1 Proof of Theorem 4.1

Since $\boldsymbol{J} = \boldsymbol{g}\boldsymbol{V}$, we note that, conditioned on $\boldsymbol{g}$, the m-th and n-th entries of $\boldsymbol{J}$, i.e., $\boldsymbol{J}_m$ and $\boldsymbol{J}_n$, $m \neq n$, are statistically independent complex Gaussian random variables with zero mean and variance $|\boldsymbol{g}|^2\sigma_V^2$. In this case, the pdf of $\boldsymbol{J}$ is given by:

$$p_{\boldsymbol{J}|\boldsymbol{g}}(J|g) = \prod_{i=1}^{T} p_{\boldsymbol{J}_i|\boldsymbol{g}}(J_i|g). \tag{B.1}$$

The pdf of $\boldsymbol{J}_i$ given $\boldsymbol{g}$ is given by:

$$p_{\boldsymbol{J}_i|\boldsymbol{g}}(J_i|g) = \frac{1}{\pi\sigma_V^2|g|^2}\exp\left(\frac{-|J_i|^2}{|g|^2\sigma_V^2}\right). \tag{B.2}$$

Substituting from (B.2) in (B.1) yields:

$$p_{\boldsymbol{J}|\boldsymbol{g}}(J|g) = \frac{1}{\pi^T \sigma_V^{2T} |g|^{2T}} \exp\left(\frac{-\|J\|^2}{|g|^2 \sigma_V^2}\right). \tag{B.3}$$

Using the fact that the pdf of $\boldsymbol{g}$ is given by:

$$p_{\boldsymbol{g}}(g) = \frac{1}{\pi \sigma_g^2} \exp\left(\frac{-|g|^2}{\sigma_g^2}\right) \tag{B.4}$$

yields

$$p_{\boldsymbol{J}}(J) = \frac{1}{\pi^{T+1} \sigma_V^{2T}\ \sigma_g^2} \int_{-\infty}^{\infty} \int_{-\infty}^{\infty} \frac{1}{|g|^{2T}} \exp\left(\frac{-\|J\|^2}{|g|^2 \sigma_V^2} - \frac{|g|^2}{\sigma_g^2}\right) dg_r dg_i, \tag{B.5}$$

where g_r and g_i are the real and imaginary parts of g. Expressing (B.5) in the polar coordinates with $|g| = r$, $g_r = r\cos(\theta)$ and $g_i = r\sin(\theta)$ yields

$$p_{\boldsymbol{J}}(J) = \frac{1}{\pi^{T+1} \sigma_V^{2T} \sigma_g^2} \int_0^{\infty} \int_0^{2\pi} \frac{1}{r^{2T}} \exp\left(\frac{-\|J\|^2}{r^2 \sigma_V^2} - \frac{r^2}{\sigma_g^2}\right) r dr d\theta \tag{B.6}$$

$$= \frac{2}{\pi^T \sigma_V^{2T} \sigma_g^2} \int_0^{\infty} \frac{1}{r^{2T-1}} \exp\left(-\frac{\|J\|^2}{r^2\ \sigma_V^2} - \frac{r^2}{\sigma_g^2}\right) dr. \tag{B.7}$$

To express this integration in the form of the modified Bessel function, we use the following change variables from [86]

$$u = \ln\left(\frac{r^2\ \sigma_V}{\|J\| \sigma_g}\right). \tag{B.8}$$

Doing so yields:

$$p_{\boldsymbol{J}}(J) = \frac{1}{\pi^T \sigma_V^{T+1} \sigma_g^{T+1} \|J\|^{T-1}} \times \int_{-\infty}^{\infty} \exp\left(-(T-1)u - 2\frac{\|J\|}{\sigma_g \sigma_V} \cosh(u)\right) du. \tag{B.9}$$

Noting that the latter integration equals $2\ K_{T-1}\left(\frac{2\ \|J\|_2}{\sigma_{hj}\ \sigma_V}\right)$ [97, (3.337.1)], where $K_\nu(\cdot)$ is the modified Bessel function of second kind of order ν, yields (4.12) and concludes the

proof.

B.2 Proof of Theorem 4.2

We begin the proof by noting that, conditioned on $\boldsymbol{g}$ being given, the vector $\boldsymbol{J}$ is independent of the phase, $\boldsymbol{\theta}_{\mu_g}$, of the jammer's channel mean μ_g. In other words, $(\boldsymbol{\theta}_{\mu_g}, \boldsymbol{g}, \boldsymbol{J})$ form the Markov chain $\boldsymbol{\theta}_{\mu_g} \to \boldsymbol{g} \to \boldsymbol{J}$, whereupon we have

$$p_{\boldsymbol{J}|\boldsymbol{g},\boldsymbol{\theta}_{\mu_g}}(J|g, \theta_{\mu_g}) = p_{\boldsymbol{J}|\boldsymbol{g}}(J|g), \tag{B.10}$$

where $p_{\boldsymbol{J}|\boldsymbol{g}}(J|g)$ is given in (B.3).

The channel $\boldsymbol{g}$ in this case is a complex Gaussian random variable with mean $\mu_g = k_g \sigma_g e^{\jmath\theta_{\mu_g}}$. Hence, conditioned on $\boldsymbol{\theta}_{\mu_g}$, the pdf of the jammer channel is given by:

$$p_{\boldsymbol{g}|\boldsymbol{\theta}_{\mu_g}}(g|\theta_{\mu_g}) = \frac{1}{\pi\sigma_g^2} \exp\left(\frac{-|g - k_g\ \sigma_g\ e^{\jmath\theta_{\mu_g}}|^2}{\sigma_g^2}\right). \tag{B.11}$$

Using (B.10) and (B.11), the joint pdf of $\boldsymbol{J}$ and $\boldsymbol{g}$ conditioned on $\boldsymbol{\theta}_{\mu_g}$ is given by:

$$p_{\boldsymbol{J},\boldsymbol{g}|\boldsymbol{\theta}_{\mu_g}}(J, g|\theta_{\mu_g}) = \frac{\exp\left(-k_g^2\right)}{\pi^{T+1}\sigma_V^{2T}\sigma_g^2|g|^{2T}} \exp\left(\frac{-\|J\|^2}{|g|^2\sigma_V^2} - \frac{\left(|g|^2 - 2\ k_g\sigma_g|g|\cos\left(\theta_g - \theta_{\mu_g}\right)\right)}{\sigma_g^2}\right), \tag{B.12}$$

where $\theta_g = \measuredangle g$. Integrating (B.12) in the polar coordinates over all realizations of $\boldsymbol{g}$ yields

$$p_{\boldsymbol{J}|\boldsymbol{\theta}_{\mu_g}}(J|\theta_{\mu_g}) = \frac{\exp\left(-k_g^2\right)}{\pi^{T+1}\sigma_V^{2T}\sigma_g^2}\int_0^\infty \frac{1}{r^{2T}}\exp\left(\frac{-\|J\|^2}{r^2\sigma_V^2} - \frac{r^2}{\sigma_g^2}\right) \times \int_0^{2\pi}\exp\left(\frac{2k_g r\cos\left(\theta_g-\theta_{\mu_g}\right)}{\sigma_g}\right)d_{\theta_{\mu_g}} r d_r \quad \text{(B.13)}$$

The inner integration in (B.13) can be readily seen to be given by:

$$\int_0^{2\pi}\exp\left(\frac{2k_g r\cos\left(\theta_g-\theta_{\mu_g}\right)}{\sigma_g}\right)d_{\theta_g} = 2\pi I_0\left(\frac{2k_g r}{\sigma_g}\right) = 2\pi\sum_{\ell=0}^{\infty}\frac{(k_g r)^{2\ell}}{\sigma_g^{2\ell}(\ell!)^2}, \quad \text{(B.14)}$$

where $I_0(\cdot)$ is the modified Bessel function of the first kind of order zero [95]. Note that the periodicity of the integrand in θ_g renders the value of the integration independent of θ_g. Substituting from (B.14) in (B.13) yields:

$$p_{\boldsymbol{J}|\boldsymbol{\theta}_{\mu_g}}(J|\theta_{\mu_g}) = \frac{\exp\left(-k_g^2\right)}{\pi^T}\sigma_V^{2T}\sigma_g^2\sum_{\ell=0}^{\infty}\frac{(k_g)^{2\ell}}{\sigma_g^{2\ell}(\ell!)^2}\int_0^\infty r^{2(\ell-T)}\exp\left(\frac{-\|J\|^2}{r^2\ \sigma_V^2} - \frac{r^2}{\sigma_g^2}\right)2rd_r. \quad \text{(B.15)}$$

Using the change of variables in (B.8) yields:

$$p_{\boldsymbol{J}|\boldsymbol{\theta}_{\mu_g}}(J|\theta_{\mu_g}) = \frac{\exp\left(-k_g^2\right)}{\pi^T}\sigma_V^{2T}\sigma_g^2\sum_{\ell=0}^{\infty}\frac{(k_g)^{2\ell}}{\sigma_g^{2\ell}(\ell!)^2}\left(\frac{\sigma_g\|J\|}{\sigma_V}\right)^{\ell-T+1} \times\int_{-\infty}^{\infty}\exp\left(-\left(T-\ell-1\right)u - \frac{2\|J\|}{\sigma_V\sigma_g}\cosh\left(u\right)\right)du. \quad \text{(B.16)}$$

Similar to the proof of Theorem 4.1 in Appendix B.1, the integration in (B.16) can be shown to be equal to $2K_{T-\ell-1}\left(2\frac{\|J\|}{\sigma_V\sigma_g}\right)$ [97, (3.337.1)]. Invoking the representation of

$K_\nu(\cdot)$ in (4.14) yields

$$p_{\boldsymbol{J}|\boldsymbol{\theta}_{\mu_g}}(J|\theta_{\mu_g}) = \frac{\exp\left(-k_g^2\right)}{\pi^T \sigma_V^{2T} \sigma_g^{2T}} \sum_{\ell=0}^{\infty} \frac{(k_g)^{2\ell}}{(\ell!)^2} \int_0^\infty \exp\left(-t - \frac{\|J\|^2}{\sigma_g^2 \sigma_V^2\ t}\right) \frac{dt}{t^{T-\ell}}. \tag{B.17}$$

The pdf in (B.17) is independent of θ_{μ_g}. Hence, removing the conditioning on $\boldsymbol{\theta}_{\mu_g}$ and noting that

$$\sum_{\ell=0}^{\infty} \frac{\left(k_g\ \sqrt{t}\right)^{2\ell}}{(\ell!)^2} = I_0\left(2\ k_g\ \sqrt{t}\right). \tag{B.18}$$

completes the proof of the theorem.

B.3 Proof of Theorem 4.3

From (4.8), it can be seen that given $\boldsymbol{h} = h$ and $\boldsymbol{X} = X$, $\boldsymbol{U}$ is a complex Gaussian random vector with mean $\mu_{\boldsymbol{U}} = hX$, and covariance $\Sigma = \sigma_Z^2 I_T$. Hence,

$$p_{\boldsymbol{U}|\boldsymbol{X}}(U|X) = \frac{1}{\pi^T \sigma_Z^{2T}} \exp\Big(\frac{\|U - hX\|^2}{\sigma_Z^2}\Big). \tag{B.19}$$

Now, the expression in (4.11) implies that

$$p_{\boldsymbol{Y}|\boldsymbol{X}}(Y|X) = \int_{\mathcal{S}} f_{\boldsymbol{U}|\boldsymbol{X}}(Y - S|X) f_{\boldsymbol{J}}(S)\ dS, \tag{B.20}$$

where $\mathcal{S} = (-\infty, \infty)^{2T}$ is the region of integration of the complex vector S.

Substituting from (4.13), (B.18) and (B.19) into (B.20) yields:

$$p_{\boldsymbol{Y}|\boldsymbol{X}}(Y|X) = \frac{\exp\left(-k_g^2\right)}{\left(\pi^2\sigma_V^2\sigma_g^2\sigma_Z^2\right)^T}\sum_{\ell=0}^{\infty}\frac{\left(k_g^2\right)^\ell}{(\ell!)^2}\int_0^\infty\int_{\mathcal{S}}\exp\left(-\frac{\|Y-S-hX\|^2}{\sigma_Z^2}\right)\times \exp\left(-t-\frac{\|S\|^2}{\sigma_g^2\sigma_V^2 t}\right)dS\frac{dt}{t^T-\ell}. \quad \text{(B.21)}$$

Using the fact that $\|Y-S-hX\|^2=\sum_{i=1}^T(|Y_i-hX_i|^2+|S_i|^2-2\,\mathrm{Re}\{(Y_i-hX_i)^*S_i\})$, yields:

$$p_{\boldsymbol{Y}|\boldsymbol{X}}(Y|X) = \frac{\exp\left(-k_g^2-\frac{1}{\sigma_Z^2}\sum_{i=1}^T|Y_i-hX_i|^2\right)}{\left(\pi^2\sigma_V^2\sigma_g^2\sigma_Z^2\right)^T}\sum_{\ell=0}^{\infty}\frac{\left(k_g^2\right)^\ell}{(\ell!)^2}\int_0^\infty\frac{\exp(-t)}{t^{T-\ell}}I(t)dt, \quad \text{(B.22)}$$

where

$$I(t) = \prod_{i=1}^T\int_{\mathcal{S}_i}\exp\left(-\left(\frac{1}{\sigma_V^2\sigma_g^2\,t}+\frac{1}{\sigma_Z^2}\right)|S_i|^2\right)\exp\left(\frac{2}{\sigma_Z^2}\,\mathrm{Re}\{(Y_i-hX_i)^*S_i\}\right)dS_i, \quad \text{(B.23)}$$

where $\mathcal{S}_i=(-\infty,\infty)^2$.

The T integrations in (B.23) can be simplified by invoking polar coordinates. Towards that end, let $S_i=r_ie^{\jmath\theta_i}$ and $dS_i=r_idr_id\theta_i$. Hence, the i-th integration in (B.23) can be expressed as :

$$I_i(t) \;=\; \int_0^{2\pi}\int_0^\infty\exp\left(-\left(\frac{1}{\sigma_V^2\sigma_g^2\,t}+\frac{1}{\sigma_Z^2}\right)r_i^2\right)\exp\left(\frac{2}{\sigma_Z^2}\,\mathrm{Re}\{(Y_i-hX_i)^*r_ie^{\jmath\theta_i}\}\right)r_idr_id\theta_i. \quad \text{(B.24)}$$

Since $\mathrm{Re}\{(Y_i-hX_i)^*r_ie^{\jmath\theta_i}\}=|Y_i-hX_i|r_i\cos(\theta_i-\phi)$, where $\phi=\measuredangle(Y_i-hX_i)$, the integra-

tion in (B.24) can be written as:

$$I_i(t) = \int_0^\infty \exp\left(-\left(\frac{1}{\sigma_V^2\sigma_g^2\ t} + \frac{1}{\sigma_Z^2}\right) r_i^2\right) \int_0^{2\pi} \exp\left(\frac{2r_i}{\sigma_Z^2}|Y_i - hX_i|\cos(\theta_i - \phi)\right) d\theta_i r_i dr_i, \tag{B.25}$$

Using the integral form of $I_0(\cdot)$, the inner integration in (B.25) can be seen to be equal to:

$$2\pi I_0\Big(\frac{2r_i}{\sigma_Z^2}|Y_i - hX_i|\Big) = 2\pi \sum_{\ell=0}^{\infty} \Big(\frac{r_i}{\sigma_Z^2}\Big)^{2\ell} \frac{|Y_i - hX_i|^{2\ell}}{(\ell!)^2}. \tag{B.26}$$

Substituting from (B.26) in (B.25) yields:

$$I_i(t) = \pi \sum_{\ell=0}^{\infty} \frac{1}{(\ell!)^2} \Big(\frac{|Y_i - hX_i|}{\sigma_Z^2}\Big)^{2\ell} \int_0^\infty \exp\left(-\left(\frac{1}{\sigma_V^2\sigma_g^2\ t} + \frac{1}{\sigma_Z^2}\right) r_i^2\right) (r_i^2)^\ell (2r_i) dr_i. \tag{B.27}$$

To further simplify this integration, we introduce the following change of variables:

$$u = \left(\frac{1}{\sigma_V^2\sigma_g^2\ t} + \frac{1}{\sigma_Z^2}\right) r_i^2, \tag{B.28}$$

which yields:

$$I_i(t) = \frac{\pi\sigma_V^2\sigma_g^2\sigma_Z^2 t}{\sigma_Z^2 + \sigma_V^2\sigma_g^2\ t} \sum_{\ell=0}^{\infty} \frac{1}{(\ell!)^2} \left(\frac{|Y_i - hX_i|^2\sigma_V^2\sigma_g^2 t}{\sigma_Z^2(\sigma_Z^2 + \sigma_V^2\sigma_g^2 t)}\right)^\ell \int_0^\infty \exp(-u)\, u^\ell du. \tag{B.29}$$

Noticing that $\int_0^\infty \exp(-u)\, u^\ell du = \ell!$ yields

$$\begin{aligned} I_i(t) &= \frac{\pi\sigma_V^2\sigma_g^2\sigma_Z^2 t}{\sigma_Z^2 + \sigma_V^2\sigma_g^2\ t} \sum_{\ell=0}^{\infty} \frac{1}{\ell!} \left(\frac{|Y_i - hX_i|^2\sigma_V^2\sigma_g^2 t}{\sigma_Z^2(\sigma_Z^2 + \sigma_V^2\sigma_g^2 t)}\right)^\ell \\ &= \frac{\pi\ \sigma_V^2\sigma_g^2\sigma_Z^2 t}{\sigma_Z^2 + \sigma_V^2\sigma_g^2\ t} \exp\left(\frac{|Y_i - hX_i|^2\sigma_V^2\sigma_g^2\ t}{\sigma_Z^2\left(\sigma_Z^2 + \sigma_V^2\sigma_g^2 t\right)}\right). \end{aligned} \tag{B.30}$$

Substituting from (B.30) in (B.23) yields:

$$I(t) = \left(\frac{\pi\ \sigma_V^2\sigma_g^2\sigma_Z^2 t}{\sigma_Z^2 + \sigma_V^2\sigma_g^2\ t}\right)^T \exp\left(\sum_{i=1}^{T}\left(\frac{|Y_i - hX_i|^2}{\sigma_Z^2} - \frac{|Y_i - hX_i|^2}{\sigma_Z^2 + \sigma_V^2\sigma_g^2 t}\right)\right). \tag{B.31}$$

Substituting from (B.31) in (B.22) and simplifying yields (4.15).

B.4 Proof of Theorem 5.1

From (4.8) we have that, given $\boldsymbol{X} = X$ and $\boldsymbol{\theta_h} = \theta_h$, $\boldsymbol{U}$ is a complex Gaussian vector with mean $\mu_{\boldsymbol{U}|\boldsymbol{X},\boldsymbol{\theta}_h} = k_h\sigma_h X e^{\jmath\theta_h}$ and covariance $\Sigma = \sigma_h X X^\dagger + \sigma_Z^2 I_T$. Hence,

$$p_{\boldsymbol{U}|\boldsymbol{X},\boldsymbol{\theta_h}}(U|X,\theta_h) = \frac{1}{\pi^T|\Sigma|}\exp\big\{(-(U - k_h\sigma_h X e^{\jmath\theta_h})^\dagger\Sigma^{-1}(U - k_h\sigma_h X e^{\jmath\theta_h}))\big\}. \tag{B.32}$$

Using (4.11), (4.13), (B.18) and (B.32), and using the same procedure used to prove Theorem 4.3, we obtain the following analog of (B.21),

$$\begin{aligned} p_{\boldsymbol{Y}|\boldsymbol{X},\boldsymbol{\theta_h}}(Y|X,\theta_h) &= \frac{\exp\left(-k_g^2\right)}{\left(\pi^2\sigma_V^2\sigma_g^2\right)^T|\Sigma|}\sum_{\ell=0}^{\infty}\frac{\left(k_g^2\right)^\ell}{(\ell!)^2} \\ &\times \int_0^\infty\!\!\int_{\mathcal{S}}\exp\big\{(-(Y - S - k_h\sigma_h X e^{\jmath\theta_h})^\dagger\Sigma^{-1}(Y - S - k_h\sigma_h X e^{\jmath\theta_h}))\big\}\exp\left(-t - \frac{\|S\|^2}{\sigma_g^2\sigma_V^2 t}\right)\frac{dSdt}{t^{T-\ell}}, \end{aligned} \tag{B.33}$$

where $\mathcal{S} = (-\infty,\infty)^{2T}$ is the region of integration of the complex vector S. Using the eigenvalue decomposition of Σ^{-1}, we obtain the analog of (B.22) as

$$p_{\boldsymbol{Y}|\boldsymbol{X},\boldsymbol{\theta_h}}(Y|X,\theta_h) = \frac{\exp\left(-k_g^2\right)}{\left(\pi^2\sigma_V^2\sigma_g^2\right)^T|\Sigma|}\sum_{\ell=0}^{\infty}\frac{\left(k_g^2\right)^\ell}{(\ell!)^2}\int_0^\infty \exp\left(-t\right)I(t)\frac{dt}{t^{T-\ell}}, \tag{B.34}$$

where

$$I(t) = \prod_{i=1}^{T}\int_{\hat{S}_i}\exp\Big\{\Big(-\lambda_i|\hat{Y}_i - k_h\sigma_h\hat{X}_i e^{\jmath\theta_h} - \hat{S}_i|^2\Big)\Big\}\exp\left(-\frac{|\hat{S}_i|^2}{\sigma_g^2\sigma_V^2 t}\right)d\hat{S}_i, \tag{B.35}$$

λ_i is the i-th eigenvalue of Σ^{-1}, and $\hat{Y}_i$, $\hat{S}_i$, and $\hat{X}_i$ are the i-th components of the vectors $\hat{Y} = Q^\dagger Y$, $\hat{S} = Q^\dagger S$ and $\hat{X} = Q^\dagger X$, respectively. We note that in writing (B.35) we used the fact that $d\hat{S} = dS$ because $|\det Q^\dagger| = 1$ [98].

Since

$|\hat{Y}_i - k_h\sigma_h\hat{X}_i e^{\jmath\theta_h} - \hat{S}_i|^2 = |\hat{Y}_i - k_h\sigma_h\hat{X}_i e^{\jmath\theta_h}|^2 + |\hat{S}_i|^2 - 2|\hat{Y}_i - k_h\sigma_h\hat{X}_i e^{j\theta_h}||\hat{S}_i|\cos\big(\theta_{\hat{S}_i} - \phi\big)$, where $\phi = \measuredangle(\hat{Y}_i - k_h\sigma_h\hat{X}_i e^{j\theta_h})$, the i-th integration in (B.35) can be written as:

$$I_i(t) = \exp\Big(-\lambda_i|\hat{Y}_i - k_h\sigma_h\hat{X}_i e^{\jmath\theta_h}|^2\Big)\int_{\hat{S}_i}\exp\Big(2\lambda_i|\hat{Y}_i - k_h\sigma_h\hat{X}_i e^{\jmath\theta_h}||\hat{S}_i|\cos(\theta_{\hat{s}_i} - \phi)\Big)\times \exp\Big(-(\lambda_i + \frac{1}{\sigma_g^2\sigma_V^2 t})|\hat{S}_i|^2\Big)d\hat{S}_i. \tag{B.36}$$

Invoking polar coordinates whereby $\hat{S}_i = r_i e^{\jmath\theta_{\hat{S}_i}}$, (B.36) can be expressed as:

$$I_i(t) = \exp\left(-\lambda_i|\hat{Y}_i - k_h\sigma_h\hat{X}_i e^{\jmath\theta_h}|^2\right)\int_0^\infty\int_0^{2\pi}\exp\left(2\lambda_i|\hat{Y}_i - k_h\sigma_h\hat{X}_i e^{\jmath\theta_h}|r_i\cos\big(\theta_{\hat{S}_i} - \phi\big)\right)d\theta_{\hat{S}_i} \times \exp\left(-\left(\lambda_i + \frac{1}{\sigma_g^2\sigma_V^2 t}\right)r_i^2\right)r_i d_{r_i}, \tag{B.37}$$

The inner integration in (B.37) equals to $2\pi I_0\left(2\lambda_i|\hat{Y}_i - k_h\sigma_h\hat{X}_i e^{\jmath\theta_h}|r_i\right)$. Hence, invoking

the analog of (B.26) in (B.37) yields:

$$I_i(t) = \pi \exp\left(-\lambda_i |\hat{Y}_i - k_h \sigma_h \hat{X}_i e^{\jmath\theta_h}|^2\right) \sum_{k=0}^{\infty} \frac{(\lambda_i^2 |\hat{Y}_i - k_h \sigma_h \hat{X}_i e^{\jmath\theta_h}|^2)^k}{(k!)^2} \times \int_0^{\infty} \exp\left(-\left(\lambda_i + \frac{1}{\sigma_g^2 \sigma_V^2 t}\right) r_i^2\right) (r_i^2)^k 2 r_i dr_i. \quad \text{(B.38)}$$

Defining the variable $u = \left(\lambda_i + \frac{1}{\sigma_V^2 \sigma_g^2 t}\right) r_i^2$, and noting that $\int_0^{\infty} \exp(-u)\, u^k du = k!$ yields:

$$\begin{aligned} I_i(t) &= \frac{\pi \sigma_g^2 \sigma_V^2 t}{1 + \lambda_i \sigma_g^2 \sigma_V^2 t} \exp\left(-\lambda_i |\hat{Y}_i - k_h \sigma_h \hat{X}_i e^{\jmath\theta_h}|^2\right) \sum_{k=0}^{\infty} \left(\frac{\lambda_i^2\ |\hat{Y}_i - k_h \sigma_h \hat{X}_i e^{\jmath\theta_h}|^2\ \sigma_g^2 \sigma_V^2 t}{1 + \lambda_i \sigma_g^2 \sigma_V^2 t}\right)^k \frac{1}{k!}, \\ &= \frac{\pi \sigma_g^2 \sigma_V^2 t}{1 + \lambda_i \sigma_g^2 \sigma_V^2 t} \exp\left(-\lambda_i |\hat{Y}_i - k_h \sigma_h \hat{X}_i e^{\jmath\theta_h}|^2\right) \exp\left(\frac{\lambda_i^2\ |\hat{Y}_i - k_h \sigma_h \hat{X}_i e^{\jmath\theta_h}|^2\ \sigma_g^2 \sigma_V^2 t}{1 + \lambda_i \sigma_g^2 \sigma_V^2 t}\right), \\ &= \frac{\pi \sigma_g^2 \sigma_V^2 t}{1 + \lambda_i \sigma_g^2 \sigma_V^2 t} \exp\left(\frac{-\lambda_i\ |\hat{Y}_i - k_h \sigma_h \hat{X}_i e^{\jmath\theta_h}|^2}{1 + \lambda_i \sigma_g^2 \sigma_V^2 t}\right). \end{aligned} \quad \text{(B.39)}$$

Using (B.39) in (B.35) yields:

$$\begin{aligned} I(t) &= \prod_{i=1}^{T} I_i(t), \\ &= \frac{\left(\pi \sigma_g^2 \sigma_V^2 t\right)^T}{\prod_{i=1}^{T} \left(1 + \lambda_i \sigma_g^2 \sigma_V^2 t\right)} \exp\left(-\sum_{i=1}^{T} \frac{\lambda_i |\hat{Y}_i - k_h \sigma_h \hat{X}_i e^{\jmath\theta_h}|^2}{1 + \lambda_i \sigma_g^2 \sigma_V^2 t}\right). \end{aligned} \quad \text{(B.40)}$$

Substituting for $I(t)$ in (B.34) yields:

$$p_{\boldsymbol{Y}|\boldsymbol{X},\boldsymbol{\theta_h}}(Y|X,\theta_h) = \frac{\exp\left(-k_g^2\right)}{\pi^T|\Sigma|}\sum_{\ell=0}^{\infty}\frac{\left(k_g^2\right)^\ell}{(\ell!)^2}\times \int_0^\infty \exp\left(-t-\sum_{i=1}^{T}\frac{\lambda_i|\hat{Y}_i - k_h\sigma_h\hat{X}_i e^{\jmath\theta_h}|^2}{1+\lambda_i\sigma_g^2\sigma_V^2 t}\right)\frac{t^\ell}{\prod_{i=1}^{T}(1+\lambda_i\sigma_g^2\sigma_V^2 t)}dt. \quad \text{(B.41)}$$

Noting that

$$\sum_{i=1}^{T}\frac{\lambda_i|\hat{Y}_i - k_h\sigma_h e^{\jmath\theta_h}\hat{X}_i|^2}{1+\lambda_i\sigma_g^2\sigma_V^2 t} = \hat{Y}^\dagger D(t)\hat{Y} + k_h^2\sigma_h^2\hat{X}^\dagger D(t)\hat{X} - 2k_h\sigma_h|\hat{Y}^\dagger D(t)\hat{X}|\cos(\theta_h-\alpha), \quad \text{(B.42)}$$

where $\alpha = \measuredangle(\hat{Y}^\dagger D(t)\hat{X})$ and $\phi_i = \measuredangle(\hat{Y}_i) - \measuredangle(\hat{X}_i)$. Using this along with the fact that $p_{\boldsymbol{\theta}_h}(\theta_h) = \frac{1}{2\pi}$, we average (B.41) over $\boldsymbol{\theta}_h$ to obtain

$$p_{\boldsymbol{Y}|\boldsymbol{X}}(Y|X) = \frac{\exp\left(-k_g^2\right)}{\pi^T|\Sigma|}\frac{1}{2\pi}\int_0^{2\pi}\exp\Big(2k_h\sigma_h|\hat{Y}^\dagger D(t)\hat{X}|\cos(\theta_h-\alpha)\Big)d\theta_h\times \int_0^\infty\sum_{\ell=0}^{\infty}\frac{\left(k_g^2 t\right)^\ell}{(\ell!)^2}\frac{1}{\prod_{i=1}^{T}(1+\lambda_i\sigma_g^2\sigma_V^2 t)}\exp\Big(-t-\hat{Y}^\dagger D(t)\hat{Y} - k_h^2\sigma_h^2\hat{X}^\dagger D(t)\hat{X}\Big)dt. \quad \text{(B.43)}$$

The first integration in (B.43) is equal to $2\pi I_0(2k_h\sigma_h|\hat{Y}^\dagger D(t)\hat{X}|)$. Substituting in (B.43) and noticing that $\sum_{\ell=0}^{\infty}\frac{(k_g^2 t)^\ell}{(\ell!)^2} = I_0(2k_g\sqrt{t})$ completes the proof.

B.5 Proof of Lemma 4.1

Given the vector of transmitted symbols, $\boldsymbol{X} = X$, and the phase of the transmitter channel mean, $\boldsymbol{\theta}_h = \theta_h$, it can be seen that the received signal vector, $\boldsymbol{Y}$, is a complex Gaussian random vector with mean vector $\mu_{Y|X,\theta_h} = k_h\sigma_h X e^{\jmath\theta_h}$, and a covariance

matrix $\Sigma_G = \mathrm{E}\{\boldsymbol{Y}\boldsymbol{Y}^\dagger|\boldsymbol{X},\boldsymbol{\theta}_h\}$. Expressing $\mathrm{Re}\{X^\dagger\Sigma_G^{-1}Ye^{-\jmath\theta_h}\}$ as $|X^\dagger\Sigma_G^{-1}Y|\cos(\theta_h-\alpha)$, where $\alpha = \measuredangle(X^\dagger\Sigma_G^{-1}Y)$, the *pdf* $p_{\boldsymbol{Y}|\boldsymbol{X},\boldsymbol{\theta}_h}(Y|X,\theta_h)$ can be expressed as

$$p_{\boldsymbol{Y}|\boldsymbol{X},\boldsymbol{\theta}_h}(Y|X,\theta_h) = \frac{1}{\pi^T|\Sigma_G|}\exp\big\{(-Y^\dagger\Sigma_G^{-1}Y)\big\}\times \\ \exp\big\{(-k_h^2\sigma_h^2X^\dagger\Sigma_G^{-1}X + 2k_h\sigma_h|X^\dagger\Sigma_G^{-1}Y|\cos(\theta_h-\alpha))\big\}. \quad \text{(B.44)}$$

Multiplying (B.44) by $p_{\boldsymbol{\theta}_h}(\theta_h) = \dfrac{1}{2\pi}$, and integrating over the interval $[0, 2\pi)$ yields the pdf in (4.19).

B.6 Proof of corollary 4.5

We will show that the likelihood functions in (4.18) and (4.19) are maximized by the transmitted vector X that maximizes $|Y^\dagger X|$. First, we notice that for any given $\boldsymbol{X} = X$, the covariance matrices $\Sigma(X)$ and $\Sigma_G(X)$ are given by:

$$\Sigma(X) = \sigma_h^2XX^\dagger + \sigma_Z^2I_T, \quad \text{(B.45)}$$

$$\Sigma_G(X) = \sigma_h^2XX^\dagger + (\sigma_g^2\sigma_V^2 + \sigma_Z^2)I_T. \quad \text{(B.46)}$$

The eigenvalues of $\Sigma^{-1}(X)$ are: $\lambda_1 = (\sigma_h^2\|X\|^2 + \sigma_Z^2)^{-1}$ and $\lambda_i = (\sigma_Z^2)^{-1}$, and the eigenvalues of $\Sigma_G^{-1}(X)$ are: $\tilde{\lambda}_1 = (\sigma_h^2\|X\|^2 + \sigma_g^2\sigma_V^2 + \sigma_Z^2)^{-1}$ and $\tilde{\lambda}_i = (\sigma_g^2\sigma_V^2 + \sigma_Z^2)^{-1}$, $i \in \{2,\ldots,T\}$. If the vectors in the constellation $\mathcal{C}$ have identical norms, it can be seen that the eigenvalues of $\Sigma^{-1}(X)$ and $\Sigma_G^{-1}(X)$, i.e., the eigenvalues in the expressions in (4.18) and (4.19), do not depend on X. However, the eigenvectors of $\Sigma^{-1}(X)$ and $\Sigma_G^{-1}(X)$, and hence both $\hat{Y}(X) = Q(X)^\dagger Y$ and $\tilde{Y} = \tilde{Q}(X)^\dagger Y$, depend on X, where $Q(X)$ and $\tilde{Q}(X)$ are the unitary matrices containing the eigenvectors of $\Sigma^{-1}(X)$ and $\Sigma_G^{-1}(X)$, respectively, cf. Theorem 5.1

and Lemma 4.1.

Using the matrix inversion lemma [99] we have

$$\Sigma^{-1}(X) = \frac{I_T}{\sigma_Z^2} - \frac{\sigma_h^2 X X^\dagger}{\sigma_Z^2\left(\sigma_Z^2 + \sigma_h^2 \|X\|^2\right)}, \tag{B.47}$$

and

$$\Sigma_G^{-1}(X) = \frac{I_T}{\sigma_g^2\sigma_V^2 + \sigma_Z^2} - \frac{\sigma_h^2 X X^\dagger}{(\sigma_g^2\sigma_V^2 + \sigma_Z^2)(\sigma_g^2\sigma_V^2 + \sigma_Z^2 + \sigma_h^2\|X\|^2)}. \tag{B.48}$$

For the likelihood function in (4.19), substituting for $\Sigma_G^{-1}(X)$ from (B.48) into this function yields:

$$\hat{p}_{\boldsymbol{Y}|\boldsymbol{X}}(Y|X) \;=\; \frac{1}{\pi^T|\Sigma_G|} I_0\left(2G|Y^\dagger X|\right) \exp\left(\frac{2G\sigma_h^2|Y^\dagger X|^2 - 2k_h\sigma_h\|Y\|^2}{\sigma_g^2\sigma_V^2 + \sigma_Z^2} - k_h\sigma_h G\|X\|^4\right), \tag{B.49}$$

where $G = k_h\sigma_h\left(\sigma_Z^2 + \sigma_g^2\sigma_V^2 + \sigma_h^2\|X\|^2\right)^{-1}$. Since $\|X\|$ is constant, and both of $I_0(\cdot)$ and $\exp(\cdot)$ are monotonically increasing, the vector $\tilde{X} \in \mathcal{C}$ that maximizes $|Y^\dagger X|$ maximizes (4.19).

We now consider the likelihood function in (4.22). Let

$$F(X,t) = \frac{I_0\left(2k_h\sigma_h|\hat{Y}^\dagger D(t)\hat{X}|\right)}{\prod_{i=1}^T\left(1 + \lambda_i\sigma_g^2\sigma_V^2 t\right)} \exp\left(-t - \left(\hat{Y}^\dagger D(t)\hat{Y} + k_h^2\sigma_h^2\hat{X}^\dagger D(t)\hat{X}\right)\right), \tag{B.50}$$

where $D(t)$, $\{\lambda_i\}_{i=1}^T$, $\hat{Y} = Q(X)^\dagger Y$ and $\hat{X} = Q(X)^\dagger X$ are as defined in Theorem 5.1. Since $F(X,t)$ is greater than zero for all t and X, maximizing $F(X,t)$ maximizes the likelihood function in (4.22). We will show that $\tilde{X} \in \mathcal{C}$ that maximizes $|Y^\dagger X|$, maximizes $F(X,t)$ at all $t \geqslant 0$. In particular, denoting $k_h^2\sigma_h^2$ by ζ, $Q^\dagger(\tilde{X})Y$ by $\tilde{Y}$, and $Q^\dagger(\tilde{X})\tilde{X}$ by $\check{X}$, we will

show that if $\tilde{X} = \arg\max |Y^\dagger X|$ then

$$|\tilde{Y}^\dagger D(t)\check{X}| > |\hat{Y}^\dagger D(t)\hat{X}| \tag{B.51}$$

and

$$\tilde{Y}^\dagger D(t)\tilde{Y} + \zeta\check{X}^\dagger D(t)\check{X} < \hat{Y}^\dagger D(t)\hat{Y} + \zeta\hat{X}^\dagger D(t)\hat{X}, \tag{B.52}$$

which implies that $F(\tilde{X}, t) > F(X, t)$, $\forall t > 0$.

To prove (B.51), we write

$$\begin{aligned}
|\tilde{Y}^\dagger D(t)\check{X}| - |\hat{Y}^\dagger D(t)\hat{X}| &= \left|\frac{\lambda_1 \tilde{Y}_1^* \check{X}_1}{1+\lambda_1\sigma_g^2\sigma_V^2 t} + \frac{\lambda_2 \sum_{i=2}^T \tilde{Y}_i^* \check{X}_i}{1+\lambda_2\sigma_g^2\sigma_V^2 t}\right| - \left|\frac{\lambda_1 \hat{Y}_1^* \hat{X}_1}{1+\lambda_1\sigma_g^2\sigma_V^2 t} + \frac{\lambda_2 \sum_{i=2}^T \hat{Y}_i^* \hat{X}_i}{1+\lambda_2\sigma_g^2\sigma_V^2 t}\right| \\
&= \left|B\sum_{i=1}^T \lambda_i \tilde{Y}_i^* \check{X}_i + B\varphi Y^\dagger \tilde{X}\right| - \left|B\sum_{i=1}^T \lambda_i \hat{Y}_i^* \hat{X}_i + B\varphi Y^\dagger X\right| \\
&= B(|Y^\dagger \Sigma^{-1}(\tilde{X})\tilde{X} + \varphi Y^\dagger \tilde{X}| - |Y^\dagger \Sigma^{-1}(X)X + \varphi Y^\dagger X|),
\end{aligned} \tag{B.53}$$

where $B = ((1+\lambda_1\sigma_g^2\sigma_V^2 t)(1+\lambda_2\sigma_g^2\sigma_V^2 t))^{-1}$ and $\varphi = \lambda_1\lambda_2\sigma_g^2\sigma_V^2 t$. In writing (B.53), we used the fact that the eigenvalue of $\Sigma^{-1}(\tilde{X})$ and $\Sigma^{-1}(X)$ do not depend on X because the entries of $\mathcal{C}$ have identical norms.

Substituting for $\Sigma^{-1}(X)$ from (B.47) into (B.53) and recalling that $|Y^\dagger \tilde{X}| > |Y^\dagger X|$ yields:

$$|\tilde{Y}^\dagger D(t)\check{X}| - |\hat{Y}^\dagger D(t)\hat{X}| = B((\sigma_Z^2 + \sigma_h^2\|X\|^2)^{-1} + \varphi)\left(|Y^\dagger \tilde{X}| - |Y^\dagger X|\right) > 0.$$

To prove (B.52), we write:

$$
\begin{aligned}
&\tilde{Y}^\dagger D(t)\tilde{Y} + \zeta\check{X}^\dagger D(t)\check{X} - \hat{Y}^\dagger D(t)\hat{Y} - \zeta\hat{X}^\dagger D(t)\hat{X} \\
&\qquad = \lambda_1 \frac{|\tilde{Y}_1|^2 + \zeta|\check{X}_1|^2 - |\hat{Y}_1|^2 - \zeta|\hat{X}_1|^2}{1+\lambda_1\sigma_g^2\sigma_V^2 t} + \lambda_2 \sum_{i=2}^{T} \frac{|\tilde{Y}_i|^2 + \zeta|\check{X}_i|^2 - |\hat{Y}_i|^2 - \zeta|\hat{X}_i|^2}{1+\lambda_2\sigma_g^2\sigma_V^2 t} \\
&\qquad = B((Y^\dagger\ \Sigma^{-1}(\tilde{X})\ Y + \zeta\ \tilde{X}^\dagger\ \Sigma^{-1}(\tilde{X})\ \tilde{X}) - (Y^\dagger\ \Sigma^{-1}(X)\ Y + \zeta\ X^\dagger\ \Sigma^{-1}(X)\ X)) \\
&\qquad = B(\sigma_Z^2 + \sigma_h^2\|X\|^2)^{-1}\sigma_h^2(|Y^\dagger X|^2 - |Y^\dagger\tilde{X}|^2) \\
&\qquad < 0. \qquad \text{(B.54)}
\end{aligned}
$$

The last equation in (B.54) follows from substituting for $\Sigma^{-1}(X)$ from (B.47) and noticing that $\tilde{X}^\dagger\ \Sigma^{-1}(\tilde{X})\ \tilde{X} = X^\dagger\ \Sigma^{-1}(X)\ X$, which completes the proof of the corollary.

Appendix C

Proofs for chaper 5

C.1 Proof of Theorem 5.1

Equation (5.2) can be written as:

$$\begin{bmatrix} Y_1 \\ Y_2 \\ \vdots \\ Y_{2T-1} \\ Y_{2T} \end{bmatrix} = \begin{bmatrix} H & 0 & \dots & 0 & 0 \\ 0 & H & \dots & 0 & 0 \\ & & \ddots & & \\ 0 & 0 & \dots & H & 0 \\ 0 & 0 & \dots & 0 & H \end{bmatrix} \begin{bmatrix} X_1 \\ X_2 \\ \vdots \\ X_{T-1} \\ X_T \end{bmatrix} + \begin{bmatrix} G & 0 & \dots & 0 & 0 \\ 0 & G & \dots & 0 & 0 \\ & & \ddots & & \\ 0 & 0 & \dots & G & 0 \\ 0 & 0 & \dots & 0 & G \end{bmatrix} \begin{bmatrix} V_1 \\ V_2 \\ \vdots \\ V_{T-1} \\ V_T \end{bmatrix} + \begin{bmatrix} Z_1 \\ Z_2 \\ \vdots \\ Z_{2T-1} \\ Z_{2T} \end{bmatrix}. \tag{C.1}$$

From this equation, it can be seen that, conditioned on $\boldsymbol{X}$, $\boldsymbol{V}$, $\boldsymbol{G} = \begin{bmatrix}\boldsymbol{g}_1^* & \boldsymbol{g}_2^*\end{bmatrix}^\dagger$, k_h and $\boldsymbol{\theta}_{\mu_h} = \begin{bmatrix}\boldsymbol{\theta}_{\mu_{h_1}} & \boldsymbol{\theta}_{\mu_{h_2}}\end{bmatrix}^\dagger$, the received signal vector, $\boldsymbol{Y}$, is Gaussian distributed with the following pdf:

$$f_{\boldsymbol{Y}|\boldsymbol{X},\boldsymbol{G},\boldsymbol{V},\boldsymbol{\theta}_{\mu_h}}(Y|X,G,V,\theta_{\mu_h}) = \\ f_{\boldsymbol{Y}_o|\boldsymbol{X},\boldsymbol{V},\boldsymbol{g_1},\boldsymbol{\theta}_{\mu_{h_1}}}(Y_o|X,V,g_1,\theta_{\mu_{h_1}}) \times f_{\boldsymbol{Y}_e|\boldsymbol{X},\boldsymbol{V},\boldsymbol{g_2},\boldsymbol{\theta}_{\mu_{h_2}}}(Y_e|X,V,g_2,\theta_{\mu_{h_2}}), \quad \text{(C.2)}$$

where $Y_o = [Y_1^*, \ldots, Y_{2i-1}^*, \ldots, Y_{2T-1}^*]^\dagger$, $Y_e = [Y_2^*, \ldots, Y_{2i}^*, \ldots, Y_{2T}^*]^\dagger$,

$$f_{\boldsymbol{Y}_o|\boldsymbol{X},\boldsymbol{V},\mathbf{g}_1,\boldsymbol{\theta}_{\mu_{h_1}}}(Y_o|X,V,g_1,\theta_{\mu_{h_1}}) = \frac{1}{\pi^T|\Sigma|}\exp\left(-\left[\tilde{Y}_o - g_1V\right]^\dagger \Sigma^{-1}\left[\tilde{Y}_o - g_1V\right]\right), \quad \text{(C.3)}$$

and

$$f_{\boldsymbol{Y}_e|\boldsymbol{X},\boldsymbol{V},\mathbf{g}_2,\boldsymbol{\theta}_{\mu_{h_2}}}(Y_e|X,V,g_2,\theta_{\mu_{h_2}}) = \frac{1}{\pi^T|\Sigma|}exp\left(-\left[\tilde{Y}_e - g_2V\right]^\dagger \Sigma^{-1}\left[\tilde{Y}_e - g_2V\right]\right), \quad \text{(C.4)}$$

where $\tilde{Y}_o = Y_o - k_h\sigma_h e^{j\boldsymbol{\theta}_{\mu_{h_1}}}X$, $\tilde{Y}_e = Y_e - k_h\sigma_h e^{j\boldsymbol{\theta}_{\mu_{h_2}}}X$, and $\Sigma = \sigma_h^2 XX^\dagger + \sigma_Z^2 I_T$. Using the eigenvalue decomposition, we write $\Sigma^{-1} = Q\Lambda Q^\dagger$. Hence,

$$\begin{aligned} f_{\boldsymbol{Y}_o|\boldsymbol{X},\boldsymbol{V},\mathbf{g}_1,\boldsymbol{\theta}_{\mu_{h_1}}}(Y_o|X,V,g_1,\theta_{\mu_{h_1}}) &= \frac{1}{\pi^T|\Sigma|}\exp\left(-\left[\check{Y}_o - g_1\hat{V}\right]^\dagger \Lambda\left[\check{Y}_o - g_1\hat{V}\right]\right), \\ &= \frac{1}{\pi^T|\Sigma|}\exp\left(-\sum_{i=1}^{T}\lambda_i|\check{y}_{2i-1} - g_1\hat{v}_i|^2\right), \end{aligned} \quad \text{(C.5)}$$

and

$$f_{\boldsymbol{Y}_e|\boldsymbol{X},\boldsymbol{V},\mathbf{g}_2,\boldsymbol{\theta}_{\mu_{h_2}}}(Y_e|X,V,g_2,\theta_{\mu_{h_2}}) = \frac{1}{\pi^T|\Sigma|}\exp\left(-\left[\check{Y}_e - g_2\hat{V}\right]^\dagger \Lambda \left[\check{Y}_e - g_2\hat{V}\right]\right),$$
$$= \frac{1}{\pi^T|\Sigma|}\exp\left(-\sum_{i=1}^{T}\lambda_i|\check{y}_{2i} - g_2\hat{v}_i|^2\right), \tag{C.6}$$

where $\hat{V} = Q^\dagger V$, $\check{Y}_o = Q^\dagger\tilde{Y}_o$ and $\check{Y}_e = Q^\dagger\tilde{Y}_e$. Using (C.5) and (C.6) in (C.2) yields:

$$f_{\boldsymbol{Y}|\boldsymbol{X},\boldsymbol{G},\boldsymbol{V},\boldsymbol{\theta}_{\mu_h}}(Y|X,G,V,\theta_{\mu_h}) = \frac{1}{\pi^{2T}|\Sigma|^2}\exp\left(-\sum_{i=1}^{T}\lambda_i\left(|\check{y}_{2i-1}-g_1\hat{v}_i|^2+|\check{y}_{2i}-g_2\hat{v}_i|^2\right)\right),$$
$$= \frac{1}{\pi^{2T}|\Sigma|^2}\exp\left(-\sum_{i=1}^{T}\lambda_i\left(|\check{y}_{2i-1}|^2 + |\check{y}_{2i}|^2 + \|g\|^2|\hat{v}_i|^2 - 2\,\mathrm{Re}\{(g_1^*\check{y}_{2i-1} + g_2^*\check{y}_{2i})\,\hat{v}_i^*\}\right)\right). \tag{C.7}$$

where $\|g\|^2 = |g_1|^2 + |g_2|^2$. Note that:

$$\mathrm{Re}\{(g_1^*\check{y}_{2i-1} + g_2^*\check{y}_{2i})\,\hat{v}_i^*\} = |g_1^*\check{y}_{2i-1} + g_2^*\check{y}_{2i}||\hat{v}_i|\cos\left(\theta_{\hat{v}_i^*} - \alpha_i\right),$$

where $\alpha_i = \angle\left(g_1^*\check{y}_{2i-1} + g_2^*\check{y}_{2i}\right)$, and $\theta_{\hat{v}_i^*} = \angle\hat{v}_i^* = -\angle\hat{v}_i$.

To obtain an expression for $f_{\boldsymbol{Y}|\boldsymbol{X},\boldsymbol{G},\boldsymbol{\theta}_{\mu_h}}(Y|X,G,\theta_{\mu_h})$, we average both sides of (C.7) over the random vector $\boldsymbol{V}$. Doing so yields:

$$f_{\boldsymbol{Y}|\boldsymbol{X},\boldsymbol{G},\boldsymbol{\theta}_{\mu_h}}(Y|X,G,\theta_{\mu_h}) = \int_{\boldsymbol{V}} f_{\boldsymbol{Y}|\boldsymbol{X},\boldsymbol{G},\boldsymbol{V},\boldsymbol{\theta}_{\mu_h}}(Y|X,G,V,\theta_{\mu_h}) f_{\boldsymbol{V}}(V)dV, \tag{C.8}$$

where $f_{\boldsymbol{V}}(V)$ is given by:

$$f_{\boldsymbol{V}}(V) = \frac{1}{\pi^T\sigma_v^{2T}}\exp\left(-\frac{\|V\|^2}{\sigma_v^2}\right). \tag{C.9}$$

Using (C.7) and (C.9) in (C.8) and taking into account that $\|V\| = \|\hat{V}\|$ and that $\cos\left(\theta_{\hat{v}_i^*} - \alpha_i\right) = \cos\left(\theta_{\hat{v}_i} + \alpha_i\right)$ yields:

$$f_{\boldsymbol{Y}|\boldsymbol{X},\boldsymbol{G},\boldsymbol{\theta}_{\mu_h}}(Y|X,G,\theta_{\mu_h}) = \frac{1}{\pi^{3T}\sigma_v^{2T}|\Sigma|^2}\exp\left(-\sum_{i=1}^{T}\lambda_i\left(|\check{y}_{2i-1}|^2 + |\check{y}_{2i}|^2\right)\right)\times$$
$$\int_{\hat{\boldsymbol{V}}}\exp\left(-2\sum_{i=1}^{T}\lambda_i|g_1^*\check{y}_{2i-1}+g_2^*\check{y}_{2i}||\hat{v}_i|\cos\left(\theta_{\hat{v}_i}+\alpha_i\right)\right)\exp\left(-\sum_{i=1}^{T}\left(\lambda_i\|g\|^2+\frac{1}{\sigma_v^2}\right)|\hat{v}_i|^2\right)d\hat{V}. \tag{C.10}$$

Using polar coordinates with $|\hat{v}_i| = r_i$, $\theta_i = \theta_{\hat{v}_i}$ and $d\hat{V} = \prod_{i=1}^{T} r_i dr_i d\theta_i$ yields:

$$f_{\boldsymbol{Y}|\boldsymbol{X},\boldsymbol{G},\boldsymbol{\theta}_{\mu_h}}(Y|X,G,\theta_{\mu_h}) = \frac{1}{\pi^{3T}\sigma_v^{2T}|\Sigma|^2}\exp\left(-\sum_{i=1}^{T}\lambda_i\left(|\check{y}_{2i-1}|^2 + |\check{y}_{2i}|^2\right)\right)\times$$
$$\prod_{i=1}^{T}\int_0^\infty r_i\exp\left(-\left(\lambda_i\|g\|^2+\frac{1}{\sigma_v^2}\right)r_i^2\right)\int_0^{2\pi}\exp\left(-2\lambda_i|g_1^*\check{y}_{2i-1}+g_2^*\check{y}_{2i}|r_i\cos\left(\theta_i+\alpha_i\right)\right)d\theta_i dr_i. \tag{C.11}$$

We note that the zeroth-order modified Bessel function of the first kind is given by

$$\begin{aligned} I_0(z) &= \frac{1}{2\pi}\int_0^{2\pi}\exp\left(-z\cos\left(\theta+\alpha\right)\right)d\theta, \\ &= \frac{1}{2\pi}\sum_{k=0}^{\infty}\frac{z^k}{(k!)^2}. \end{aligned}$$

Hence, the inner integration in (C.11) can be expressed as:

$$2\pi I_0\left(2\lambda_i|g_1^*\check{y}_{2i-1}+g_2^*\check{y}_{2i}|r_i\right) = 2\pi\sum_{\ell=0}^{\infty}\frac{\left(\lambda_i^2|g_1^*\check{y}_{2i-1}+g_2^*\check{y}_{2i}|^2r_i^2\right)^\ell}{(\ell!)^2}. \tag{C.12}$$

Using (C.12) in (C.11) yields:

$$f_{\boldsymbol{Y}|\boldsymbol{X},\boldsymbol{G},\boldsymbol{\theta}_{\mu_h}}(Y|X,G,\theta_{\mu_h}) = \frac{1}{\pi^{2T}\sigma_v^{2T}|\Sigma|^2}\exp\left(-\sum_{i=1}^{T}\lambda_i\left(|\check{y}_{2i-1}|^2+|\check{y}_{2i}|^2\right)\right)$$
$$\times\prod_{i=1}^{T}\sum_{\ell=0}^{\infty}\frac{\left(\lambda_i^2|g_1^*\check{y}_{2i-1}+g_2^*\check{y}_{2i}|^2\right)^{\ell}}{(\ell!)^2}\int_0^{\infty}r_i^{2\ell}\exp\left(-\left(\lambda_i\|g\|^2+\frac{1}{\sigma_v^2}\right)r_i^2\right)2r_idr_i \tag{C.13}$$
$$=\frac{1}{\pi^{2T}|\Sigma|^2}\exp\left(-\sum_{i=1}^{T}\lambda_i\left(|\check{y}_{2i-1}|^2+|\check{y}_{2i}|^2\right)\right)\prod_{i=1}^{T}\left(\frac{1}{\lambda_i\sigma_v^2\|g\|^2+1}\right)$$
$$\times\sum_{\ell=0}^{\infty}\left(\frac{\lambda_i^2\sigma_v^2|g_1^*\check{y}_{2i-1}+g_2^*\check{y}_{2i}|^2}{\lambda_i\sigma_v^2\|g\|^2+1}\right)^{\ell}\frac{1}{(\ell!)} \tag{C.14}$$
$$=\frac{1}{\prod_{i=1}^{T}(\lambda_i\sigma_v^2\|g\|^2+1)}\exp\left(-\sum_{i=1}^{T}\lambda_i\left(|\check{y}_{2i-1}|^2+|\check{y}_{2i}|^2\right)\right)\exp\left(\sum_{i=1}^{T}\frac{\lambda_i^2\sigma_v^2|g_1^*\check{y}_{2i-1}+g_2^*\check{y}_{2i}|^2}{\lambda_i\sigma_v^2\|g\|^2+1}\right), \tag{C.15}$$

where, to write (C.14), we have used the fact that the integration in (C.13) is equal to $(\ell!)\left(\frac{\sigma_v^2}{\lambda_i\sigma_v^2\|g\|^2+1}\right)^{\ell+1}$, and to write (C.15), we have replaced the summation in (C.14) with the exponential function.

Let S_1 be the summation in the argument of the last exponential in (C.15). This summation is given by

$$S_1=\sum_{i=1}^{T}\frac{\lambda_i^2\sigma_v^2}{\lambda_i\sigma_v^2\|g\|^2+1}\Big(|\check{y}_{2i-1}|^2|g_1|^2+|\check{y}_{2i}|^2|g_2|^2+2|\check{y}_{2i-1}||\check{y}_{2i}||g_1||g_2|\cos\left(\theta_{g_1}-\theta_{g_2}-\theta_i\right)\Big), \tag{C.16}$$

where $\theta_{g_\ell}=\angle g_\ell$, $\ell\in\{1,2\}$, and $\theta_i=\angle\check{y}_{2i-1}-\angle\check{y}_{2i}$. Define S_2 to be the following (C.16), i.e.,

$$S_2=\sum_{i=1}^{T}\frac{\lambda_i^2\sigma_v^2|\check{y}_{2i-1}||\check{y}_{2i}|\cos\left(\theta_{g_1}-\theta_{g_2}-\theta_i\right)}{\lambda_i\sigma_v^2\|g\|^2+1}. \tag{C.17}$$

It can be shown that:

$$
\begin{aligned}
S_2 &= \Big(\sum_{i=1}^{T} \frac{\lambda_i^2\sigma_v^2|\check{y}_{2i-1}||\check{y}_{2i}|\cos(\theta_i)}{\lambda_i\sigma_v^2\|g\|^2+1}\Big)\cos(\theta_{g_1}-\theta_{g_2}) + \Big(\sum_{i=1}^{T} \frac{\lambda_i^2\sigma_v^2|\check{y}_{2i-1}||\check{y}_{2i}|\sin(\theta_i)}{\lambda_i\sigma_v^2\|g\|^2+1}\Big)\sin(\theta_{g_1}-\theta_{g_2}),\\
&= \bar{C}_{\check{Y}}(\|g\|^2)\left(\cos(\beta)\cos(\theta_{g_1}-\theta_{g_2}) + \sin(\beta)\sin(\theta_{g_1}-\theta_{g_2})\right),\\
&= \bar{C}_{\check{Y}}(\|g\|^2)\cos(\theta_{g_1}-\theta_{g_2}-\beta),
\end{aligned}
\tag{C.18}
$$

where $\bar{C}_{\check{Y}}(\|g\|^2) = \sqrt{C_1^2+C_2^2}$, $\beta = \arctan\left(\frac{C_2}{C_1}\right)$, and $C_1 = \sum_{i=1}^{T} \frac{\lambda_i^2\sigma_v^2|\check{y}_{2i-1}||\check{y}_{2i}|\cos(\theta_i)}{\lambda_i\sigma_v^2\|g\|^2+1}$, and $C_2 = \sum_{i=1}^{T} \frac{\lambda_i^2\sigma_v^2|\check{y}_{2i-1}||\check{y}_{2i}|\sin(\theta_i)}{\lambda_i\sigma_v^2\|g\|^2+1}$. Using $\tilde{\Lambda}$ to denote the diagonal matrix whose ℓ-th element is given by $\tilde{\Lambda}_\ell = \frac{\lambda_\ell^2\sigma_v^2}{\lambda_\ell\sigma_v^2\|g\|^2+1}$, it can be verified that $C_1 = \mathrm{Re}\{\check{Y}_o^\dagger\ \tilde{\Lambda}\ \check{Y}_e\}$ and $C_2 = \mathrm{Im}\{\check{Y}_o^\dagger\ \tilde{\Lambda}\ \check{Y}_e\}$. Hence,

$$
\begin{aligned}
\bar{C}_{\check{Y}}^2(\|g\|^2) &= \sigma_v^4 \sum_{\substack{m=1\\n=1}}^{T} \frac{|\check{y}_{2m-1}||\check{y}_{2n-1}||\check{y}_{2m}||\check{y}_{2n}|\cos(\theta_m-\theta_n)}{\lambda_m^{-2}\lambda_n^{-2}(\lambda_m\sigma_v^2\|g\|^2+1)(\lambda_n\sigma_v^2\|g\|^2+1)},\\
&= |\check{Y}_o^\dagger\ \tilde{\Lambda}\ \check{Y}_e|^2.
\end{aligned}
\tag{C.19}
$$

Using (C.18) and (C.19) in (C.16) yields:

$$
S_1 = \Big(\sum_{i=1}^{T} \frac{\lambda_i^2\sigma_v^2\left(\ |\check{y}_{2i-1}|^2|g_1|^2 + |\check{y}_{2i}|^2|g_2|^2\ \right)}{\lambda_i\sigma_v^2\|g\|^2+1} + 2|g_1||g_2||\check{Y}_o^\dagger\ \ \tilde{\Lambda}\ \ \check{Y}_e|\cos(\theta_{g_1}-\theta_{g_2}-\beta)\Big).
\tag{C.20}
$$

Substituting from (C.20) in (C.15) yields

$$f_{\boldsymbol{Y}|\boldsymbol{X},\boldsymbol{G},\boldsymbol{\theta}_{\mu_h}}(Y|X,G,\theta_{\mu_h}) = \frac{1}{\pi^{2T}|\Sigma|^2\prod_{i=1}^{T}(\lambda_i\sigma_v^2\|g\|^2+1)}\exp\left(-\sum_{i=1}^{T}\lambda_i\left(|\check{y}_{2i-1}|^2+|\check{y}_{2i}|^2\right)\right)$$
$$\times\exp\left(\sum_{i=1}^{T}\frac{\lambda_i^2\sigma_v^2\left(|\check{y}_{2i-1}|^2|g_1|^2+|\check{y}_{2i}|^2|g_2|^2\right)}{\lambda_i\sigma_v^2\|g\|^2+1}+2|g_1||g_2||\check{Y}_o^{\dagger}\ \tilde{\Lambda}\ \check{Y}_e|\cos\left(\theta_{g_1}-\theta_{g_2}-\beta\right)\right). \tag{C.21}$$

To obtain an expression for $f_{\boldsymbol{Y}|\boldsymbol{X},\boldsymbol{\theta}_{\mu_h}}(Y|X,\theta_{\mu_h})$, we average $f_{\boldsymbol{Y}|\boldsymbol{X},\boldsymbol{G},\boldsymbol{\theta}_{\mu_h}}(Y|X,G,\theta_{\mu_h})$ over the distributions of $\boldsymbol{g}_1$ and $\boldsymbol{g}_2$. In particular, we write

$$f_{\boldsymbol{Y}|\boldsymbol{X},\boldsymbol{\theta}_{\mu_h}}(Y|X,\theta_{\mu_h}) = \int_{g_1}\int_{g_2} f_{\boldsymbol{Y}|\boldsymbol{X},\boldsymbol{G},\boldsymbol{\theta}_{\mu_h}}(Y|X,G,\theta_{\mu_h})f_{\boldsymbol{g}_1}(g_1)f_{\boldsymbol{g}_2}(g_2)dg_1dg_2, \tag{C.22}$$

where we have used the fact that $\boldsymbol{g}_1$ and $\boldsymbol{g}_2$ are independent and identically distributed.

We will derive $f_{\boldsymbol{g}_1}(g_1)$ and the derivation of $f_{\boldsymbol{g}_2}(g_2)$ follows *mutatis mutandis*.

$$\begin{aligned}
f_{\boldsymbol{g}_1}(g_1) &= \frac{1}{2\pi}\int_0^{2\pi} f_{\boldsymbol{g}_1|\bar{\theta}_{\mu_{g_1}}}(g_1|\theta_{\mu_{g_1}})d\theta_{\mu_{g_1}},\\
&= \frac{1}{2\pi^2\sigma_g^2}\int_0^{2\pi}\exp\left(\frac{-|g_1-k_g\sigma_g e^{j\theta_{\mu_{g_1}}}|^2}{\sigma_g^2}\right)d\theta_{\mu_{g_1}},\\
&= \frac{\exp\left(-k_g^2-\frac{|g_1|^2}{\sigma_g^2}\right)}{2\pi^2\sigma_g^2}\int_0^{2\pi}\exp\left(\frac{2k_g|g_1|\cos\left(\theta_{\mu_{g_1}}-\theta_{g_1}\right)}{\sigma_g}\right)d\theta_{\mu_{g_1}}\\
&= \frac{1}{2\pi^2\sigma_g^2}\exp\left(-k_g^2-\frac{|g_1|^2}{\sigma_g^2}\right)I_0\left(\frac{2k_g|g_1|}{\sigma_g}\right).
\end{aligned} \tag{C.23}$$

Analogously, we have

$$f_{\boldsymbol{g}_2}(g_2) = \frac{1}{2\pi^2\sigma_g^2}\exp\left(-k_g^2 - \frac{|g_2|^2}{\sigma_g^2}\right) I_0\left(\frac{2k_g|g_2|}{\sigma_g}\right). \tag{C.24}$$

Using (C.21), (C.23) and (C.24) in (C.22) yields:

$$f_{\boldsymbol{Y}|\boldsymbol{X},\boldsymbol{\theta}_{\mu_h}}(Y|X,\theta_{\mu_h}) =$$
$$\frac{\exp\left(-2k_g^2\right)}{\pi^{2T+2}\sigma_g^4|\Sigma|^2}\exp\left(-\sum_{i=1}^{T}\lambda_i\left(|\check{y}_{2i-1}|^2+|\check{y}_{2i}|^2\right)\right)\iint\limits_{g_1\ g_2}\frac{I_o\left(\frac{2k_g|g_1|}{\sigma_g}\right)I_o\left(\frac{2k_g|g_2|}{\sigma_g}\right)}{\prod_{i=1}^{T}\left(\lambda_i\sigma_v^2\|g\|^2+1\right)}\exp\left(-\frac{|g_1|^2+|g_2|^2}{\sigma_g^2}\right)$$
$$\times\exp\left(\sum_{i=1}^{T}\frac{\lambda_i^2\sigma_v^2\left(|\check{y}_{2i-1}|^2|g_1|^2+|\check{y}_{2i}|^2|g_2|^2\right)}{\lambda_i\sigma_v^2\|g\|^2+1}+2|g_1||g_2||\check{Y}_o^\dagger\tilde{\Lambda}\check{Y}_e|\cos\left(\theta_{g_1}-\theta_{g_2}-\beta\right)\right)dg_1dg_2, \tag{C.25}$$

Note that $\boldsymbol{g}_1$ and $\boldsymbol{g}_2$ are complex variables. Hence, the double integration in (C.25) is equivalent to quadruple real integrations.

Let χ_0 be the integration in (C.25). Using polar representation, we write $|g_\ell| = r_\ell$, and $dg_\ell = r_\ell dr_\ell d\theta_{g_\ell}$, $\ell \in \{1,2\}$, and hence

$$\chi_0 = \int_0^\infty\int_0^\infty\frac{I_o\left(\frac{2k_gr_1}{\sigma_g}\right)I_o\left(\frac{2k_gr_2}{\sigma_g}\right)}{\prod_{i=1}^{T}\left(\lambda_i\sigma_v^2(r_1^2+r_2^2)+1\right)}\exp\left(\sum_{i=1}^{T}\frac{\lambda_i^2\sigma_v^2\left(|\check{y}_{2i-1}|^2r_1^2+|\check{y}_{2i}|^2r_2^2\right)}{\lambda_i\sigma_v^2(r_1^2+r_2^2)+1}-\frac{r_1^2+r_2^2}{\sigma_g^2}\right)$$
$$\times\int_0^{2\pi}\int_0^{2\pi}\exp\left(2r_1r_2|\check{Y}_o^\dagger\ \tilde{\Lambda}\ \check{Y}_e|\cos\left(\theta_{g_1}-\theta_{g_2}-\beta\right)\right)d\theta_{g_1}d\theta_{g_2}r_1r_2dr_1dr_2. \tag{C.26}$$

Let χ_1 be the inner double integration in (C.26), it can be shown that

$$\begin{aligned}\chi_1 &= 4\pi^2 I_0\left(2r_1r_2|\check{Y}_o^\dagger\ \tilde{\Lambda}\ \check{Y}_e|\right),\\ &= 4\pi^2 I_0\left(2r_1r_2\ \bar{C}_{\check{Y}}\left(r_1^2+r_2^2\right)\right),\end{aligned} \tag{C.27}$$

Using the following change of variable: $\rho^2 = r_1^2 + r_2^2$, $\phi = \arctan\left(\frac{r_2}{r_1}\right)$, $r_1 = \rho\cos(\phi)$, $r_2 = \rho\sin(\phi)$, $dr_1dr_2 = \rho d\rho d\phi$ yields:

$$\begin{aligned}f_{\boldsymbol{Y}|\boldsymbol{X},\boldsymbol{\theta}_{\mu_h}}(Y|X,\theta_{\mu_h}) &= \frac{2\exp\left(-2k_g^2\right)}{\pi^{2T}\sigma_g^4|\Sigma|^2}\exp\left(-\sum_{i=1}^{T}\lambda_i\left(|\check{y}_{2i-1}|^2+|\check{y}_{2i}|^2\right)\right)\\ &\times\int_0^\infty\int_0^{\frac{\pi}{2}}\frac{2\rho^3\sin(\phi)\cos(\phi)}{\prod_{i=1}^{T}(\lambda_i\sigma_v^2\rho^2+1)}I_0\left(\frac{2k_g\rho\cos(\phi)}{\sigma_g}\right)I_0\left(\frac{2k_g\rho\sin(\phi)}{\sigma_g}\right)I_0\left(\rho^2\sin(2\phi)\,\bar{C}_{\check{Y}}\left(\rho^2\right)\right)\\ &\times\exp\left(\sum_{i=1}^{T}\frac{\lambda_i^2\sigma_v^2\left(|\check{y}_{2i-1}|^2\cos^2(\phi)+|\check{y}_{2i}|^2\sin^2(\phi)\right)\rho^2}{\lambda_i\sigma_v^2\rho^2+1}-\frac{\rho^2}{\sigma_g^2}\right)d\phi d\rho.\end{aligned} \tag{C.28}$$

Using the change of variables: $u = \sin^2(\phi)$, $du = 2\sin(\phi)\cos(\phi)\,d\phi$, $t = \frac{\sigma_v^2\ \rho^2}{\sigma_v^2\ \rho^2+1}$ and $\frac{dt}{\sigma_v^2(1-t)^2} = 2\rho d\rho$ and defining $\bar{t} = 1-t$ and $\bar{u} = 1-u$ yields:

$$\begin{aligned}f_{\boldsymbol{Y}|\boldsymbol{X},\boldsymbol{\theta}_{\mu_h}}(Y|X,\theta_{\mu_h}) &= \frac{\exp\left(-2k_g^2\right)}{\pi^{2T}\sigma_g^4\sigma_v^4|\Sigma|^2}\exp\left(-\sum_{i=1}^{T}\lambda_i\left(|\check{y}_{2i-1}|^2+|\check{y}_{2i}|^2\right)\right)\int_0^1\int_0^1\frac{t\ \bar{t}^{T-3}}{\prod_{i=1}^{T}(\lambda_i t+\bar{t})}\\ &\times I_0\left(\frac{2k_g}{\sigma_g\sigma_v}\sqrt{\frac{t\bar{u}}{\bar{t}}}\right)I_0\left(\frac{2k_g}{\sigma_g\sigma_v}\sqrt{\frac{tu}{\bar{t}}}\right)I_0\left(2t\sqrt{u\bar{u}}\bar{C}_{\check{Y}}\left(\frac{t}{\sigma_v^2\bar{t}}\right)\right)\\ &\times\exp\left(\sum_{i=1}^{T}\frac{\lambda_i^2\left(|\check{y}_{2i-1}|^2\bar{u}+|\check{y}_{2i}|^2u\right)t}{\lambda_i t+\bar{t}}-\frac{t}{\sigma_g^2\sigma_v^2\bar{t}}\right)dudt,\end{aligned} \tag{C.29}$$

It can be shown that the argument of the last Bessel function can be written as:

$$2t\sqrt{u\bar{u}}\bar{C}_{\check{Y}}\left(\frac{t}{\sigma_v^2\bar{t}}\right) = |\check{Y}_o^\dagger\ \bar{\Lambda}(u,t)\ \check{Y}_e|.$$

where $\bar{\Lambda}(u,t)$ is a diagonal matrix whose ℓ-th element is given by $\tilde{\Lambda}_\ell = \dfrac{4\ \lambda_\ell^2 u\bar{u}\ t^2}{\lambda_\ell t + \bar{t}}$.

To obtain an expression for $f_{\boldsymbol{Y}|\boldsymbol{X}}(Y|X)$ we average $f_{\boldsymbol{Y}|\boldsymbol{X},\boldsymbol{\theta}_{\mu_h}}(Y|X,\theta_{\mu_h})$ over the independent uniformly distributed phases $\boldsymbol{\theta}_{\mu_{h_1}}$ and $\boldsymbol{\theta}_{\mu_{h_2}}$. In particular, we write

$$f_{\boldsymbol{Y}|\boldsymbol{X}}(Y|X) = \frac{1}{(2\pi)^2}\int_0^{2\pi}\int_0^{2\pi} f_{\boldsymbol{Y}|\boldsymbol{X},\boldsymbol{\theta}_{\mu_h}}(Y|X,\theta_{\mu_h})d\theta_{\mu_{h_1}}d\theta_{\mu_{h_2}}. \tag{C.30}$$

Using (C.29) in (C.30) yields:

$$f_{\boldsymbol{Y}|\boldsymbol{X}}(Y|X) = \frac{\exp\left(-2k_g^2\right)}{4\pi^{2T+2}\sigma_g^4\sigma_v^4|\Sigma|^2}\int_0^{2\pi}\int_0^{2\pi}\exp\left(-\sum_{i=1}^{T}\lambda_i\left(|\check{y}_{2i-1}|^2+|\check{y}_{2i}|^2\right)\right)\Psi(\theta_{\mu_{h_1}},\theta_{\mu_{h_2}})d\theta_{\mu_{h_1}}d\theta_{\mu_{h_2}}, \tag{C.31}$$

where

$$\Psi(\theta_{\mu_{h_1}},\theta_{\mu_{h_2}}) = \int_0^1\int_0^1 \frac{t\bar{t}^{T-3}}{\prod_{i=1}^{T}(\lambda_i t+\bar{t})} I_0\left(|\check{Y}_o^\dagger\bar{\Lambda}(u,t)\check{Y}_e|\right) I_0\left(\frac{2k_g}{\sigma_g\sigma_v}\sqrt{\frac{\bar{u}t}{\bar{t}}}\right) I_0\left(\frac{2k_g}{\sigma_g\sigma_v}\sqrt{\frac{ut}{\bar{t}}}\right) \times \exp\left(\sum_{i=1}^{T}\frac{\lambda_i^2\left(|\check{y}_{2i-1}|^2\bar{u}+|\check{y}_{2i}|^2u\right)t}{\lambda_i t+\bar{t}} - \frac{t}{\sigma_g^2\sigma_v^2\bar{t}}\right)dudt, \tag{C.32}$$

The desired pdf is given by the expressions in (C.31) and (C.32). These expressions can be presented more succinctly by introducing matrix notation. In particular, using the fact that $\check{Y}_o = Q^\dagger\tilde{Y}_o = Q^\dagger\left(Y_o - k_h\sigma_h e^{\jmath\boldsymbol{\theta}_{\mu_{h_1}}}X\right)$ and $\check{Y}_e = Q^\dagger\tilde{Y}_e = Q^\dagger\left(Y_e - k_h\sigma_h e^{\jmath\boldsymbol{\theta}_{\mu_{h_2}}}X\right)$, along

with the fact that $\Sigma^{-1} = Q\Lambda Q^{\dagger}$, for (C.31) we can write

$$\sum_{i=1}^{T} \lambda_i |\check{y}_{2i-1}|^2 = (Y_o - k_h \sigma_h e^{\jmath \boldsymbol{\theta}_{\mu_{h_1}}} X)\Sigma^{-1}(Y_o - k_h \sigma_h e^{\jmath \boldsymbol{\theta}_{\mu_{h_1}}} X), \tag{C.33}$$

$$\sum_{i=1}^{T} \lambda_i |\check{y}_{2i}|^2 = (Y_e - k_h \sigma_h e^{\jmath \boldsymbol{\theta}_{\mu_{h_2}}} X)^{\dagger}\Sigma^{-1}(Y_e - k_h \sigma_h e^{\jmath \boldsymbol{\theta}_{\mu_{h_2}}} X), \tag{C.34}$$

and, for (C.32) we can write:

$$\sum_{i=1}^{T} \frac{\lambda_i^2 |\check{y}_{2i-1}|^2 \bar{u} t}{\lambda_i t + \bar{t}} = \bar{u}(Y_o - k_h \sigma_h e^{\jmath \boldsymbol{\theta}_{\mu_{h_1}}} X)^{\dagger} \Upsilon(\Sigma, t)(Y_o - k_h \sigma_h e^{\jmath \boldsymbol{\theta}_{\mu_{h_1}}} X), \tag{C.35}$$

where $\Upsilon(\Sigma, t) = \Sigma(I_T + \frac{\bar{t}}{t}\Sigma^{-1})^{-1}$. Analogously, it can be shown that:

$$\sum_{i=1}^{T} \frac{\lambda_i^2 |\check{y}_{2i}|^2 u t}{\lambda_i t + \bar{t}} = u(Y_e - k_h \sigma_h e^{\jmath \boldsymbol{\theta}_{\mu_{h_2}}} X)^{\dagger} \Upsilon(\Sigma, t)(Y_e - k_h \sigma_h e^{\jmath \boldsymbol{\theta}_{\mu_{h_2}}} X), \tag{C.36}$$

$$|\check{Y}_o^{\dagger}\ \bar{\Lambda}(u, t)\ \check{Y}_e| = 4u\bar{u}t|(Y_o - k_h \sigma_h e^{\jmath \boldsymbol{\theta}_{\mu_{h_1}}} X)^{\dagger} \Upsilon(\Sigma, t)(Y_e - k_h \sigma_h e^{\jmath \boldsymbol{\theta}_{\mu_{h_2}}} X)|, \tag{C.37}$$

and

$$\prod_{i=1}^{T} (\lambda_i t + \bar{t}) = |\Lambda t + \bar{t} I_T|. \tag{C.38}$$

Using equations (C.33), (C.34), (C.35), (C.36), (C.37), and (C.38) in (C.31) and (C.32) completes the proof.

C.2 Proof of Lemma 5.1

To prove this lemma, we assume in (C.1) that the signal resulting form the jammer transmission at the i-th receive antenna, $\boldsymbol{J}_i = \boldsymbol{g}_i \boldsymbol{V}$, $i \in \{1, 2\}$ is Gaussian distributed, i.e., $\boldsymbol{J}_i \sim \mathcal{CN}\left(\boldsymbol{0}_T, \sigma_g^2 \sigma_v^2 I_T\right)$. Under this assumption, it can be seen from (C.1) that, conditioned on the vector of transmitted symbols, $\boldsymbol{X}$, the k-factor of the transmitter channel, k_h, and the phases vector of the transmitter channel mean $\boldsymbol{\theta}_{\mu_h} = [\ \boldsymbol{\theta}^*_{\mu_{h_1}}\ \boldsymbol{\theta}^*_{\mu_{h_2}}\ ]^\dagger$, the pdf of the received signal vector, $\boldsymbol{Y}$, is given by:

$$f_{\boldsymbol{Y}|\boldsymbol{X},\boldsymbol{\theta}_{\mu_h}}(Y|X, \theta_{\mu_h}) = \quad f_{\boldsymbol{Y}_o|\boldsymbol{X},\boldsymbol{\theta}_{\mu_{h_1}}}(Y_o|X, \theta_{\mu_{h_1}}) f_{\boldsymbol{Y}_e|\boldsymbol{X},\boldsymbol{\theta}_{\mu_{h_2}}}(Y_e|X, \theta_{\mu_{h_2}}), \tag{C.39}$$

where $\boldsymbol{Y}_o$ and $\boldsymbol{Y}_e$ are Gaussian distributed with the following pdfs:

$$f_{\boldsymbol{Y}_o|\boldsymbol{X},\boldsymbol{\theta}_{\mu_{h_1}}}(Y_o|X, \theta_{\mu_{h_1}}) = \frac{1}{\pi^T |\Sigma_N|} \exp\left(-(Y_o - k_h \sigma_h e^{j\theta_{\mu_{h_1}}} X)^\dagger \Sigma_N^{-1} (Y_o - k_h \sigma_h e^{j\theta_{\mu_{h_1}}} X)\right), \tag{C.40}$$

and

$$f_{\boldsymbol{Y}_e|\boldsymbol{X},\boldsymbol{\theta}_{\mu_{h_2}}}(Y_e|X, \theta_{\mu_{h_2}}) = \frac{1}{\pi^T |\Sigma_N|} \exp\left(-(Y_e - k_h \sigma_h e^{j\theta_{\mu_{h_2}}} X)^\dagger \Sigma_N^{-1} (Y_e - k_h \sigma_h e^{j\theta_{\mu_{h_2}}} X)\right), \tag{C.41}$$

where $\Sigma_N = \sigma_h^2 XX^\dagger + (\sigma_g^2\sigma_v^2 + \sigma_Z^2)I_T$. Using the eigndecomposition $\Sigma_N^{-1} = Q_N \Lambda_N Q_N^\dagger$, yields:

$$\begin{aligned} f_{\boldsymbol{Y}_o|\boldsymbol{X},\boldsymbol{\theta}_{\mu_{h_1}}}(Y_o|X,\theta_{\mu_{h_1}}) &= \frac{1}{\pi^T|\Sigma_N|}\exp\left(-\sum_{i=1}^{T}\lambda_i|\hat{y}_{2i-1} - k_h\sigma_h\hat{x}_i e^{j\theta_{\mu_{h_1}}}|^2\right) \\ &= \frac{1}{\pi^T|\Sigma_N|}\exp\left(-\sum_{i=1}^{T}\lambda_i(|\hat{y}_{2i-1}|^2 + k_h^2\sigma_h^2|\hat{x}_i|^2)\right) \\ &\quad \times \exp\left(2k_h\sigma_h\sum_{i=1}^{T}\lambda_i|\hat{y}_{2i-1}||\hat{x}_i|\cos\Big(\theta_{\mu_{h_1}} + \alpha_i\Big)\right), \end{aligned} \tag{C.42}$$

where $\hat{y}_{2i-1}$, $\hat{y}_{2i}$ and $\hat{x}_i$ are the i-th elements of $\hat{Y}_o = Q_N^\dagger Y_o$, $\hat{Y}_e = Q_N^\dagger Y_e$, $\hat{X} = Q_N^\dagger X$, respectively, and $\alpha_i = \angle\hat{x}_i - \angle\hat{y}_{2i-1}$.

Denoting the summation in the argument of the last exponential in (C.42) by S_N, we write

$$\begin{aligned} S_N &= \Big(\sum_{i=1}^{T}\lambda_i|\hat{y}_{2i-1}||\hat{x}_i|\cos(\alpha_i)\Big)\cos\Big(\theta_{\mu_{h_1}}\Big) + \Big(\sum_{i=1}^{T}\lambda_i|\hat{y}_{2i-1}||\hat{x}_i|\sin(\alpha_i)\Big)\sin\Big(\theta_{\mu_{h_1}}\Big) \\ &= \sqrt{W_1^2 + W_2^2}\left(\cos(\beta_o)\cos\Big(\theta_{\mu_{h_1}}\Big) + \sin(\beta_o)\sin\Big(\theta_{\mu_{h_1}}\Big)\right) \\ &= \sqrt{W_1^2 + W_2^2}\cos\Big(\theta_{\mu_{h_1}} - \beta_o\Big), \end{aligned} \tag{C.43}$$

where $W_1 = \sum_{i=1}^{T}\lambda_i|\hat{y}_{2i-1}||\hat{x}_i|\cos(\alpha_i)$, $W_2 = \sum_{i=1}^{T}\lambda_i|\hat{y}_{2i-1}||\hat{x}_i|\sin(\alpha_i)$, and $\beta_o = \arctan\left(\frac{W_2}{W_1}\right)$.

It can be shown that $W_1 = \mathrm{Re}\{\hat{Y}_o^\dagger\ \Lambda_N\ \hat{X}\}$ and $W_2 = \mathrm{Im}\{\hat{Y}_o^\dagger\ \Lambda_N\ \hat{X}\}$, which yields that

$$\begin{aligned} W_1^2 + W_2^2 &= \sum_{m,n=1}^{T} \lambda_m \lambda_n |\hat{y}_{2m-1}||\hat{y}_{2n-1}||\hat{x}_{2m}||\check{x}_{2n}| \cos(\alpha_m - \alpha_n) \\ &= |\hat{Y}_o^\dagger\ \Lambda_N\ \hat{X}|^2, \end{aligned} \tag{C.44}$$

where Λ_N is the diagonal matrix of eigenvalues of Σ_N^{-1}. Using (C.43) and (C.44) in (C.42) yields:

$$\begin{aligned} f_{\boldsymbol{Y}_o|\boldsymbol{X},\boldsymbol{\theta}_{\mu_{h_1}}}(Y_o|X,\theta_{\mu_{h_1}}) = \frac{1}{\pi^T|\Sigma_N|} \exp\left(-\sum_{i=1}^{T} \lambda_i(|\hat{y}_{2i-1}|^2 + k_h^2\sigma_h^2|\hat{x}_i|^2)\right) \\ \times \exp\left(2k_h\sigma_h|\hat{Y}_o^\dagger \Lambda_N \hat{X}| \cos\Big(\theta_{\mu_{h_1}} - \beta_o\Big)\right). \end{aligned} \tag{C.45}$$

Analogously, it can be shown that:

$$\begin{aligned} f_{\boldsymbol{Y}_e|\boldsymbol{X},\boldsymbol{\theta}_{\mu_{h_2}}}(Y_e|X,\theta_{\mu_{h_2}}) = \frac{1}{\pi^T|\Sigma_N|} \exp\left(-\sum_{i=1}^{T} \lambda_i(|\hat{y}_{2i}|^2 + k_h^2\sigma_h^2|\hat{x}_i|^2)\right) \\ \times \exp\left(2k_h\sigma_h|\hat{Y}_e^\dagger \Lambda_N \hat{X}| \cos\Big(\theta_{\mu_{h_2}} - \beta_e\Big)\right). \end{aligned} \tag{C.46}$$

Using (C.45) and (C.46) in (C.39) yields:

$$\begin{aligned} f_{\boldsymbol{Y}|\boldsymbol{X},\boldsymbol{\theta}_{\mu_h}}(Y|X,\theta_{\mu_h}) = \frac{1}{\pi^{2T}|\Sigma_N|^2} \exp\left(-\sum_{i=1}^{T} \lambda_i(|\hat{y}_{2i-1}|^2 + |\hat{y}_{2i}|^2 + 2k_h^2\sigma_h^2|\hat{x}_i|^2)\right) \\ \times \exp\left(2k_h\sigma_h|\hat{Y}_o^\dagger \Lambda_N \hat{X}| \cos\Big(\theta_{\mu_{h_1}} - \beta_o\Big)\right) \exp\left(2k_h\sigma_h|\hat{Y}_e^\dagger \Lambda_N \hat{X}| \cos\Big(\theta_{\mu_{h_2}} - \beta_e\Big)\right). \end{aligned} \tag{C.47}$$

To obtain $f_{\boldsymbol{Y}|\boldsymbol{X}}(Y|X)$, we average the right hand side of (C.47)

over $\boldsymbol{\theta}_{\mu_{h_1}}$ and $\boldsymbol{\theta}_{\mu_{h_2}}$, which yields:

$$f_{\boldsymbol{Y}|\boldsymbol{X}}(Y|X) = \frac{1}{\pi^{2T}|\Sigma_N|^2} \exp\left(-\sum_{i=1}^{T} \lambda_i(|\hat{y}_{2i-1}|^2 + |\hat{y}_{2i}|^2 + 2k_h^2\sigma_h^2|\hat{x}_i|^2)\right) \times I_0\left(2k_h\sigma_h|\hat{Y}_o^\dagger\ \Lambda_N\ \hat{X}|\right) I_0\left(2k_h\sigma_h|\hat{Y}_e^\dagger\ \Lambda_N\ \hat{X}|\right). \quad \text{(C.48)}$$

It can be readily verified that:

$$\sum_{i=1}^{T} \lambda_i|\hat{y}_{2i-1}|^2 = Y_o\Sigma_N^{-1}Y_o, \quad \text{(C.49)}$$

$$\sum_{i=1}^{T} \lambda_i|\hat{y}_{2i}|^2 = Y_e^\dagger\ \Sigma_N^{-1}\ Y_e, \quad \text{(C.50)}$$

and

$$\sum_{i=1}^{T} \lambda_i|\hat{x}_i|^2 = X^\dagger\ \Sigma_N^{-1}\ X. \quad \text{(C.51)}$$

Using (C.49), (C.50), and (C.51) in (C.48) completes the proof.

References

[1] K. Pelechrinis, M. Iliofotou, and S. V. Krishnamurthy. Denial of service attacks in wireless networks: The case of jammers. *IEEE Commun. Surv. Tutorial*, 13(2):245–257, February 2011.

[2] Y. Zou, J. Zhu, X. Wang, and L. Hanzo. A survey on wireless security: Technical challenges, recent advances, and future trends. *IEEE Proc.*, 104(9):1727–1765, September 2016.

[3] Kanika Grover, Alvin Lim, and Qing Yang. Jamming and anti-jamming techniques in wireless networks: A survey. *Int. J. Ad Hoc Ubiquitous Comput.*, 17(4):197–215, December 2014.

[4] M. Petracca, M. Vari, F. Vatalaro, and G. Lubello. Performance evaluation of GSM robustness against smart jamming attacks. In *5th International Symposium on Communications, Control and Signal Processing*, pages 1–6, 2012.

[5] S. Yubo, Z. Kan, Y. Bingxin, and C. Xi. A GSM/UMTS Selective Jamming System. In *International Conference on Multimedia Information Networking and Security*, pages 813–815, 2010.

[6] R. Krenz and S. Brahma. Jamming LTE signals. In *IEEE Int. Black Sea Conf. Commun. and Ntwrking (BlackSeaCom)*, pages 72–76, May 2015.

[7] Y. Arjoune and S. Faruque. Smart Jamming Attacks in 5G New Radio: A Review. In *2020 10th Annual Computing and Communication Workshop and Conference (CCWC)*, pages 1010–1015, 2020.

[8] D. Fang, Y. Qian, and R. Q. Hu. Security for 5G Mobile Wireless Networks. *IEEE Access*, pages 4850–4874, 2018.

[9] Mathy Vanhoef and Frank Piessens. Advanced Wi-Fi attacks using commodity hardware. In *Proceedings of the 30th Annual Computer Security Applications Conference*, pages 256–265, 2014.

[10] Emekcan Aras, Nicolas Small, Gowri Sankar Ramachandran, Stéphane Delbruel, Wouter Joosen, and Danny Hughes. Selective jamming of LoRaWAN using commodity hardware. In *Proceedings of the 14th EAI International Conference on Mobile and Ubiquitous Systems: Computing, Networking and Services*, pages 363–372, 2017.

[11] IEEE standard for local and metropolitan area networks–part 15.4: Low-rate wireless personal area networks (LR-WPANs). *IEEE Std 802.15.4-2011 (Revision of IEEE Std 802.15.4-2006)*, pages 1–314, 2011.

[12] J. Rewienski, M. Groth, L. Kulas, and K. Nyka. Investigation of continuous wave jamming in an IEEE 802.15.4 network. In *2018 22nd International Microwave and Radar Conference (MIKON)*, pages 242–246, 2018.

[13] H. Pirayesh, P. K. Sangdeh, and H. Zeng. Securing ZigBee communications against constant jamming attack using neural network. *IEEE Internet of Things J.*, 2020.

[14] S. Köppel. Bluetooth jamming. In *ETH Zürich Switzerland*, 2013.

[15] A. Mpitziopoulos, D. Gavalas, C. Konstantopoulos, and G. Pantziou. A survey on jamming attacks and countermeasures in WSNs. *IEEE Commun. Surv. Tutorial*, 11(4):42–56, April 2009.

[16] R. D. Pietro and G. Oligeri. Jamming mitigation in cognitive radio networks. *IEEE Network*, 27(3):10–15, May 2013.

[17] J. Z. Moghaddam, M. Usman, F. Granelli, and H. Farrokhi. Cognitive Radio and Device-to-Device Communication: A Cooperative Approach for Disaster Response. In *Proc. IEEE Glob. Commun. Conf.*, pages 1–6, 2016.

[18] J. Wang, M. Ghosh, and K. Challapali. Emerging cognitive radio applications: A survey. *IEEE Commun. Mag.*, pages 74–81, 2011.

[19] Ó. Puñal, C. Pereira, A. Aguiar, and J. Gross. Experimental Characterization and Modeling of RF Jamming Attacks on VANETs. *IEEE Trans. Veh. Technol.*, 64(2):524–540, 2015.

[20] G. Dimitrakopoulos and P. Demestichas. Intelligent Transportation Systems. *IEEE Vec. Technol. Mag.*, pages 77–84, 2010.

[21] F. J. Martinez, C. Toh, J. Cano, C. T. Calafate, and P. Manzoni. Emergency services in future intelligent transportation systems based on vehicular communication networks. *IEEE Intelligent Transportation Systems Magazine*, pages 6–20, 2010.

[22] Rachna Kumari and Mainak Mukhopadhyay. Design of GPS antijamming algorithm using adaptive array antenna to mitigate the noise and interference. *Ambient Intelligence Humanized Computing*, February 2019.

[23] L. Avanco, A. E. Guelfi, E. Pontes, A. A. A. Silva, S. T. Kofuji, and F. Zhou. An effective intrusion detection approach for jamming attacks on rfid systems. In *2015 International EURASIP Workshop on RFID Technology (EURFID)*, pages 73–80, 2015.

[24] P. M. B. Mansingh, T. J. Titus, and V. S. S. Devi. A Secured Biometric Voting System Using RFID Linked with the Aadhar Database. In *6th International Conference on Advanced Computing and Communication Systems (ICACCS)*, pages 1116–1119, 2020.

[25] Mina Labib, Sean Ha, Walid Saad, and Jeffrey H. Reed. A Colonel Blotto game for anti-jamming in the Internet of Things. In *Proc. IEEE Glob. Commun. Conf.*, pages 1–6, San Diego, 2015.

[26] J. G. Proakis and M. Salehi. *Digital Communications*. McGraw-Hill, 2008.

[27] O. Holland, H. Bogucka, and A. Medeisis. *The Universal Software Radio Peripheral (USRP) Family of Low-Cost SDRs*, pages 3–23. Wiley, 2015.

[28] Matthias Wilhelm, Ivan Martinovic, Jens B. Schmitt, and Vincent Lenders. Short paper: Reactive jamming in wireless networks: How realistic is the threat? In *Proc. 4th ACM Conf. Wireless Ntwrk Security*, pages 47–52, New York, 2011.

[29] Matthias Schulz, Francesco Gringoli, Daniel Steinmetzer, Michael Koch, and Matthias Hollick. Massive reactive smartphone-based jamming using arbitrary waveforms and adaptive power control. pages 111–121, 2017.

[30] David J. Thuente and Mithun Acharya. Intelligent Jamming in Wireless Networks with Applications to 802.11b and Other Networks. In *Proc. IEEE Military Commun. (MILCOM)*, pages 1075–1081, 2006.

[31] D. J. Thuente, B. Newlin, and M. Acharya. Jamming Vulnerabilities of IEEE 802.11e. In *Proc. IEEE Military Commun. (MILCOM)*, pages 1–7, 2007.

[32] M. J. L. Pan, T. C. Clancy, and R. W. McGwier. Jamming attacks against OFDM timing synchronization and signal acquisition. In *Proc. IEEE Military Commun. (MILCOM)*, pages 1–7, 2012.

[33] C. Shahriar, M. La Pan, M. Lichtman, T. C. Clancy, R. McGwier, R. Tandon, S. Sodagari, and J. H. Reed. PHY-Layer Resiliency in OFDM Communications: A Tutorial. *IEEE Commun. Surv. Tutorial*, pages 292–314, 2015.

[34] C. Shahriar, S. Sodagari, R. McGwier, and T. C. Clancy. Performance impact of asynchronous off-tone jamming attacks against OFDM. In *Proc. IEEE Int. Conf. Commun. (ICC)*, pages 2177–2182, 2013.

[35] M. J. La Pan, T. C. Clancy, and R. W. McGwier. Phase warping and differential scrambling attacks against OFDM frequency synchronization. In *2013 IEEE International Conference on Acoustics, Speech and Signal Processing*, pages 2886–2890, 2013.

[36] A. El-Keyi, O. ÜReten, H. Yanikomeroglu, and T. Yensen. LTE for Public Safety Networks: Synchronization in the Presence of Jamming. *IEEE Access*, pages 20800–20813, 2017.

[37] T. C. Clancy. Efficient OFDM denial: Pilot jamming and pilot nulling. In *Proc. IEEE Int. Conf. Commun. (ICC)*, Kyoto, June 2011.

[38] C. Shahriar, S. Sodagari, and T. C. Clancy. Performance of pilot jamming on MIMO channels with imperfect synchronization. In *Proc. IEEE Int. Conf. Commun. (ICC)*, pages 898–902, 2012.

[39] S. Sodagari and T. C. Clancy. Efficient jamming attacks on MIMO channels. In *Proc. IEEE Int. Conf. Commun. (ICC)*, pages 852–856, 2012.

[40] S. Sodagari and T.C. Clancy. On singularity attacks in MIMO channels. *Transactions on Emerging Telecommunications Technologies*, 26(3):482–490, 2015.

[41] G. Patwardhan and D. Thuente. Jamming Beamforming: A New Attack Vector in Jamming IEEE 802.11ac Networks. In *Proc. IEEE Military Commun. (MILCOM)*, pages 1534–1541, 2014.

[42] M. Lichtman, J. D. Poston, S. Amuru, C. Shahriar, T. C. Clancy, R. M. Buehrer, and J. H. Reed. A communications jamming taxonomy. *IEEE Security Privacy*, 14(1):47–54, January 2016.

[43] T. Basar. The Gaussian test channel with an intelligent jammer. *IEEE Trans. Inf. Theory*, 29(1):152–157, January 1983.

[44] V. Navda, A. Bohra, S. Ganguly, and D. Rubenstein. Using Channel Hopping to Increase 802.11 Resilience to Jamming Attacks. In *Proc. IEEE Int. Conf. Comp. Commun. (INFOCOM)*, pages 2526–2530, May 2007.

[45] C. Popper, M. Strasser, and S. Capkun. Anti-jamming broadcast communication using uncoordinated spread spectrum techniques. *IEEE J. Select. Areas Commun.*, 28(5):703–715, 2010.

[46] A. Liu, P. Ning, H. Dai, and Y. Liu. USD-FH: Jamming-resistant wireless communication using frequency Hopping with Uncoordinated Seed Disclosure. In *The 7th IEEE International Conference on Mobile Ad-hoc and Sensor Systems (IEEE MASS 2010)*, pages 41–50, 2010.

[47] Y. Liu, P. Ning, H. Dai, and A. Liu. Randomized Differential DSSS: Jamming-Resistant Wireless Broadcast Communication. In *2010 Proceedings IEEE INFOCOM*, pages 1–9, 2010.

[48] Wenyuan Xu, Timothy Wood, Wade Trappe, and Yanyong Zhang. Channel Surfing and Spatial Retreats: Defenses Against Wireless Denial of Service. In *Proc.ACM Wrkshp Wireless Security (WISE)*, pages 80–89, Philadelphia, 2004.

[49] X. He, H. Dai, and P. Ning. Dynamic Adaptive Anti-Jamming via Controlled Mobility. *IEEE Trans. Wireless Commun.*, pages 4374–4388, 2014.

[50] R. C. Hansen. *Phased Array Antennas*. Wiley, 2009.

[51] Ö. C. Dabak, F. Erdem, T. Sönmez, L. Alatan, and S. S. Koç. Interference suppression in a GPS receiver with 4 element array design and implementation of beamforming algorithms. In *2016 IEEE/ION Position, Location and Navigation Symposium (PLANS)*, pages 645–652, 2016.

[52] M. Li, A. G. Dempster, A. T. Balaei, C. Rizos, and F. Wang. Switchable Beam Steering/null Steering Algorithm for CW Interference Mitigation in GPS C/A Code Receivers. *IEEE Transactions on Aerospace and Electronic Systems*, 47(3):1564–1579, 2011.

[53] Q. Li, W. Wang, D. Xu, and X. Wang. A Robust Anti-Jamming Navigation Receiver with Antenna Array and GPS/SINS. *IEEE Commun. Lett.*, pages 467–470, 2014.

[54] S. Lim, S. Han, J. Lee, Y. Eun, and J. Choi. Decoy Signal Based Strategic Beamforming Against High-Power Reactive Jamming. *IEEE Trans. Veh. Technol.*, pages 10054–10058, 2018.

[55] Sung-Ho Lim, Sungmin Han, Jaeseok Lee, and Ji-Woong Choi. Tactical beamforming against high-power reactive jammer. In *2016 Eighth International Conference on Ubiquitous and Future Networks (ICUFN)*, pages 92–95, 2016.

[56] C. A. Cole, C. Shahriar, and T. C. Clancy. An Anti-jam Communications Technique via Spatial Hiding Precoding. In *Proc. IEEE Military Commun. (MILCOM)*, pages 490–494, October 2014.

[57] Shyamnath Gollakota, Fadel Adib, Dina Katabi, and Srinivasan Seshan. Clearing the RF Smog: Making 802.11n Robust to Cross-Technology Interference. *ACM SIGCOMM Comp. Commun. Rev.*, pages 170–181, August 2011.

[58] Q. Yan, H. Zeng, T. Jiang, M. Li, W. Lou, and Y. T. Hou. Jamming Resilient Communication Using MIMO Interference Cancellation. *IEEE Trans. Info. Forensics Security.*, 11(7):1486–1499, 2016.

[59] C. Shahriar, R. McGwier, and T. C. Clancy. Performance impact of pilot tone randomization to mitigate OFDM jamming attacks. In *2013 IEEE 10th Consumer Communications and Networking Conference (CCNC)*, pages 813–816, 2013.

[60] W. Shen, P. Ning, X. He, H. Dai, and Y. Liu. MCR Decoding: A MIMO approach for defending against wireless jamming attacks. In *2014 IEEE Conference on Communications and Network Security*, pages 133–138, 2014.

[61] Hongwei Zhao, Baowang Lian, and Juan Feng. Space-time adaptive processing for gps anti-jamming receiver. *Physics Procedia*, 33:1060–1067, 2012.

[62] D. Lu, R. Wu, and H. Liu. Global positioning system anti-jamming algorithm based on period repetitive CLEAN. *IET Radar, Sonar & Navigation*, pages 164–169, February 2013.

[63] U J Schwarz. MATHEMATICAL-STATISTICAL DESCRIPTION OF ITERATIVE BEAM REMOVING TECHNIQUE (METHOD CLEAN). *Astronomy & astrophysics*, pages 345–356, 1978.

[64] D. Borio, L. Camoriano, L. Lo Presti, and P. Mulassano. Analysis of the one-pole Notch Filter for Interference Mitigation: Wiener Solution and Loss Estimations. In *ION GNSS*, 2006.

[65] D. Borio, L. Camoriano, and L. Lo Presti. Two-pole and Multi-pole Notch filters: A Computationally Effective Solution for GNSS Interference Detection and Mitigation. *IEEE Systems Journal*, pages 38–47, 2008.

[66] Y. Chien. Design of GPS Anti-Jamming Systems Using Adaptive Notch Filters. *IEEE Systems Journal*, 9:451–460, 2015.

[67] Alan V. Oppenheim, Ronald W. Schafer, and John R. Buck. *Discrete-Time Signal Processing (2nd Ed.)*. Prentice-Hall, Inc., 1999.

[68] Mohammad Javad Rezaei, Mohsen Abedi, and Mohammad Reza Mosavi. New GPS anti-jamming system based on multiple short-time Fourier transform. *IET Radar, Sonar & Navigation*, pages 807–815, 2016.

[69] F.J Owens and M.S Murphy. A short-time Fourier transform. *Signal Processing*, pages 3–10, 1988.

[70] K. Luo, R. H. Gohary, and H. Yanikomeroglu. The capacity of a broadcast channel with Gaussian jamming and a friendly eavesdropper. In *Proc. IEEE Inform. Theory Wkshp. (ITW)*, pages 327–331, October 2015.

[71] Konstantinos Pelechrinis, Ioannis Broustis, Srikanth V. Krishnamurthy, and Christos Gkantsidis. ARES: An anti-jamming reinforcement system for 802.11 networks. In *Proc. Int. Conf. Emerg. Ntwrk. Experiments and Technologies*, Rome, Italy, 2009.

[72] D. Fang, Y. Qian, and R. Q. Hu. Security for 5G Mobile Wireless Networks. *IEEE Access*, pages 4850–4874, 2018.

[73] R. H. Gohary, Y. Huang, Z. Luo, and J. Pang. A generalized iterative water-filling algorithm for distributed power control in the presence of a jammer. *IEEE Trans. Signal Processing*, 57(7):2660–2674, July 2009.

[74] M. K. Hanawal, M. J. Abdel-Rahman, and M. Krunz. Game theoretic anti-jamming dynamic frequency hopping and rate adaptation in wireless systems. In *Int. Symp. Model. Opt. Mobile, Ad Hoc, and Wireless Ntwrks (WiOpt)*, pages 247–254, Hammamet, Tunisia, May 2014.

[75] Y. Wu, B. Wang, K. J. R. Liu, and T. C. Clancy. Anti-jamming games in multi-channel cognitive radio networks. *IEEE J. Select. Areas Commun.*, 30(1):4–15, January 2012.

[76] M. Medard. Capacity of correlated jamming channels. In *Proc. Allerton Conf. Commun, Control, Comput.*, pages 1043—-1052, October 1997.

[77] A. Bayesteh, M. Ansari, and A. K. Khandani. Effect of jamming on the capacity of MIMO channels. In *Proc. Allerton Conf. Commun, Control, Comput.*, pages 401–410, October 2004.

[78] S. Shafiee and S. Ulukus. Capacity of multiple access channels with correlated jamming. In *Proc. IEEE Military Commun. (MILCOM)*, pages 218–224, October 2005.

[79] C. A. Cole, C. Shahriar, and T. C. Clancy. An anti-jam communications technique via spatial hiding precoding. In *Proc. IEEE Military Commun. (MILCOM)*, pages 490–494, October 2014.

[80] Cecil C. Craig. On the frequency function of xy. *Ann. Math. Statist.*, 7(1):1–15, March 1936.

[81] K. S. Miller. *Multidimensional Gaussian distributions*. John Wiley and Sons, New York, 1964.

[82] A. Gut. *An Intermediate Course in Probability*. Springer Texts in Statistics. Springer, New York, 2009.

[83] A. Papoulis, S.U. Pillai, and S.U. Pillai. *Probability, Random Variables, and Stochastic Processes*. McGraw-Hill, 2002.

[84] Marvin K. Simon. *Probability Distributions Involving Gaussian Random Variables: A Handbook for Engineers, Scientists and Mathematicians*. Springer-Verlag, Berlin, 2006.

[85] R. K. Mallik and N. C. Sagias. Distribution of inner product of complex Gaussian random vectors and its applications. *IEEE Trans. Commun.*, 59(12):3353–3362, December 2011.

[86] N. O'Donoughue and J. M. F. Moura. On the product of independent complex Gaussians. *IEEE Trans. Signal Processing*, 60(3):1050–1063, March 2012.

[87] T. Betlehem and A. J. Coulson. Distribution of the sum of a complex Gaussian and the product of two complex Gaussians. In *Australian Commun. Theory Wkshp (AusCTW)*, pages 126–129, Wellington, January 2012.

[88] K. A. Almahorg and R. H. Gohary. Maximum Likelihood Detection in the Presence of Non-Gaussian Jamming. *IEEE Trans. Signal Processing*, pages 5722–5735, 2020.

[89] W. Khawaja, I. Guvenc, D. W. Matolak, U. Fiebig, and N. Schneckenburger. A survey of air-to-ground propagation channel modeling for unmanned aerial vehicles. *IEEE Commun. Surv. Tutorial*, 21(3):2361–2391, 2019.

[90] G. N. Watson. *A Treatise on the Theory of Bessel Functions*. Cambridge University Press, Cambridge, 2nd edition, 1944.

[91] B. M. Hochwald, T. L. Marzetta, T. J. Richardson, W. Sweldens, and R. Urbanke. Systematic design of unitary space-time constellations. *IEEE Trans. Inf. Theory*, 46(6):1962–1973, September 2000.

[92] MATLAB. *version 9.9.0.1538559 (R2020b)*. The MathWorks Inc., Natick, Massachusetts, 2020.

[93] K. A. Almahorg and R. H. Gohary. Maximum likelihood detection in the presence of non-Gaussian jamming. *IEEE Trans. Signal Processing*, 68:5722–5735, 2020.

[94] Glenn Shafer. Dempster-shafer theory. *Encyclopedia of artificial intelligence*, 1:330–331, 1992.

[95] Milton Abramowitz and Irene A. Stegun, editors. *Handbook of Mathematical Functions with Formulas, Graphs and Mathematical Tables*. Dover Publications, Inc., New York, 1965.

[96] B. Dwork. *Generalized Hypergeometric Functions*. Clarendon Press, Oxford, England, 1990.

[97] I. Gradshteyn and I. Ryzhik. *Table of Integrals, Series and Products*. Academic Press, 2007.

[98] R. J. Muirhead. *Aspects of Multivariate Statistical Theory*. Wiley, New York, 1982.

[99] Kenneth S. Miller. On the inverse of the sum of matrices. *Mathematics Magazine*, 54(2):67–72, 1981.